

# Tensor Factorized Recursive Hamiltonian Downfolding to Optimize the Scaling Complexity of the Electronic Correlations Problem on Classical and Quantum Computers

Ritam Banerjee, Ananthakrishna Gopal, Soham Bhandary, Janani Seshadri, and

Anirban Mukherjee\*

*TCS Corporate Incubation*

E-mail: m.anirban7@tcs.com

## Abstract

This paper presents a new variant of post-Hartree-Fock Hamiltonian downfolding-based quantum chemistry methods with optimized scaling for high-cost simulations like coupled cluster (CC), full configuration interaction (FCI), and multi-reference CI (MRCI) on classical and quantum hardware. This improves the applicability of these calculations to practical use cases.

High-accuracy quantum chemistry calculations, such as CC, involve memory and time-intensive tensor operations, which are the primary bottlenecks in determining the properties of many-electron systems. The complexity of these operations scales exponentially with the system size. We aim to find properties of chemical systems by optimizing this scaling through mathematical transformations on the Hamiltonian and the state space. By defining a bi-partition of the many-body Hilbert space into electron-occupied and electron-unoccupied blocks for a given orbital, we perform a downfolding

transformation that decouples the electron-occupied block from its complement.

We represent high-rank electronic integrals and cluster amplitude tensors as low-rank tensor factors of a downfolding transformation, mapping the full many-body Hamiltonian into a smaller dimensional block-Hamiltonian recursively. This reduces the computational complexity of solving the residual equations for Hamiltonian downfolding on CPUs from  $\mathcal{O}(N^7)$  for CCSD(T) and  $\mathcal{O}(N^9) - \mathcal{O}(N^{10})$  for CI and MRCI to  $\mathcal{O}(N^3)$ . Additionally, we create a quantum circuit encoding of the tensor factors, generating circuits of  $\mathcal{O}(N^2)$  depth with  $\mathcal{O}(\log N)$  qubits. We demonstrate super-quadratic speedups of expensive quantum chemistry algorithms on both classical and quantum computers.

## Contents

<b>1</b>	<b>Introduction</b>	<b>5</b>
<b>2</b>	<b>System Description</b>	<b>9</b>
<b>3</b>	<b>Recursive Hamiltonian downfolding in Tensor factorized representation</b>	<b>10</b>
<b>4</b>	<b>Case Study: Multireference Downfolding with Singles and Paired Doubles</b>	<b>15</b>
<b>5</b>	<b>Case Study: Unitary Multireference Downfolding with Singles and Doubles</b>	<b>19</b>
<b>6</b>	<b>Case Study: Single configuration spin restricted downfolding with singles and doubles</b>	<b>25</b>
6.1	T1-Residual Equation . . . . .	27
6.2	T2-Residual Equation . . . . .	28
<b>7</b>	<b>Quantum Circuits for Block encoding tensor operations</b>	<b>31</b>
7.1	Realizing Tensor Operations . . . . .	32
7.1.1	Qubitization circuit for Matrix-Matrix multiplication with isometries	32

Theorem . . . . .	32
7.1.2 Matrix-multiplication with Quantum circuits only with Unitary operators . . . . .	34
Theorem . . . . .	34
7.1.3 Quantum Circuit for Tensor Product . . . . .	36
Theorem . . . . .	36
7.1.4 Quantum Circuit for Tensor Contraction . . . . .	39
Theorem . . . . .	39
7.1.5 Tensor Contraction . . . . .	41
7.1.6 Tensor Dot . . . . .	42
7.1.7 Hadamard Product . . . . .	42
7.2 Complexity Analysis of Single Reference Recursive Hamiltonian Downfolding(Singles Doubles) . . . . .	43
7.3 Implementing Downfolding Expressions on Quantum Circuits . . . . .	45
7.3.1 Depth of a Quantum Circuit in S,CNOT,H,T basis that block encodes a two-rank tensor . . . . .	47
7.3.2 Expression 1 . . . . .	47
7.3.3 Expression 2 . . . . .	47
7.3.4 Expression 3 . . . . .	49
7.3.5 Expression 4 . . . . .	50
7.3.6 Expression 5 . . . . .	51
7.3.7 Expression 6 . . . . .	53
7.3.8 Expression 7 . . . . .	54
7.3.9 Expression 8 . . . . .	55
7.3.10 Expression 9 . . . . .	56
7.3.11 Expression 10 . . . . .	57
7.3.12 Expression 11 . . . . .	59

7.4	Error from Quantum Phase Estimation and Downfolding . . . . .	63
7.5	Benchmarking . . . . .	64
<b>8</b>	<b>Results and Discussion</b>	<b>74</b>
<b>9</b>	<b>Future Directions</b>	<b>78</b>
<b>A</b>	<b>Lowdin Decomposition of The Hamiltonian H For Primary Space (P) and Secondary Space (Q)</b>	<b>78</b>
A.1	Normal Ordering $\eta_{(N)}P_{(N)}HQ_{(N)}\eta_{(N)}$ . . . . .	79
<b>B</b>	<b>Normal ordering <math>\eta_{(N)}P_{(N)}HP_{(N)}</math></b>	<b>81</b>
<b>C</b>	<b>Normal ordering <math>Q_{(N)}HQ_{(N)}\eta_{(N)}</math></b>	<b>82</b>
C.1	Algebraic Downfolding equations Deduced From Bloch Equation . . . . .	83
C.2	Tensor Factorization of three rank tensors-Convex Polyadic decomposition of three rank tensors . . . . .	85
C.3	Qubitization circuit for Matrix-Matrix multiplication with isometries . . . . .	87
	Theorem . . . . .	87
C.4	Matrix-multiplication with Quantum circuits only with Unitary operators . . . . .	89
	Theorem . . . . .	89
	<b>Acknowledgement</b>	<b>91</b>
	<b>Declaration</b>	<b>91</b>
	<b>References</b>	<b>91</b>

# 1 Introduction

Quantum chemistry calculations, particularly those beyond Hartree-Fock (HF) or density functional theory (DFT), are essential for accurately computing the properties of molecules and materials, which are crucial for research in multiple industry verticals that deals with molecules, chemical processes, crystals and advanced materials.<sup>3-6</sup>

To formulate the electronic problem, we use the Born-Oppenheimer approximation which allows the construction of the electronic Hamiltonian as a function of the nuclear coordinates. The electronic Hamiltonian is constituted of one-electron and two-electron integrals,  $h_{ij}^{(1)}$  and  $h_{ijkl}^{(2)}$  respectively, which are  $N^2$  and  $N^4$  dimensional objects where  $N$  is the system size (number of molecular orbitals). Here the Hamiltonian,  $H$ , for a system with  $N$  orbitals is a massive object with a  $2^{2N} \times 2^{2N}$  matrix representation. The eigenvalues and eigenvectors of  $H$  describe the static and the dynamic properties of a many-electron system. However, the computational complexity for the eigenvalue decomposition of  $H$  scales exponentially with  $N$  making the brute-force approach non-scalable. There are multitudes of alternate ways to solve the problem, like coupled cluster theories - coupled cluster singles doubles (CCSD) with perturbative triples (CCSD(T)) and perturbative quadruples (CCSD(TQ)).<sup>7-10</sup> The coupled cluster theories are inherently size-extensive and size-consistent. There are also different variants of configuration interaction theories that account for the electronic correlations, like configuration interaction singles doubles (CISD) and full configuration interaction (FCI).<sup>11</sup> For the cases with unequal number of up-spin and down-spin electrons, open shell properties of electronic systems are calculated with unrestricted coupled cluster theories. For molecules with d-block elements, for spin triplets, for free radicals or for studying bond-breaking scenarios, multi-reference effects of electronic systems need to be accounted for. These cases are handled using multi-reference coupled cluster (MRCC) theories.<sup>12,12-14</sup> There also exist multiple variants of MRCC that can be either state-specific or state-universal.<sup>15</sup>

High accuracy quantum chemistry calculations like coupled cluster, have recently been accelerated on GPUs using density-fitting based resolution-of-identity (RI) and tensor hyper-

contraction approaches.<sup>2,9,16</sup> An alternative way to solve the electronic Hamiltonian involves subsystem partitioning, either explicitly like density-matrix embedding theory (DMET)<sup>17,18</sup> or implicitly like DMFT<sup>19</sup> and cluster DMFT.<sup>20</sup> There are also a host of renormalization group approaches like numerical renormalization group<sup>21</sup> and its density matrix variant, the density matrix renormalization group (DMRG),<sup>22</sup> that generates a low energy description starting from a tensor-network based ansatz. Among these, DMRG approach<sup>23,24</sup> leverages tensor decomposition to depict wavefunctions in a tensor network representation to make the calculations cost-efficient. Current state-of-the-art complexities are  $> \mathcal{O}(N^3)$ . New innovations are ongoing in this area, particularly for tree-tensor networks<sup>25</sup> in molecular quantum chemistry, to optimize the compute-resources and thereby enhance the volume of data for chemical complexes of diverse types and sizes.

Constructing effective Hamiltonians on a reduced set of orbitals from the parent Hamiltonian, is another approach to lowering the computational scaling complexity of incorporating electronic correlation energies. The effective Hamiltonian is a lower-dimensional representation of the full many-body Hamiltonian  $H$ , which describes the physics of a reduced subspace. Constructing an effective Hamiltonian is a central goal in physics, with applications in the study of quantum phase transitions<sup>26-29</sup> and quantum chemistry simulations.<sup>30-32</sup> The concept of effective Hamiltonian emerges in a diverse set of many-body methods: many-body perturbation theory,<sup>33-35</sup> Scheiffer-Wolff transformation,<sup>36</sup> similarity transformation,<sup>37,38</sup> continuous unitary transformation,<sup>39</sup> Hamiltonian truncation,<sup>40</sup> Feshbach-Lowdin-Fano method,<sup>32</sup> multireference perturbation theory,<sup>41</sup> Hamiltonian Monte Carlo,<sup>42</sup> Numerical renormalization group<sup>43,44</sup> and Hamiltonian downfolding.<sup>45-48</sup>

We focus on the approach of downfolding that allows electronic Hamiltonians to be solved in a smaller active space.<sup>10</sup> In traditional approaches to downfolding, both similarity transformation and unitary transformation variants exist. To perform downfolding in a standard manner, one must choose between a small primary space and a large complementary space. If downfolding is implemented exactly, then the eigenvalues of the downfolded effective Hamil-

tonian in the smaller primary space via an appropriate transformation will only contain a subset of the eigenvalues of the full space. In practice, however, downfolding is as costly to implement as solving the many-body Hamiltonian for getting eigenvalues. Therefore, an alternative is sought. We must solve for the downfolded Hamiltonian, including solving the algebraic equations of the transformation parameters which are similar to solving the residual equations in coupled cluster theory. In this area, there is a family of coupled cluster based downfolding approaches. Some recent approaches split the transformation operation and exploit the sub-algebra of the operators to simplify expressions.<sup>45,49,50</sup> The unitary route to downfolding is inspired by the unitary coupled cluster ansatz which must be truncated up to a double-commutator level to obtain a DUCC Hamiltonian.<sup>51</sup> In standard downfolding approaches, the similarity or the unitary transformation operator has  $N^2$  singles and  $N^4$  doubles excitation operators.

In this work, downfolding is recursively performed. At each step, the highest molecular orbital is decoupled from the rest. This enables us to make a natural choice of a large primary space(P) of  $(N - 1)$  orbitals and a small secondary space(Q) of just 1 orbital. In the standard downfolding approach, the secondary space has more orbitals than primary space and the Bloch equation is solved with respect to a reference state. In our case, at each step, the P and Q sub-spaces form a sequence of blocks. The unitary transformation can be constructed in closed form offering direct access to the many body wave-functions. This is not possible from the standard approach. Combined with tensor factorization and the multi-reference nature of the Bloch equation used in our approach, we can solve the algebraic equations with  $\mathcal{O}(N^3)$  -  $\mathcal{O}(N^4)$  complexity compared to  $N_C \times \mathcal{O}(N^7)$  complexity in the standard approach. Downfolding methods are also used to construct effective Hamiltonians with lesser degrees of freedom that can be used for subsequent calculations like DMFT, quantum monte carlo, DMRG etc.

With recent efforts in the direction of quantum computing, there has also been a parallel development of quantum algorithms towards solving the complex electronic correlation

problem. One of the leading efforts in that direction is due to the quantum phase estimation (QPE) algorithm based on qubitization.<sup>52</sup> The time evolution operator used in phase estimation,  $e^{iHt}$ , is reconstructed using quantum signal processing<sup>53,54</sup> from the quantum walk operator,  $e^{i\arccos(H/\|H\|_1)}$ , where  $\|H\|_1$  is the 1-norm of the Hamiltonian. In a series of works,<sup>55-57</sup> the authors present tensor factorization based approaches to compactly represent the electronic Hamiltonian on a quantum circuit for performing QPE with optimal depth and optimal number of qubits. Tensor hypercontraction and qubitization based QPE substantially reduces the quantum resource requirements compared to double and single factorization based QPE, as can be seen in a variety of practical problems of interest: simulating catalyst for carbon capture,<sup>58</sup> FeMoCo co-factor of nitrogenase for biological nitrogen fixation,<sup>59</sup> for simulating lithium based battery materials,<sup>60</sup> electronic structure of cytochrome P450.<sup>61</sup> There are also alternate techniques like first quantization based approaches<sup>62</sup> and Krylov subspace based approaches<sup>63-65</sup> that enable low cost implementation of QPE on quantum computers. There is also a family of works that classify the quantum algorithms from the perspective of quantum computational complexities as compared to the classical complexities. Under that classification and with a decent projection of the level of future quantum hardware, a demand for innovative algorithms that have super-quadratic or cubic quantum advantage over classical computing on GPUs is imminent.<sup>66,67</sup>

These variants of QPE have shown a need for  $\mathcal{O}(N)$  logical qubits and  $\mathcal{O}(N^2/\epsilon) - \mathcal{O}(N^4/\epsilon)$  Toffolis for a  $N$  orbital electronic system, where  $\epsilon$  is the accuracy with respect to the exact energy. In this work we develop a method to port the recursive downfolding approach in tensor factorized representation onto the quantum circuits by block encoding<sup>52</sup> a family of tensors, matrices and their operations. We construct the residual equation amplitudes in its tensor factorized form on the quantum circuit with  $\mathcal{O}(N^2\log(1/\epsilon))$  depth and  $\mathcal{O}(\log N)$  logical qubits, and use that to compute the updated cluster coefficients at each step of the Downfolding recursion. We collect the energy contributions for each downfolded orbital which cumulatively sums over to give the total electronic correlation energy.



In subsequent sections, we will showcase the detailed methodology for a general recursive Hamiltonian downfolding approach with tensor factorization (Fig2). From there, we will reduce to a family of theories: multi-reference recursive Hamiltonian downfolding theories and single reference recursive Hamiltonian downfolding theories. For each of these theories and with different levels of cluster interactions: singles, doubles, triples and quadruples, we will show the reduction in computational scaling complexity for both memory and time. We will also show the quantum computational scaling complexities for qubits-count, T-depth and CNOT depth by implementing quantum circuits for each level of theory in S, CNOT, H,T basis. Finally we will show a diverse array of examples, spanning small, medium and large sized molecules and benchmark our downfolding energy values, storage requirements and run-times with the standard post-HF theories: MP2 and coupled cluster. Additionally, we will provide a comparison of quantum circuit depth and qubit-count estimates for our qubitized recursive Hamiltonian downfolding with standard QPE algorithm implementations.

## 2 System Description

We consider a system of  $N$ -correlated Hartree-Fock MOs corresponding to a chemical system. The fermionic Fock-space Hamiltonian in MO basis is represented as,

$$H_{(N)} = \sum_{ab} h_{ab}^{1,(N)} f_a^\dagger f_b + \sum_{abcd} h_{abcd}^{2,(N)} f_a^\dagger f_b^\dagger f_c f_d, \quad (1)$$

where  $h_{ab}^{1,(N)}$  and  $h_{abcd}^{2,\sigma\sigma',(N)}$  represents the one-electron and two-electron ERI tensors of the block-Hamiltonian respectively. The two-electron integrals can be represented in the tensor factorized form using a convex polyadic decomposition of the Cholesky factorized block-ERI as follows,<sup>68,69</sup>

$$h_{abcd}^2 = \sum_x L_{ab}^x L_{cd}^x = \sum_{p,q} B_{ap}^1 B_{bp}^2 B_{xp}^3 B_{cq}^1 B_{dq}^2 B_{xq}^3 \quad (2)$$

For the case of molecular systems,  $a, b, c, d$  contains information of both the spatial component and the spin component of the molecular orbitals such that  $a \equiv (i, \sigma)$ , where  $\sigma \in \{\uparrow, \downarrow\}$ . In the one-body term,  $h_{ab}^{1,(N)}$ ,  $a \equiv (i, \sigma)$  and  $b \equiv (j, \sigma)$ . In the two body term,  $h_{abcd}^{2,(N)}$ , the spin orbital ordering is given by  $(i, \sigma), (j, \sigma'), (k, \sigma'), (l, \sigma)$ . The index  $(N)$  denotes the coefficients for the system with  $N$  correlated MO's. It will be useful to denote the downfolding orbital number with  $N$ . Here  $\sigma$  and  $\sigma'$  represents the  $\alpha/\beta$  or  $\uparrow / \downarrow$  spin orbitals.

*Energy Level Grouping of the HF-MO's*

The HF MOs get grouped into virtual orbitals  $\mathcal{V}$ , core orbitals  $\mathcal{C}$ , and active space orbitals  $\mathcal{A}$ . We specify the absolute energy difference of the HF Orbitals (labeled  $k$ 's) from the HOMO(highest occupied molecular orbital) energy  $E_{HOMO}$  as  $\epsilon_k = |E_i - E_{HOMO}|$ . The spin orbital labels comprising the molecular orbitals are lexicographic-ally ordered  $1, 2, \dots, N$  and correspond to a two element tuple  $(i, \sigma)$ . The indices  $1, \dots, N$  of the ordering are tagged to the molecular orbital energies obtained from Hartree-Fock theory,

$$\epsilon_1 \leq \epsilon_2 \leq \dots \leq \epsilon_k \leq \dots \leq \epsilon_N \tag{3}$$

If  $k \in \mathcal{V}$  then within Hartree-Fock theory the MO is unoccupied  $n_{k\uparrow} + n_{k\downarrow} = 0$ . If  $k \in \mathcal{C}$  then  $n_{k\uparrow} + n_{k\downarrow} = 2$ . And if  $k \in \mathcal{A}$  then  $n_{k\uparrow} + n_{k\downarrow} = 0, 1, 2$

### 3 Recursive Hamiltonian downfolding in Tensor factorized representation

In this section, we will introduce the most general form of the tensor factorized recursive Hamiltonian downfolding. As per the notations defined in the previous section, the molecular orbitals are arranged in an ascending order w.r.t to the molecular orbital (MO) energies. Then, the MOs can be systematically downfolded starting from the highest energy MOs scaling down towards the low energy HOMO-LUMO window. For decoupling the outermost

orbital  $N \in \mathcal{V}$ , we partition the many-body Hilbert space  $\mathcal{H}^{\otimes 2N}$  into a primary space ( $P_{(N)}$ ) and a secondary space ( $Q_{(N)}$ ):

$$P_{(N)} = (1 - \hat{n}_N) \quad (4)$$

$$Q_{(N)} = \hat{n}_N \quad (5)$$

Here  $\hat{n}_a = f_a^\dagger f_a$ ,  $\{f_a^\dagger, f_b\} = \delta_{ab}$ ,  $\{f_a^\dagger, f_a\} = 0$ . Together  $P_{(N)} + Q_{(N)} = I^{\otimes 2N}$  comprise the complete Hilbert space. We seek a similarity transformation  $S_{(N)} = \exp(\eta_{(N)})$  generated by  $\eta_{(N)}$  such that the Bloch equation is satisfied,

$$Q_{(N)} S_{(N)}^{-1} H_{(N)} S_{(N)} P_{(N)} = 0 \quad (6)$$

For  $\eta_{(N)}$  satisfying the *linearization* condition  $Q_{(N)} \eta_{(N)} P_{(N)} = \eta_{(N)}$  i.e. equivalent to  $\eta_{(N)}^2 = 0$  a linear representation of the similarity transform  $S_{(N)} = 1 + \eta_{(N)}$  can be obtained. A general choice of  $\eta_{(N)}$  comprises of all possible  $m$ -particle  $m$ -hole excitations coupling  $P_{(N)}$  and  $Q_{(N)}$ ,

$$\begin{aligned} S_{(N)} &= 1 + \eta_{(N)} \\ &= 1 + \left[ \sum_{m=1}^{N_e} \sum_{\substack{a_1 \leq \dots \leq a_m, \\ a_{m+1} \leq \dots \leq a_{2m-1} < N}} \sum_k A_{a_1, k}^1 \dots A_{a_{2m-1}, k}^{2m-1} E_{a_1, \dots, a_m}^+ E_{a_{m+1}, \dots, a_{2m-1}}^- \right] f_N. \end{aligned} \quad (7)$$

The summation is over the collective indices  $a_1, \dots, a_m$  where  $a_i = (i, \sigma_i)$  and these are energy ordered eq.(3). Here the cluster operators  $E_{a_1, \dots, a_m}^+$  and  $E_{a_{m+1}, \dots, a_{2m-1}}^-$  are defined as,

$$E_{a_1, \dots, a_m}^+ = f_{a_1}^\dagger \dots f_{a_m}^\dagger \quad (8)$$

$$E_{a_{m+1}, \dots, a_{2m-1}}^- = f_{a_{m+1}} \dots f_{a_{2m-1}}. \quad (9)$$

This enables creation of  $m$  particles and  $m - 1$  holes respectively. All these excitations generated by  $\eta_{(N)}$  comprise  $2^{N-1}$  sub-configuration of many body states where the  $N$ th

spin orbital is in occupied state and will be decoupled. The index  $m$  ranges from 1 to  $N_e$ , because we can excite all the  $N_e$  electrons in the system at maximum. Therefore, the generator comprises of  $N - 1$  singles excitation amplitudes,  $\binom{N}{4} - \binom{N}{3}$  doubles excitation amplitude,  $\binom{N}{6} - \binom{N}{5}$  triples excitation amplitude all the way to  $\binom{N}{2\lceil N_e/2 \rceil} - \binom{N}{2\lceil N_e/2 \rceil - 1}$   $N_e$ -cluster excitation amplitude. The ceil accounts for the fact that the number of electrons can be odd viz. open shell and if its even then that would correspond to closed shell. With the form of  $\eta_{(N)}$  given in eq(7) and the tensor factors for the electronic integrals given in eq(2), we can write down the operator ordered Bloch equation for the 1st downfolding step (fig 2) as follows,

$$Q_{(N)}S_{(N)}^{-1}HS_{(N)}P_{(N)} = 0 \implies \sum_{a_1, \dots, a_p} r_{a_1, \dots, a_{2p}}^{(N)} E_{a_1 \dots a_m}^+ E_{a_{m+1} \dots a_{2m-1}}^- f_N = 0 . \quad (10)$$

To normal order the strings of fermionic operations in the Bloch equation eq(10) we establish some identities below:

1. operator ordering- :  $E_{a_1 \dots a_m}^+ E_{a_{m+1} \dots a_{2m-1}}^- f_N f_a^\dagger f_b :$

$$\begin{aligned} & E_{a_1 \dots a_m}^+ E_{a_{m+1} \dots a_{2m-1}}^- f_N f_a^\dagger f_b = \\ & \sum_{j=m+1}^{2m-1} \delta_{a_j, a} e^{ij\pi} E_{a_1 \dots a_m}^+ f_{a_{m+1}} \dots f_{a_{j-1}} f_{a_{j+1}} \dots f_{a_{2m-1}} f_N f_b \prod_{j=1}^m (1 - \delta_{a_j, a}) \\ & + \sum_{j=m+1}^{2m-1} \sum_{q=1}^m \theta(l - a_q) \theta(a_{q+1} - l) e^{i(q+1)\pi} f_{a_1}^\dagger \dots f_{a_q}^\dagger f_l^\dagger f_{a_{q+1}}^\dagger \dots f_{a_m}^\dagger f_{a_{m+1}} \dots f_{a_{j-1}} f_l f_{a_{j+1}} \dots f_{a_{2m-1}} f_N \prod_{j=1}^m (1 - \delta_{a_j, l}) \\ & + \sum_{j=1}^m \theta(l - a_j) \theta(a_{j+1} - l) e^{ij\pi} f_{a_1}^\dagger \dots f_{a_j}^\dagger f_l^\dagger f_{a_{j+1}}^\dagger \dots f_{a_m}^\dagger f_{a_{m+1}} \dots f_{a_{2m-1}} f_N \end{aligned} \quad (11)$$

2. operator ordering :  $f_{a_1}^\dagger \dots f_{a_m}^\dagger f_{a_{m+1}} \dots f_{a_{2m-1}} f_N f_l^\dagger f_k^\dagger :$  for  $k > l$

$$\begin{aligned} & : f_{a_1}^\dagger \dots f_{a_m}^\dagger f_{a_{m+1}} \dots f_{a_{2m-1}} f_N f_l^\dagger f_k^\dagger : \\ & = \sum_{j=1}^m \sum_{q=m+1}^{2m-1} \Theta(a_j - l) \Theta(k - a_q) \delta_{a_j, l} \delta_{a_q, k} f_{a_1}^\dagger \dots f_{a_{j-1}}^\dagger f_k^\dagger f_{a_{j+1}}^\dagger \dots f_{a_m}^\dagger f_{a_{m+1}} \dots f_{a_{q-1}} f_l f_{a_{q+1}} \dots f_{a_{2m-1}} f_N \end{aligned} \quad (12)$$

$$\begin{aligned}
& \times \prod_{i=1}^m (1 - \delta_{a_i, l})(1 - \delta_{a_i, k}) \\
& + \sum_{j=1}^m \Theta(l - a_j) \Theta(k - a_j) \delta_{a_j, l} f_{a_1}^\dagger \cdots f_{a_{j-1}}^\dagger f_k^\dagger f_{a_{j+1}}^\dagger \cdots f_{a_m}^\dagger f_{a_{m+1}} \cdots f_{a_{2m-1}} f_N \prod_{i=1}^m (1 - \delta_{a_i, k}) \\
& + \sum_{j=1}^m \Theta(k - a_j) \Theta(a_j - l) \delta_{a_j, k} f_{a_1}^\dagger \cdots f_{a_{j-1}}^\dagger f_l^\dagger f_{a_{j+1}}^\dagger \cdots f_{a_m}^\dagger f_{a_{m+1}} \cdots f_{a_{2m-1}} f_N \prod_{i=1}^m (1 - \delta_{a_i, l}) \\
& + \sum_{j=m+1}^{2m-1} \Theta(l - a_j) \Theta(k - a_j) \delta_{a_j, k} f_{a_1}^\dagger \cdots f_{a_m}^\dagger f_{a_{m+1}} \cdots f_{a_{j-1}} f_l^\dagger f_{a_{j+1}} \cdots f_{a_{2m-1}} f_N \prod_{i=1}^m (1 - \delta_{a_i, l})(1 - \delta_{a_i, k}) \\
& + \sum_{j=m+1}^{2m-1} \Theta(k - a_j) \Theta(a_j - l) \delta_{a_j, l} f_{a_1}^\dagger \cdots f_{a_m}^\dagger f_{a_{m+1}} \cdots f_{a_{j-1}} f_k^\dagger f_{a_{j+1}} \cdots f_{a_{2m-1}} f_N \prod_{i=1}^m (1 - \delta_{a_i, k}) \\
& + \Theta(l - N) \delta_{N, k} f_{a_1}^\dagger \cdots f_{a_m}^\dagger f_{a_{m+1}} \cdots f_{a_{2m-1}} f_l^\dagger f_N \prod_{i=1}^m (1 - \delta_{a_i, k}) \\
& + \Theta(k - N) \delta_{N, l} f_{a_1}^\dagger \cdots f_{a_m}^\dagger f_{a_{m+1}} \cdots f_{a_{2m-1}} f_k^\dagger f_N \prod_{i=1}^m (1 - \delta_{a_i, l}) \tag{13}
\end{aligned}$$

With the above operator ordering expressions for fermionic strings given by eq(11) and eq(13), we can represent the residual expression of eq(10) in its tensor factorized form as,

$$\begin{aligned}
r_{a_1, \dots, a_{2p}}^{(j)} &= h_{a_1, \dots, a_{2p}}^{(j)} + \sum_{a_{2m}, \dots, a_p, k, l} C_{a_{2m}, \dots, a_{2p+1}} A_{a_{2m}, k}^{1, (j)} \cdots A_{a_{2p+1}, k}^{2p+1, (j)} B_{a_{2m}, l}^{2m, (j)} \cdots B_{a_{2p+1}, l}^{2p+1, (j)} \cdots B_{a_1, l}^{1, (j)} \\
&+ \sum_{a_{2p+1}, \dots, \max(a_{2l-1}, 2r-1, 2q-1)} D_{a_1, \dots, a_{2k-1}, a_{2k-1}, \dots, a_{2p-1}} A_{a_1, l}^{1, (j)} \cdots A_{a_{2k-1}, l}^{2k-1, (j)} A_{a_{2k}, l}^{2k, (j)} \cdots A_{a_{2l-1}, l}^{2l-1, (j)} \\
&\times B_{N, q}^{N, (j)} B_{a_{2r-1}, w}^{2r-1, (j)} \cdots B_{a_{2k}, w}^{2k, (j)} B_{a_{2k-1}, w}^{2k-1, (j)} \cdots B_{a_1, w}^{1, (j)} A_{a_1, s}^{1, (j)} \cdots A_{a_{2k-1}, s}^{2k-1, (j)} A_{a_{2k}, s}^{2k, (j)} \cdots A_{a_{2q-1}, s}^{2q-1, (j)} . \tag{14}
\end{aligned}$$

We now give an example of how the components of the residual expression arising from  $\eta PHP$  for the first downfolding step can be computed. From eq.(11) we can find that the fermionic operator  $f_a^\dagger$  can match with one of the indices in the set of the fermionic operators corresponding to  $\eta_{(N)}$ . This will lead to the following term,

$$\eta PHP \longrightarrow \sum_{a_1, \dots, a_{2m-1}, a} h_{ab}^{1, (N)} A_{a_1 k}^1 \cdots A_{a_{2m-1} k}^{2m-1} E_{a_1 \dots a_m}^+ E_{a_{m+1} \dots a_{2m-1}}^- f_N f_a^\dagger f_b , \tag{15}$$

$$\begin{aligned}
&= \sum_{a'_i s, a \neq a_j} A_{a_1 k}^1 \cdots A_{a_{j-1} k}^{j-1} A_{a_{j+1} k}^{j+1} \cdots A_{a_{2m-1} k}^{2m-1} \sum_{p, a, a_j} \delta_{a_j, a} (-1)^{p+1} \theta(a_p - b) \theta(b - a_{p-1}) A_{a_j, k}^j h_{a, b}^{1, (N)} E_{a_1 \dots a_m}^+ \\
&\quad E_{a_{m+1} \dots a_{j-1} a_{j+1} \dots a_{p-1} b a_p \dots a_{2m-1}}^- f_N
\end{aligned} \tag{16}$$

Similarly for the two-electron Hamiltonian terms, the contribution of the residuals in  $\eta PHP$  is given by,

$$\begin{aligned}
\eta PHP &\longrightarrow h_{abcd}^{2, (N)} A_{a_1 k}^1 \cdots A_{a_{2m-1} k}^{2m-1} E_{a_1 \dots a_m}^+ \\
&\quad \sum_{ab, a_j, a_k} \delta_{a, a_j} \delta_{b, a_k} h_{abcd}^2 \sum_k A_{a_1 k}^1 \cdots A_{a_{2m-1} k}^{2m-1} \rightarrow \\
&\quad \sum_k A_{a_1 k}^1 \cdots A_{a_{j-1}, k}^{j-1} A_{a_{j+1}, k}^{j+1} \cdots A_{a_{s-1}, k}^{s-1} A_{a_{s+1}, k}^{s+1} \cdots A_{a_{2m-1} k}^{2m-1} \sum_a A_{a, k}^j B_{a, l}^1 \sum_b A_{b, l}^s B_{b, l}^1 B_{p, l}^2 \sum_t B_{c, t}^1 B_{d, t}^1 B_{p, t}^2
\end{aligned} \tag{17}$$

From above, we find that in the tensor factorized representation for downfolding, all contractions involves matrices. And the computational complexity of computing the residual for each downfolding step scales as,

$$O(N^3) \tag{18}$$

At the end of the first downfolding recursion step, when the transformation parameters are determined, the form of the new decoupled block-Hamiltonian is given by,

$$\begin{aligned}
&P_{(N)} S_{(N)}^{-1} H_{(N)} S_{(N)} P_{(N)} = P_{(N)} H_{(N)} P_{(N)} + P_{(N)} H_{(N)} Q_{(N)} \eta_{(N)} \\
&= \sum_{m=1}^{N_e} \sum_{\substack{a_1 \leq \dots \leq a_m, \\ a_{m+1} \leq \dots a_j \dots \leq a_{2m-1} < N}} \delta_{a, a_j} A_{a_1 k}^1 \cdots A_{a_m k}^m A_{a_{m+1} k}^{m+1} \cdots A_{a_{j-1} k}^{j-1} A_{a_{j+1} k}^{j+1} \cdots A_{a_{2m-1} k}^{2m-1} h_{ab} \\
&\times f_{a_1}^\dagger \cdots f_{a_m}^\dagger f_{a_{m+1}} \cdots f_{a_{2m-1}} f_b \\
&+ \sum_{m=1}^{N_e} \sum_{\substack{a_1 \leq \dots \leq a_m, \\ a_{m+1} \leq \dots a_j \dots a_l \leq a_{2m-1} < N}} \delta_{a, a_j} \delta_{b, a_l} A_{a_1 k}^1 \cdots A_{a_m k}^m A_{a_{m+1} k}^{m+1} \cdots A_{a_{j-1} k}^{j-1} A_{a_{j+1} k}^{j+1} \cdots A_{a_{l-1} k}^{l-1} A_{a_{l+1} k}^{l+1} \cdots A_{a_{2m-1} k}^{2m-1} \\
&\times B_{a_q}^1 B_{b_q}^2 B_{p_q}^3 B_{c_s}^1 B_{d_s}^2 B_{p_s}^3 f_{a_1}^\dagger \cdots f_{a_m}^\dagger f_{a_{m+1}} \cdots f_{a_{2m-1}} f_c f_d
\end{aligned} \tag{19}$$

From here, we find that the n-cluster interaction terms in the Hamiltonian get renormalized in their tensor factorized representations as,

$$\begin{aligned} \tilde{h}_{a_1 \dots a_{2m-1}, c, d} &= \sum_{k, q, s} A_{a_1 k}^1 \dots A_{a_m k}^m A_{a_{m+1} k}^{m+1} \dots A_{a_{j-1} k}^{j-1} A_{a_{j+1} k}^{j+1} \dots A_{a_{l-1} k}^{l-1} A_{a_{l+1} k}^{l+1} \dots A_{a_{2m-1} k}^{2m-1} \\ &\times B_{a_j q}^1 B_{a_l q}^2 B_{pq}^3 B_{cs}^1 B_{ds}^2 B_{ps}^3 \end{aligned} \quad (20)$$

For all these cases, the general diagram representing the tensor operations is given in fig.1

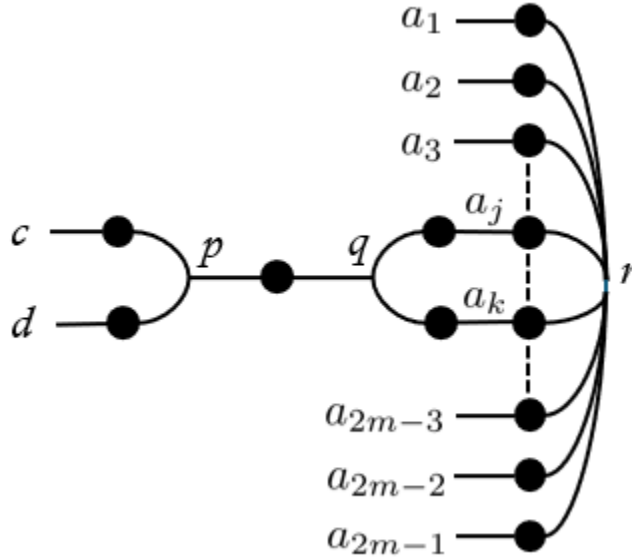


Figure 1: This figure represents the fusion of the one body term  $h^1$  having two-rank tensor  $h_{ab}$  with  $\eta$  for the residual contribution in Bloch equation from  $\eta PHP$

## 4 Case Study: Multireference Downfolding with Singles and Paired Doubles

In this section we will discuss a specific case of recursive Hamiltonian downfolding with singles and paired doubles cluster amplitudes. We replace the form for  $\eta_{(N)}$  given in eq.(7), into the Bloch equation (eq.(6)) and normal-order the fermionic operators comprising the Bloch equation. For the Bloch equation to be satisfied, the coefficients of the independent

N.O. fermionic terms must vanish: singles excitation - ( $i\sigma \rightarrow N\sigma$ ), doubles excitations - ( $(k\sigma, l\sigma') \rightarrow (j\sigma', N\sigma)$ ), paired doubles excitations- ( $(i \uparrow, j \downarrow) \rightarrow (N \downarrow, N \uparrow)$ ), triples excitations ( $(l'\sigma'', k'\sigma', j'\sigma) \rightarrow (j\sigma, k\sigma', N\sigma'')$ ), quadruples excitations ( $(l'\sigma''', k'\sigma'', j'\sigma', i'\sigma) \rightarrow (i\sigma, j\sigma', k\sigma'', N\sigma''')$ ). This calculation is presented in the appendices (A-C.1). As a result, the Bloch equation leads to the following multireference downfolding equations:

$$\mathbf{A}^{(N),\sigma} = \mathbf{t}^{1,\sigma} \cdot \mathbf{h}_{\mathbf{N}}^{1,\sigma} \mathbf{t}^{1,\sigma} + \mathbf{t}^{1,\sigma} \cdot \mathbf{h}^{1,\sigma} - h_{NN}^{1,\sigma} \mathbf{t}^{1,\sigma} - \mathbf{h}_{\mathbf{N}}^{1,\sigma} \quad (21)$$

$$\begin{aligned} \mathbf{B}^{(N),\sigma\nu} &= \left( \mathbf{t}^{1,\sigma} \otimes \mathbf{h}_{\mathbf{N}}^{1,\nu} \otimes \mathbf{t}^{1,\nu} \right)_{312} + \mathbf{t}^{1,\sigma} \cdot \left( \mathbf{h}_{\mathbf{N}}^{2,\sigma\nu} \otimes \mathbf{t}^{1,\sigma} + \left( \mathbf{h}_{\mathbf{N}}^{2,\sigma\nu} \otimes \mathbf{t}^{1,\sigma} \right)_{2143} \right. \\ &\quad \left. + \delta_{\nu,-\sigma} \mathbf{h}_{\mathbf{N}\mathbf{N}}^2 \otimes \mathbf{t}^2 + \mathbf{h}^{2,\sigma\nu} + \left( \mathbf{h}^{2,\sigma\nu} \right)_{2143} \right) - \delta_{\nu,-\sigma} \left( \delta_{\sigma\downarrow} \mathbf{h}_{\mathbf{N}}^{1,\sigma} \otimes \mathbf{t}^2 + \delta_{\sigma\uparrow} \mathbf{h}_{\mathbf{N}}^{1,\sigma} \otimes (\mathbf{t}^2)_{21} \right) - \mathbf{h}_{\mathbf{N}}^{2,\sigma\nu} \end{aligned} \quad (22)$$

$$\begin{aligned} \mathbf{C}^{(N)} &= \mathbf{t}^2 \cdot \left( \mathbf{h}_{\mathbf{N}}^{1,\uparrow} \otimes \mathbf{t}^{1,\uparrow} + \mathbf{h}^{1,\uparrow} \right) - \mathbf{h}_{\mathbf{N}}^{1,\downarrow} \otimes \mathbf{t}^{1,\uparrow} \\ &\quad + \left( (\mathbf{t}^2)_{21} \cdot \left( \mathbf{h}_{\mathbf{N}}^{1,\downarrow} \otimes \mathbf{t}^{1,\downarrow} + \mathbf{h}^{1,\downarrow} \right) \right)_{21} - \mathbf{h}_{\mathbf{N}}^{1,\uparrow} \otimes \mathbf{t}^{1,\downarrow} + \mathbf{t}^2 \cdot \left( \mathbf{h}_{\mathbf{N}}^{2,\uparrow\downarrow} \otimes \mathbf{t}^{1,\uparrow} + \left( \mathbf{h}_{\mathbf{N}}^{2,\uparrow\downarrow} \otimes \mathbf{t}^{1,\downarrow} \right)_{2143} \right. \\ &\quad \left. + \mathbf{h}^{2,\uparrow\downarrow} + \left( \mathbf{h}^{2,\uparrow\downarrow} \right)_{2143} + \mathbf{h}_{\mathbf{N}\mathbf{N}}^2 \otimes \mathbf{t}^2 \right) - h_{NNNN}^2 \mathbf{t}^2 - \mathbf{h}_{\mathbf{N}\mathbf{N}}^2 - (h_{NN}^{1,\downarrow} + h_{NN}^{1,\uparrow}) \mathbf{t}^2 \end{aligned} \quad (23)$$

$$\begin{aligned} \mathbf{D}^{(N),\sigma} &= \mathbf{t}^2 \otimes \left( \mathbf{h}_{\mathbf{N}}^{1,\sigma} \otimes \mathbf{t}^{1,\sigma} + \mathbf{h}^{1,\sigma} \right) \\ &\quad + (\mathbf{t}^2 \cdot \mathbf{h}_{\mathbf{N}}^{2,\uparrow\sigma} \otimes \mathbf{t}^{1,\uparrow})_{3124} + ((\mathbf{t}^2)_{21} \cdot \mathbf{h}_{\mathbf{N}}^{2,\downarrow\sigma} \otimes \mathbf{t}^{1,\downarrow})_{4123} + ((\mathbf{t}^2)_{21} \cdot (\mathbf{h}_{\mathbf{N}}^{2,\sigma\downarrow})_{2134} \otimes \mathbf{t}^{1,\uparrow})_{4132} \\ &\quad + (\mathbf{t}^2 \cdot (\mathbf{h}_{\mathbf{N}}^{2,\sigma\uparrow})_{2134} \otimes \mathbf{t}^{1,\uparrow})_{3142} + \delta_{\sigma\downarrow} \mathbf{t}^2 \otimes \mathbf{h}_{\mathbf{N}\mathbf{N}}^2 \otimes \mathbf{t}^2 - \delta_{\sigma\uparrow} (\mathbf{t}^2)_{21} \otimes \mathbf{h}_{\mathbf{N}\mathbf{N}}^2 \otimes \mathbf{t}^2 + \left( \mathbf{t}^2 \otimes \mathbf{h}^{2,\uparrow\sigma} \right)_{3124} \\ &\quad + \left( \mathbf{t}^2 \otimes (\mathbf{h}^{2,\sigma\uparrow})_{2134} \right)_{3124} + ((\mathbf{t}^2)_{21} \otimes \mathbf{h}^{2,\downarrow\sigma})_{4123} + ((\mathbf{t}^2)_{21} \otimes (\mathbf{h}^{2,\sigma\downarrow})_{2134})_{4132} \\ &\quad - (\mathbf{h}_{\mathbf{N}}^{2,\uparrow\sigma} \otimes \mathbf{t}^{1,\downarrow})_{1243} - (\mathbf{h}_{\mathbf{N}}^{2,\uparrow\sigma} \otimes \mathbf{t}^{1,\downarrow})_{1234} - \mathbf{h}^{1,\sigma} \otimes \mathbf{t}^2 \end{aligned} \quad (24)$$

$$\mathbf{E}^{(N),\sigma\nu} = \mathbf{t}^{1,\sigma} \otimes \mathbf{h}_{\mathbf{N}}^{2,\mu\nu} \otimes \mathbf{t}^{1,\mu} + \delta_{\sigma,-\nu} \mathbf{h}_{\mathbf{N}\mathbf{N}}^2 \otimes \mathbf{t}^2 \otimes \mathbf{t}^{1,\sigma} - \delta_{\sigma\downarrow} (\mathbf{h}_{\mathbf{N}}^{2,\uparrow\nu} \otimes \mathbf{t}^2)_{32154} - \delta_{\sigma\downarrow} (\mathbf{h}_{\mathbf{N}}^{2,\downarrow\nu} \otimes \mathbf{t}^2)_{32154} \quad (25)$$

$$\mathbf{F}^{(N),\sigma\nu\rho} = \mathbf{h}_{\mathbf{N}}^{2,\sigma\mu} \otimes \mathbf{t}^{1,\sigma} \otimes \mathbf{t}^2 + \mathbf{h}_{\mathbf{N}\mathbf{N}}^2 \otimes \mathbf{t}^2 \otimes \mathbf{t}^2 \quad (26)$$

Here  $\mathbf{t}^{1,\sigma}$  is a vector of length,  $n_1 = (N - 1)$ , comprising of singles excitation amplitudes.  $\mathbf{t}_{\mathbf{N}}^{2,\sigma\nu}$  is a  $(N - 1)^2$ -length vector comprised of doubles excitation amplitudes,  $(\mathbf{t}_{\mathbf{N}}^2)_{ab} = t_{ab}^{2,(N)}$ . The vectors  $\mathbf{h}_{\mathbf{N}}^1$ ,  $\mathbf{h}_{\mathbf{N}}^2$  of dimensions  $(N - 1)$  and  $(N - 1)^3$  comprise of one-electron tensors,  $\mathbf{h}_{\mathbf{N}_i}^1 = h_i^{1,(N)}$  and two-electron tensors,  $(\mathbf{h}_{\mathbf{N}}^2)_{ijk} = h_{Nijk}^{2,(N)}$ , coupling the Nth molecular



orbital to the other molecular orbitals.  $\mathbf{h}_{\mathbf{N}\mathbf{N}}^2$  comprises the two-electron tensor contributions ( $(\mathbf{h}_{\mathbf{N}\mathbf{N}}^2)_{ij} = h_{\mathbf{N}\mathbf{N}ij}^2$ ) that couple all the paired excitations of the Nth MO with other spin orbitals. Here  $\mathbf{K} \otimes \mathbf{L}$  denotes the tensor-product ( $\otimes$ ) of two vectors whose elements are  $(\mathbf{K} \otimes \mathbf{L})_{ij} = K_i L_j$ . In the above expressions  $(\mathbf{h}^{2,\sigma\nu})_{abcd}$  represents a permutation of indexes of the tensor, for e.g.  $((\mathbf{h}^{2,\sigma\nu})_{3124})_{ijkl} = (\mathbf{h}^{2,\sigma\nu})_{kijl}$ , and  $(\cdot)$  represents tensor contraction. These downfolding equations (eq.(21)-(24)) correspond to a rectangular system of multi-variable quadratic polynomials. There are  $m = 8N^6 + 8N^5 + 2N^4 + 4N^3 + N^2 + 1$  polynomial equations in  $n = N^3 + N^2 + 2(N - 1)$  parameters.

### *Computational complexity of the multireference downfolding technique*

The term  $t_{ijk}^2 h_{abcN}^2 t_{abc}^2$  in the equation set eq.(26) has the highest cost  $O(N^7)$  of being generated, if the full the ERI in MO representation is used. On the other hand we can compress the ERI via tensor factorization,  $h_{abcN}^2 = \sum_{pq} X_{ap} X_{bp} M_{pq} X_{cq} X_{Nq}$ , using convex polyadic decomposition or perform interpolative-separable density fitting.<sup>9,70</sup> Similarly we can do tensor factorization of  $t_{abc}^2 = \sum_k A_{ak} B_{bk} C_{ck}$ . Then the compute cost will reduce to  $O(N_{THC} N^2)$ .

### *Hamiltonian RG flow from Downfolding*

The similarity transformation  $S_{(N)}$  on the starting Hamiltonian  $H_{(N)} = H$  leads to a renormalized Hamiltonian  $H_{(N-1)}$  in the primary space  $P_{(N)}$  with a self-similar form,

$$\begin{aligned}
H_{(N-1)} &= P_{(N)} S_{(N)}^{-1} H_{(N)} S_{(N)} P_{(N)} \\
&= P_{(N)} H_{(N)} P_{(N)} + P_{(N)} H_{(N)} Q_{(N)} \eta_{(N)} \\
&= (1 - \hat{n}_{N\uparrow})(1 - \hat{n}_{N\downarrow}) \left[ \sum_{ij=1,\sigma}^{N-1} h_{ij}^{1,(N-1)} f_{i\sigma}^\dagger f_{j\sigma} + \sum_{\substack{ijkl=1, \\ \sigma\sigma'}}^{N-1} h_{ijkl}^{2,(N-1)} f_{i\sigma}^\dagger f_{j\sigma'}^\dagger f_{k\sigma'} f_{l\sigma} \right] \quad (27)
\end{aligned}$$

The one and two-electron tensors comprising the renormalized Hamiltonian  $H_{(N-1)}$  can be written in terms of the one and two-electron tensors of  $H_{(N)}$  (eq(1)) and the amplitudes

$t^{1,(N)}$  and  $t^{2,(N)}$  of the generator  $\eta$  (eq(7)).

$$h_{ij}^{1,\sigma,(N-1)} = h_{ij}^{1,\sigma,(N)} + h_{iN}^{1,\sigma,(N)} t_j^{1,\sigma,(N)} \quad (28)$$

$$h_{ijkl}^{2,\sigma\nu,(N-1)} = h_{ijkl}^{2,\sigma\nu,(N)} + h_{ijkN}^{2,\sigma\nu,(N)} t_l^{1,\sigma,(N)} + \delta_{\nu,-\sigma} h_{ijNN}^{2,(N)} t_{kl}^{2,(N)} + h_{iN}^{1,(N)} t_{jkl}^{2,(N)} \quad (29)$$

The effect of downfolding the electronic correlations coupling  $Q_{(N)}$  to  $P_{(N)}$  was to renormalize the one-electron (eq.(28)) and two-electron interaction tensor contributions (eq.(29)) in the primary space using the excitation amplitudes of the generator  $\eta$  (eq.(7)). From the RG flow equation of the Hamiltonian  $H_{(N-1)}$  (eq.(27)) we make two important observations. Firstly, the indices in the one and two-electron tensors ( $h_{ij}^{1,(N-1)}, h_{ijkl}^{2,(N-1)}$ ) runs over MO from 1 to N-1 i.e. leaving out the Nth MO. The Nth orbital gets decoupled with only an overall diagonal contribution. This remains true even if  $N \in \mathcal{C}$  where  $P_{(N)} = \hat{n}_\uparrow \hat{n}_\downarrow$  and for  $N \in \mathcal{A}$  :  $P_{(N)} = \hat{n}_\uparrow \hat{n}_\downarrow$  or  $(1 - \hat{n}_\uparrow)(1 - \hat{n}_\downarrow)$ . However, in that case, the energetic contribution from the diagonal term may change. Secondly, no new many-body excitation clusters are created. This results from the choice of  $\eta$  where paired doubles at the Nth MO get excited  $t_{ij}^{2,(N)}$ . The choice of  $\eta$  automatically terminates the hierarchy of the three-particle or higher-order clusters. Such a description allows the self-similar representation of the Hamiltonian to prevail. The next set of RG equations that describes the Hamiltonian coefficients for a system of  $(N - 2)$  MOs are derived from the  $(N - 1)$  MOs (eq. (28), eq. (29)).

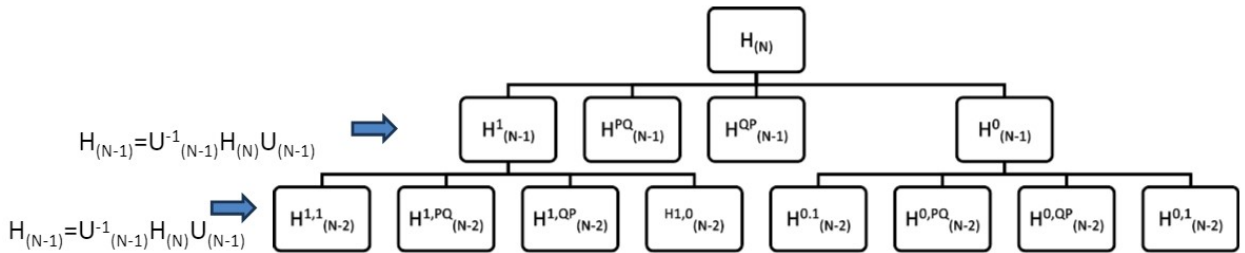


Figure 2: Hamiltonian Downfolding: The scheme shows decoupling of molecular orbitals. At each step the Hamiltonian is mapped to a direct sum of reduced dimensional blocks. When  $H_{(N)}$  undergoes the decoupling

*Flow towards diagonalization*

After  $s$  downfolding steps, we obtain a reduced Hamiltonian,

$$\begin{aligned}
H_{(s)} = & \prod_{\substack{a=N, \\ \sigma=\uparrow,\downarrow}}^{N-p} (1 - \hat{n}_{a\sigma}) \prod_{\substack{a=N-p-1, \\ \sigma=\uparrow,\downarrow}}^{N-s+1} \hat{n}_{a\sigma} \left[ \sum_{ij=1,\sigma}^{N-s} h_{ij}^{1,(N-s)} f_{i\sigma}^\dagger f_{j\sigma} \right. \\
& + \left. \sum_{l=N-p}^{N-s} h_{l,l,l,l}^{2,\uparrow,\downarrow,(l)} + \sum_{l=N-p,\sigma}^{N-s} h_{l,l}^{1,\sigma,(l)} + \sum_{\substack{ijkl=1, \\ \sigma\sigma'}}^{N-s} h_{ijkl}^{2,(N-s)} f_{i\sigma}^\dagger f_{j\sigma'}^\dagger f_{k\sigma'} f_{l\sigma} \right]. \quad (30)
\end{aligned}$$

## 5 Case Study: Unitary Multireference Downfolding with Singles and Doubles

In this section we will look into the formalism for recursive Hamiltonian downfolding with singles and doubles excitations. We will study the generation of unitary transformation operators corresponding to the similarity transformation operators used in each downfolding step. This will lead to a series of downfolding transformations that preserves the hermiticity of the Hamiltonian in the reduced subspace. A detailed step-wise description is presented below.

### *Step-1*

The electronic Hamiltonian in MO basis with  $N$  spin orbitals is constructed as,

$$H_{(N)} = \sum_{pq,\sigma} h_{pq}^{1,\sigma,(N)} f_{p\sigma}^\dagger f_{q\sigma} + \sum_{pqrs,\sigma\sigma'} h_{pqrs}^{2,\sigma\sigma',(N)} f_{p\sigma}^\dagger f_{q\sigma'}^\dagger f_{r\sigma'} f_{s\sigma} \quad (31)$$

Here,  $f_{i\sigma}^\dagger$  is a creation operator for  $i^{th}$  molecular orbital with spin state  $\sigma$ . Similarly,  $f_{i\sigma}$  is an annihilation operator for  $i^{th}$  molecular orbital with spin state  $\sigma$ . All dummy indices corresponding to the orbital numbers are denoted by English letters whereas spin states are denoted by greek letters. In this section, orbital indices denoted by p,q,r,s... have been considered to span over all spin orbitals. Whereas, indices denoted by a,b,c...i,j,k,l...m,n span over all spin orbitals except the outermost orbital, the  $N^{th}$  orbital here.

*Step-2*

We partition the many body Hilbert space into a model space and its complement.<sup>37</sup> Our iterative downfolding needs us to decouple only the outermost orbital at a time. So we define our two subspace projection operators,  $P_N$  and  $Q_N$ , as,

$$P_{(N)} = (1 - \hat{n}_{N\uparrow})(1 - \hat{n}_{N\downarrow}) \quad (32)$$

$$Q_{(N)} = \hat{n}_{N\uparrow} + \hat{n}_{N\downarrow} + \hat{n}_{N\uparrow}\hat{n}_{N\downarrow} \quad (33)$$

where  $\hat{n}_{k\sigma} = f_{k\sigma}^\dagger f_{k\sigma}$  and  $P_{(N)} + Q_{(N)} = I^{\otimes 2N}$ . The P-space projection removes contributions from the  $N^{th}$  molecular orbital.

*Step-3*

At first, we construct a non-Hermitian generator  $\eta^{(N)}$  for a  $N^{th}$  MO decoupling similarity transformation, given by,

$$\eta^{(N)} = \eta^{1,(N)} + \eta^{2,(N)} + \eta^{3,(N)} \quad (34)$$

where,

$$\eta^{1,(N)} = \sum_{i,\sigma} \eta_{i,\sigma}^{1,(N)} = \sum_{i,\sigma} t_{i,\sigma}^{1,(N)} (1 - \hat{n}_{i-\sigma})(1 - \hat{n}_{N-\sigma}) f_{N\sigma}^\dagger f_{i\sigma} \quad (35)$$

$$\eta^{2,(N)} = \sum_{ijk,\sigma\sigma'} \eta_{ijk,\sigma\sigma'}^{2,(N)} = \sum_{ijk,\sigma\sigma'} t_{ijk,\sigma\sigma'}^{2,(N)} (1 - \hat{n}_{N-\sigma}) f_{N\sigma}^\dagger f_{i\sigma'}^\dagger f_{j\sigma'} f_{k\sigma} \quad (36)$$

$$\eta^{3,(N)} = \sum_{ij} \eta_{ij}^{3,(N)} = \sum_{ij} t_{ij}^{3,(N)} f_{N\uparrow}^\dagger f_{N\downarrow}^\dagger f_{i\downarrow} f_{j\uparrow} \quad (37)$$

This generator accounts for all possible singles and doubles excitations involving the  $N^{th}$  molecular orbital. Here,  $t_{i,\sigma}^{1,(N)}$ ,  $t_{ijk,\sigma\sigma'}^{2,(N)}$  and  $t_{ij}^{3,(N)}$  denote singles, mixed-doubles (excitations to only one  $N^{th}$  spin orbital) and paired-doubles (excitations to both  $N^{th}$  spin orbitals) ex-

citation amplitudes respectively. Here we will see that  $\eta^{(N)}$  is nilpotent with degree 2, i.e,  $(\eta^{(N)})^2 = 0, (\eta^{(N)})^3 = 0 \dots$ , and the polynomial expansion of the similarity transformation  $S^{(N)} = e^{\eta^{(N)}}$  naturally terminates at  $O(\eta^{(N)})$  with  $S^{(N)} = 1 + \eta^{(N)}$ .

*Step-4*

This choice of generator allows for a decomposition of the similarity transformation  $S^{(N)}$  into a product of three separate similarity transformations,  $S^{1,(N)}, S^{2,(N)}, S^{3,(N)}$  for singles, mixed-doubles and paired-doubles excitations, respectively, given by the generators,  $\eta^{1,(N)}, \eta^{2,(N)}$  and  $\eta^{3,(N)}$  as,

$$S^{(N)} = e^{(\eta^{1,(N)} + \eta^{2,(N)} + \eta^{3,(N)})} = e^{\eta^{1,(N)}} e^{\eta^{2,(N)}} e^{\eta^{3,(N)}} = S^{1,(N)} S^{2,(N)} S^{3,(N)} \quad (38)$$

This is due to the set of commutation relations,

$$[\eta^{1,(N)}, \eta^{2,(N)}] = [\eta^{2,(N)}, \eta^{3,(N)}] = [\eta^{3,(N)}, \eta^{1,(N)}] = 0 \quad (39)$$

Again, the individual similarity transformations,  $\{S^{i,(N)}\}$  for  $i \in \{1, 2, 3\}$ , can be written as products of similarity transformations given by ,

$$S^{1,(N)} = e^{\eta^{1,(N)}} = e^{\sum_{i,\sigma} \eta_{i,\sigma}^{1,(N)}} = \prod_{i,\sigma} e^{\eta_{i,\sigma}^{1,(N)}} = \prod_{i,\sigma} S_{i,\sigma}^{1,(N)} \quad (40)$$

$$S^{2,(N)} = e^{\eta^{2,(N)}} = e^{\sum_{ijk,\sigma\sigma'} \eta_{ijk,\sigma\sigma'}^{2,(N)}} = \prod_{ijk,\sigma\sigma'} e^{\eta_{ijk,\sigma\sigma'}^{2,(N)}} = \prod_{ijk,\sigma\sigma'} S_{ijk,\sigma\sigma'}^{2,(N)} \quad (41)$$

$$S^{3,(N)} = e^{\eta^{3,(N)}} = e^{\sum_{ij} \eta_{ij}^{3,(N)}} = \prod_{ij} e^{\eta_{ij}^{3,(N)}} = \prod_{ij} S_{ij}^{3,(N)} \quad (42)$$

The above decompositions were made possible due to the following commutation relations,

$$\left[ \eta_{i,\sigma}^{1,(N)}, \eta_{j,\sigma'}^{1,(N)} \right] = 0 \quad \forall i, j, \sigma, \sigma' \quad (43)$$

$$\left[ \eta_{ijk,\sigma\sigma'}^{2,(N)}, \eta_{abc,\mu\mu'}^{2,(N)} \right] = 0 \quad \forall i, j, k, a, b, c, \sigma, \sigma', \mu, \mu' \quad (44)$$

$$\left[ \eta_{ij}^{3,(N)}, \eta_{ab}^{3,(N)} \right] = 0 \quad \forall i, j, a, b \quad (45)$$

So, the similarity transformation that decouples the  $N^{th}$  Molecular orbital and gives rise to a one-step downfolded effective Hamiltonian given by,

$$H_{(N-1)} = (S^{(N)})^{-1} H_{(N)} S^{(N)} \quad (46)$$

$$= \prod_{ijklmn, \mu\sigma\sigma'} e^{-\eta_{mn}^{3,(N)}} e^{-\eta_{jkl, \sigma\sigma'}^{2,(N)}} e^{-\eta_{i, \mu}^{1,(N)}} H_{(N)} e^{\eta_{i, \mu}^{1,(N)}} e^{\eta_{jkl, \sigma\sigma'}^{2,(N)}} e^{\eta_{mn}^{3,(N)}} \quad (47)$$

### Step-5

The effective Hamiltonian is non-Hermitian after undergoing the similarity transformation. The Hermitian counterpart can be formulated by constructing analogous unitary transformations from the generators of the similarity transformation. The Unitary operators for the similarity transformation generators,  $\eta_{i, \sigma}^{1,(N)}$ ,  $\eta_{ijk, \sigma\sigma'}^{2,(N)}$  and  $\eta_{ij}^{3,(N)}$ , can be written as,<sup>71</sup>

$$U_{i, \sigma}^{1,(N)} = e^{\operatorname{arctanh}\left(\eta_{i, \sigma}^{1,(N)} - \left(\eta_{i, \sigma}^{1,(N)}\right)^\dagger\right)} \quad (48)$$

$$U_{ijk, \sigma\sigma'}^{2,(N)} = e^{\operatorname{arctanh}\left(\eta_{ijk, \sigma\sigma'}^{2,(N)} - \left(\eta_{ijk, \sigma\sigma'}^{2,(N)}\right)^\dagger\right)} \quad (49)$$

$$U_{ij}^{3,(N)} = e^{\operatorname{arctanh}\left(\eta_{ij}^{3,(N)} - \left(\eta_{ij}^{3,(N)}\right)^\dagger\right)} \quad (50)$$

The generators satisfy the conditions:

$$Q \eta_{i\sigma}^{1,(N)} P = \eta_{i\sigma}^{1,(N)} \quad (51)$$

$$P \eta_{i\sigma}^{1,(N)} P = P \eta_{i\sigma}^{1,(N)} Q = Q \eta_{i\sigma}^{1,(N)} Q = 0 \quad (52)$$

$$Q \eta_{ijk, \sigma\sigma'}^{2,(N)} P = \eta_{ijk, \sigma\sigma'}^{2,(N)} \quad (53)$$

$$P \eta_{ijk, \sigma\sigma'}^{2,(N)} P = P \eta_{ijk, \sigma\sigma'}^{2,(N)} Q = Q \eta_{ijk, \sigma\sigma'}^{2,(N)} Q = 0 \quad (54)$$

$$Q \eta_{ij}^{3,(N)} P = \eta_{ij}^{3,(N)} \quad (55)$$

$$P\eta_{ij}^{3,(N)}P = P\eta_{ij}^{3,(N)}Q = Q\eta_{ij}^{3,(N)}Q = 0 \quad (56)$$

$$\left(\eta_{i\sigma}^{1,(N)}\right)^2 = \left(\eta_{ijk,\sigma\sigma'}^{2,(N)}\right)^2 = \left(\eta_{ij}^{3,(N)}\right)^2 = 0 \quad (57)$$

which leads to a series of simplifications, given by,

$$U_{i\sigma}^{1,(N)} = \frac{1 + \eta_{i\sigma}^{1,(N)} - \left(\eta_{i\sigma}^{1,(N)}\right)^\dagger}{\left(1 + \eta_{i\sigma}^{1,(N)} \left(\eta_{i\sigma}^{1,(N)}\right)^\dagger + \left(\eta_{i\sigma}^{1,(N)}\right)^\dagger \eta_{i\sigma}^{1,(N)}\right)^{1/2}} \quad (58)$$

$$U_{ijk,\sigma\sigma'}^{2,(N)} = \frac{1 + \eta_{ijk,\sigma\sigma'}^{2,(N)} - \left(\eta_{ijk,\sigma\sigma'}^{2,(N)}\right)^\dagger}{\left(1 + \eta_{ijk,\sigma\sigma'}^{2,(N)} \left(\eta_{ijk,\sigma\sigma'}^{2,(N)}\right)^\dagger + \left(\eta_{ijk,\sigma\sigma'}^{2,(N)}\right)^\dagger \eta_{ijk,\sigma\sigma'}^{2,(N)}\right)^{1/2}} \quad (59)$$

$$U_{ij}^{3,(N)} = \frac{1 + \eta_{ij}^{3,(N)} - \left(\eta_{ij}^{3,(N)}\right)^\dagger}{\left(1 + \eta_{ij}^{3,(N)} \left(\eta_{ij}^{3,(N)}\right)^\dagger + \left(\eta_{ij}^{3,(N)}\right)^\dagger \eta_{ij}^{3,(N)}\right)^{1/2}} \quad (60)$$

These equations can further be simplified into,

$$U_{i\sigma}^{1,(N)} = \frac{1 + \eta_{i\sigma}^{1,(N)} - \left(\eta_{i\sigma}^{1,(N)}\right)^\dagger}{\left(1 + |t_{i\sigma}^{1,(N)}|^2(1 - \hat{n}_{i-\sigma})(1 - \hat{n}_{N-\sigma}) \left((1 - \hat{n}_{i\sigma})\hat{n}_{N\sigma} + (1 - \hat{n}_{N\sigma})\hat{n}_{i\sigma}\right)\right)^{1/2}} \quad (61)$$

$$U_{ijk,\sigma\sigma'}^{2,(N)} = \frac{1 + \eta_{ijk,\sigma\sigma'}^{2,(N)} - \left(\eta_{ijk,\sigma\sigma'}^{2,(N)}\right)^\dagger}{\left(1 + t_{ijk\sigma\sigma'}^{2,(N)} \left(t_{ijk\sigma\sigma'}^{2,(N)}\right)^* (1 - \hat{n}_{N-\sigma}) \left((1 - \hat{n}_{j\sigma})(1 - \hat{n}_{i\sigma'})\hat{n}_{k\sigma'}\hat{n}_{N\sigma} + (1 - \hat{n}_{N\sigma})(1 - \hat{n}_{k\sigma'})\hat{n}_{i\sigma'}\hat{n}_{j\sigma}\right)\right)^{1/2}} \quad (62)$$

$$U_{ij}^{3,(N)} = \frac{1 + \eta_{ij}^{3,(N)} - \left(\eta_{ij}^{3,(N)}\right)^\dagger}{\left(1 + t_{ij}^{3,(N)} \left(t_{ij}^{3,(N)}\right)^* \left((1 - \hat{n}_{j\uparrow})(1 - \hat{n}_{i\downarrow})\hat{n}_{N\downarrow}\hat{n}_{N\uparrow} + (1 - \hat{n}_{N\uparrow})(1 - \hat{n}_{N\downarrow})\hat{n}_{i\downarrow}\hat{n}_{j\uparrow}\right)\right)^{1/2}} \quad (63)$$

Separating the unitary operators into their Nth orbital projection spaces we obtain even

simpler expressions,

$$\begin{aligned}
U_{i\sigma}^{1,(N)} &= \left(1 + \eta_{i\sigma}^{1,(N)} - \left(\eta_{i\sigma}^{1,(N)}\right)^\dagger\right) \hat{n}_{N-\sigma} \\
&+ \left(1 + \eta_{i\sigma}^{1,(N)} - \left(\eta_{i\sigma}^{1,(N)}\right)^\dagger\right) \left(1 - P_{i\sigma}^{1,(N)} + P_{i\sigma}^{1,(N)} \hat{n}_{i-\sigma} + \frac{P_{i\sigma}^{1,(N)}(1 - \hat{n}_{i-\sigma})}{\left(1 + t_{i\sigma}^{1,(N)} \left(t_{i\sigma}^{1,(N)}\right)^*\right)^{1/2}}\right) (1 - \hat{n}_{N-\sigma})
\end{aligned} \tag{64}$$

$$\text{where } P_{i\sigma}^{1,(N)} = (1 - \hat{n}_{i\sigma})\hat{n}_{N\sigma} + (1 - \hat{n}_{N\sigma})\hat{n}_{i\sigma} \tag{65}$$

$$\begin{aligned}
U_{ijk,\sigma\sigma'}^{2,(N)} &= \left(1 + \eta_{ijk,\sigma\sigma'}^{2,(N)} - \left(\eta_{ijk,\sigma\sigma'}^{2,(N)}\right)^\dagger\right) \hat{n}_{N-\sigma} \\
&+ \left(1 + \eta_{ijk,\sigma\sigma'}^{2,(N)} - \left(\eta_{ijk,\sigma\sigma'}^{2,(N)}\right)^\dagger\right) \left(1 - P_{ijk,\sigma\sigma'}^{2,(N)} + \frac{P_{ijk,\sigma\sigma'}^{2,(N)}}{\left(1 + t_{ijk,\sigma\sigma'}^{2,(N)} \left(t_{ijk,\sigma\sigma'}^{2,(N)}\right)^*\right)^{1/2}}\right) (1 - \hat{n}_{N-\sigma})
\end{aligned} \tag{66}$$

$$\text{where } P_{ijk,\sigma\sigma'}^{2,(N)} = (1 - \hat{n}_{j\sigma})(1 - \hat{n}_{i\sigma'})\hat{n}_{k\sigma'}\hat{n}_{N\sigma} + (1 - \hat{n}_{N\sigma})(1 - \hat{n}_{k\sigma'})\hat{n}_{i\sigma'}\hat{n}_{j\sigma} \tag{67}$$

$$U_{ij}^{3,(N)} = \left(1 + \eta_{ij}^{3,(N)} - \left(\eta_{ij}^{3,(N)}\right)^\dagger\right) \left(1 - P_{ij}^{3,(N)} + \frac{P_{ij}^{3,(N)}}{\left(1 + t_{ij}^{3,(N)} \left(t_{ij}^{3,(N)}\right)^*\right)^{1/2}}\right) \tag{68}$$

$$\text{where } P_{ij}^{3,(N)} = (1 - \hat{n}_{j\uparrow})(1 - \hat{n}_{i\downarrow})\hat{n}_{N\downarrow}\hat{n}_{N\uparrow} + (1 - \hat{n}_{N\uparrow})(1 - \hat{n}_{N\downarrow})\hat{n}_{i\downarrow}\hat{n}_{j\uparrow} \tag{69}$$

Our Downfolding transformation for one step downfolded Hermitian Hamiltonian,  $H_{(N-1)}$  is given by,

$$\begin{aligned}
H_{(N-1)} &= (U^{(N)})^\dagger H_{(N)} U^{(N)} \\
&= \prod_{ijklmn,\mu\sigma\sigma'} e^{-\text{arctanh}\left(\eta_{mn}^{3,(N)} - \left(\eta_{mn}^{3,(N)}\right)^\dagger\right)} e^{-\text{arctanh}\left(\eta_{jkl,\sigma\sigma'}^{2,(N)} - \left(\eta_{jkl,\sigma\sigma'}^{2,(N)}\right)^\dagger\right)} e^{-\text{arctanh}\left(\eta_{i,\sigma}^{1,(N)} - \left(\eta_{i,\sigma}^{1,(N)}\right)^\dagger\right)}
\end{aligned}$$



$$H_{(N)} e^{\operatorname{arctanh}\left(\eta_{i,\sigma}^{1,(N)} - \left(\eta_{i,\sigma}^{1,(N)}\right)^\dagger\right)} e^{\operatorname{arctanh}\left(\eta_{jkl,\sigma\sigma'}^{2,(N)} - \left(\eta_{jkl,\sigma\sigma'}^{2,(N)}\right)^\dagger\right)} e^{\operatorname{arctanh}\left(\eta_{mn}^{3,(N)} - \left(\eta_{mn}^{3,(N)}\right)^\dagger\right)} \quad (70)$$

In this manner we construct a closed-form unitary operator representation for downfolding Hamiltonian with Singles and doubles and similar construction can be made for the general multireference case with all excitations singles, doubles and beyond. Note that in the unitary operator no higher order electronic clusters are generated beyond the singles and doubles contribution in  $\eta$  albeit the unitary operator constructed from the similarity map fulfills the  $U^\dagger U = U U^\dagger = I$  form. This is different from the unitary transformation in the DUCC formalism<sup>51</sup> where the action of the unitary operator on the Hamiltonian is truncated beyond double commutator making the approach perturbative with respect to the electronic cluster amplitudes. After our multireference downfolding cases we will take the case of single configuration downfolding in the next section

## 6 Case Study: Single configuration spin restricted downfolding with singles and doubles

This is a specific case of single configuration downfolding where we start from the Hartree Fock state and incorporate the downfolding correlations by doing a sequence of similarity transformations on the Hartree-Fock state  $|\Psi\rangle$  We first define the partition,

$$P_N = (1 - \hat{n}_{N\uparrow})(1 - \hat{n}_{N\downarrow}), \quad Q_N = 1 - P_N \quad (71)$$

Let's now define the generator of similarity transformations in the space of  $P_N$  and  $Q_N$ ,

$$\begin{aligned} \eta_{(N)} &= \sum_{i\sigma} t_{Ni}(1 - \hat{n}_{N-\sigma}) f_{N\sigma}^\dagger f_{i\sigma} + \sum_{bij,\sigma\sigma'} t_{Nbij}(1 - \hat{n}_{N-\sigma}) f_{N\sigma}^\dagger f_{b\sigma'}^\dagger f_{j\sigma'} f_{i\sigma} \\ &+ \sum_{ij} t_{NNij} f_{N\uparrow}^\dagger f_{N\downarrow}^\dagger f_{j\downarrow} f_{i\uparrow} \end{aligned} \quad (72)$$

The  $\eta_{(N)}$  satisfies the equation,

$$Q_{(N)}\eta_{(N)}P_{(N)} = \eta_{(N)}, \eta_{(N)}^2 = 0 \quad (73)$$

Now we can write down the subset of coupled cluster equations for downfolding one molecular orbital as,

$$\langle \Psi_i^{N,\sigma} | Q_N S_N^{-1} H S_N P_{N\sigma} | \Psi \rangle = 0 \quad (74)$$

$$\langle \Psi_{ij}^{aN,\sigma\sigma'} | Q_N S_N^{-1} H S_N P_N | \Psi \rangle = 0 \quad (75)$$

$$\langle \Psi_{ij}^{NN} | Q_N S_N^{-1} H S_N P_N | \Psi \rangle = 0 \quad (76)$$

where,

$$|\Psi_i^{N\sigma}\rangle = f_{N\sigma}^\dagger f_{i\sigma} |\Psi\rangle \quad (77)$$

$$|\Psi_{ij}^{aN,\sigma\sigma'}\rangle = f_{Ng\sigma}^\dagger f_{a\sigma'}^\dagger f_{j\sigma'} f_{i\sigma} |\Psi\rangle \quad (78)$$

$$|\Psi_{ij}^{NN}\rangle = f_{N\uparrow}^\dagger f_{a\downarrow}^\dagger f_{j\downarrow} f_{i\uparrow} |\Psi\rangle \quad (79)$$

Before writing down the algebraic expressions for the recursive Hamiltonian downfolding amplitude equations, we will define a modified ERI operator,  $w^2$ , given by,

$$w_{ijab}^2 = 2h_{ijab}^2 - h_{ijba}^2 \quad (80)$$

and a permutation operator,  $\mathcal{P}$ , given by,

$$\mathcal{P}\{\dots\}_{abij} = \{\dots\}_{abij} + \{\dots\}_{baji} \quad (81)$$

## 6.1 T1-Residual Equation

Solving equation 74, we get the  $t^1$  amplitude equation for  $N$ th orbital downfolding step as,

$$\sum_{i=1}^{11} T_i = 0 \quad (82)$$

where  $f_{ij}$  are elements of (N-1) step downfolded fock matrix and,

$$T_1 = f_{Ni} \quad (83)$$

$$T_2 = -2 \sum_k f_{kN} t_{Nk}^1 t_{Ni}^1 \quad (84)$$

$$T_3 = f_{NN} t_{Ni}^1 - \sum_k w_{klNN}^2 t_{NNkl}^2 t_{Ni}^1 - \sum_{k,d \neq N} w_{klNd}^2 t_{Ndkl}^2 t_{Ni}^1 \quad (85)$$

$$T_4 = -\sum_k f_{ki} t_{Nk}^1 - \sum_{klc} w_{klcN}^2 t_{cNkl}^2 t_{Nk}^1 - \sum_{kl,d \neq N} w_{klNd}^2 t_{Ndkl}^2 t_{Nk}^1 \quad (86)$$

$$T_5 = 2 \sum_{kc} f_{kc} t_{cNki}^2 + 2 \sum_{klc} w_{klcN}^2 t_{Nl}^1 t_{cNki}^2 - \sum_{kc} f_{kc} t_{cNik}^2 - \sum_{klc} w_{klcN}^2 t_{Nl}^1 t_{cNik}^2 \quad (87)$$

$$T_6 = \sum_k f_{kN} t_{Ni}^1 t_{Nk}^1 \quad (88)$$

$$T_7 = \sum_k w_{NkiN}^2 t_{Nk}^1 \quad (89)$$

$$T_8 = \sum_{kc} w_{NkcN}^2 t_{cNik}^2 + \sum_{k,d \neq N} w_{NkNd}^2 t_{Ndik}^2 \quad (90)$$

$$T_9 = \sum_k w_{NkNN}^2 t_{Ni}^1 t_{Nk}^1 \quad (91)$$

$$T_{10} = -\sum_{kl} w_{kliN}^2 t_{NNkl}^2 - \sum_{kl,c \neq N} w_{klic}^2 t_{Nckl}^2 \quad (92)$$

$$T_{11} = -\sum_{kl} w_{kliN}^2 t_{Nk}^1 t_{Nl}^1 \quad (93)$$

## 6.2 T2-Residual Equation

Solving equations 75 and 76, we get the  $t^2$  amplitude equation for  $N$ th orbital downfolding step as,

$$\sum_{i=1}^{13} T_i = 0 \quad (94)$$

where,

$$T_1 = h_{ijaN}^2 + h_{ijNb}^2 \quad (95)$$

$$\begin{aligned} T_2 = & \sum_{kl} h_{klij}^2 t_{aNkl}^2 + \sum_{kl} h_{klij}^2 t_{Nbkl}^2 + \sum_{kl} h_{kliN}^2 t_{Nj}^1 t_{aNkl}^2 + \sum_{kl} h_{kliN}^2 t_{Nj}^1 t_{Nbkl}^2 + \sum_{kl} h_{klNj}^2 t_{Ni}^1 t_{aNkl}^2 \\ & + \sum_{kl} h_{klNj}^2 t_{Ni}^1 t_{Nbkl}^2 + \sum_{klc} h_{klcN}^2 t_{cNij}^2 t_{aNkl}^2 + \sum_{klc} h_{klcN}^2 t_{cNij}^2 t_{Nbkl}^2 \\ & + \sum_{kl, c \neq N} h_{klNc}^2 t_{Ncij}^2 t_{aNkl}^2 + \sum_{kl, c \neq N} h_{klNc}^2 t_{Ncij}^2 t_{Nbkl}^2 \end{aligned} \quad (96)$$

$$T_3 = \sum_{kl} h_{klij}^2 t_{Nk}^1 t_{Nl}^1 \quad (97)$$

$$\begin{aligned} T_4 = & \sum_c h_{aNcN}^2 t_{cNij}^2 + \sum_c h_{NbcN}^2 t_{cNij}^2 + \sum_{d \neq N} h_{aNNd}^2 t_{Ndi}^2 \\ & + \sum_{d \neq N} h_{NbdN}^2 t_{Ndi}^2 - \sum_{kc} h_{akcN}^2 t_{Nk}^1 t_{cNij}^2 - \sum_{k, d \neq N} h_{akNd}^2 t_{Nk}^1 t_{Ndi}^2 \\ & - \sum_{kc} h_{kbcN}^2 t_{Nk}^1 t_{cNij}^2 - \sum_{k, d \neq N} h_{kbNd}^2 t_{Nk}^1 t_{Ndi}^2 \end{aligned} \quad (98)$$

$$T_5 = h_{aNnN}^2 t_{Ni}^1 t_{Nj}^1 + h_{NbNn}^2 t_{Ni}^1 t_{Nj}^1 \quad (99)$$

$$\begin{aligned} T_6 = & \mathcal{P} \sum_c f_{ac} t_{cNij}^2 + \mathcal{P} f_{NN} t_{Nbij}^2 - \mathcal{P} \sum_{klc} w_{klcN}^2 t_{aNkl}^2 t_{cNij}^2 - \mathcal{P} \sum_{kl} w_{klNN}^2 t_{NNkl}^2 t_{Nbij}^2 \\ & - \mathcal{P} \sum_{kl, d \neq N} w_{klNd}^2 t_{Ndkl}^2 t_{NNij}^2 - \mathcal{P} \sum_{kl, d \neq N} w_{klNd}^2 t_{Ndkl}^2 t_{Nbij}^2 - \mathcal{P} \sum_k f_{kN} t_{Nk}^1 t_{NNij}^2 \\ & - \mathcal{P} \sum_k f_{kN} t_{Nk}^1 t_{Nbij}^2 + \mathcal{P} \sum_{kc} w_{akcN}^2 t_{Nk}^1 t_{cNij}^2 + \mathcal{P} \sum_k w_{NkNN}^2 t_{Nk}^1 t_{Nbij}^2 \end{aligned} \quad (100)$$

$$T_7 = -\mathcal{P} \sum_k f_{ki} t_{aNkj}^2 - \mathcal{P} \sum_{klc} w_{klcN}^2 t_{cNil}^2 t_{aNkj}^2 - \mathcal{P} \sum_{kl, d \neq N} w_{klNd}^2 t_{Ndil}^2 t_{aNkj}^2$$

$$\begin{aligned}
& -\mathcal{P} \sum_k f_{kN} t_{Ni}^1 t_{aNkj}^2 - \mathcal{P} \sum_{kl} w_{kliN}^2 t_{Ni}^1 t_{aNkj}^2 \\
& -\mathcal{P} \sum_k f_{ki} t_{Nbkj}^2 - \mathcal{P} \sum_{klc} w_{klcN}^2 t_{cNi}^2 t_{Nbkj}^2 - \mathcal{P} \sum_{kl, d \neq N} w_{klNd}^2 t_{Ndil}^2 t_{Nbkj}^2 \\
& -\mathcal{P} \sum_k f_{kN} t_{Ni}^1 t_{Nbkj}^2 - \mathcal{P} \sum_{kl} w_{kliN}^2 t_{Ni}^1 t_{Nbkj}^2
\end{aligned} \tag{101}$$

$$T_8 = \mathcal{P} h_{aNiN}^2 t_{Nj}^1 + \mathcal{P} h_{NbiN}^2 t_{Nj}^1 - \mathcal{P} \sum_k h_{kbiN}^2 t_{Nk}^1 t_{Nj}^1 \tag{102}$$

$$T_9 = -\mathcal{P} \sum_k h_{akij}^2 t_{Nk}^1 - \mathcal{P} \sum_k h_{akiN}^2 t_{Nj}^1 t_{Nk}^1 \tag{103}$$

$$\begin{aligned}
T_{10} = & 2\mathcal{P} \sum_{kc} h_{akic}^2 t_{cNkj}^2 + 2\mathcal{P} \sum_k h_{NkiN}^2 t_{Nbkj}^2 - 2\mathcal{P} \sum_{kl} h_{lkiN}^2 t_{Ni}^1 t_{NNkj}^2 \\
& - 2\mathcal{P} \sum_{kl} h_{lkiN}^2 t_{Ni}^1 t_{Nbkj}^2 + 2\mathcal{P} \sum_{kc} h_{akNc}^2 t_{Ni}^1 t_{cNkj}^2 + 2\mathcal{P} \sum_k h_{NkNN}^2 t_{Ni}^1 t_{Nbkj}^2 \\
& - \mathcal{P} \sum_{klc} h_{lkNc}^2 t_{NNil}^2 t_{cNkj}^2 - \mathcal{P} \sum_{kl, d \neq N} h_{lkdN}^2 t_{dNil}^2 t_{NNkj}^2 \\
& - \mathcal{P} \sum_{kld} h_{lkdN}^2 t_{dNil}^2 t_{Nbkj}^2 - \mathcal{P} \sum_{klc} h_{lkNc}^2 t_{Nail}^2 t_{cNkj}^2 - \mathcal{P} \sum_{kl} h_{lkNN}^2 t_{Nail}^2 t_{Nbkj}^2 \\
& + \mathcal{P} \sum_{klc} w_{lkNc}^2 t_{aNil}^2 t_{cNkj}^2 + \mathcal{P} \sum_{kl} w_{lkNN}^2 t_{NNil}^2 t_{Nbkj}^2 \\
& + \mathcal{P} \sum_{kl, d \neq N} w_{lkdN}^2 t_{Ndil}^2 t_{NNkj}^2 + \mathcal{P} \sum_{kl, d \neq N} w_{lkdN}^2 t_{Ndil}^2 t_{Nbkj}^2
\end{aligned} \tag{104}$$

$$\begin{aligned}
T_{11} = & -\mathcal{P} \sum_k h_{akiN}^2 t_{NNkj}^2 - \mathcal{P} \sum_k h_{NkiN}^2 t_{bNkj}^2 - \mathcal{P} \sum_{k, c \neq N} h_{akic}^2 t_{Nckj}^2 + \mathcal{P} \sum_{kl} h_{lkiN}^2 t_{Ni}^1 t_{bNkj}^2 \\
& + \mathcal{P} \sum_{kl} h_{lkiN}^2 t_{Ni}^1 t_{NNkj}^2 - \mathcal{P} \sum_k h_{akNN}^2 t_{Ni}^1 t_{NNkj}^2 - \mathcal{P} \sum_k h_{NkNN}^2 t_{Ni}^1 t_{bNkj}^2 \\
& - \mathcal{P} \sum_{k, c \neq N} h_{akNc}^2 t_{Ni}^1 t_{Nckj}^2 + 1/2 \mathcal{P} \sum_{kld} h_{lkdN}^2 t_{dNil}^2 t_{bNkj}^2 + 1/2 \mathcal{P} \sum_{kld} h_{lkdN}^2 t_{dNil}^2 t_{NNkj}^2 \\
& + 1/2 \mathcal{P} \sum_{kl, c \neq N} h_{lkNc}^2 t_{NNil}^2 t_{Nckj}^2 + 1/2 \mathcal{P} \sum_{kl} h_{lkNN}^2 t_{Nail}^2 t_{NNkj}^2 + 1/2 \mathcal{P} \sum_{kl, c \neq N} h_{lkNc}^2 t_{Nail}^2 t_{Nckj}^2 \\
& - 1/2 \mathcal{P} \sum_{kl} w_{lkNN}^2 t_{aNil}^2 t_{NNkj}^2 - 1/2 \mathcal{P} \sum_{kl} w_{lkNN}^2 t_{NNil}^2 t_{bNkj}^2 - 1/2 \mathcal{P} \sum_{kl, c \neq N} w_{lkNc}^2 t_{aNil}^2 t_{Nckj}^2 \\
& - 1/2 \mathcal{P} \sum_{kl, d \neq N} w_{lkdN}^2 t_{Ndil}^2 t_{bNkj}^2 - 1/2 \mathcal{P} \sum_{kl, d \neq N} w_{lkdN}^2 t_{Ndil}^2 t_{NNkj}^2
\end{aligned} \tag{105}$$

$$\begin{aligned}
T_{12} = & -\mathcal{P} \sum_k h_{NkNi}^2 t_{aNkj}^2 - \mathcal{P} \sum_k h_{bkNi}^2 t_{NNkj}^2 - \mathcal{P} \sum_{k,c \neq N} h_{bkci}^2 t_{Nckj}^2 \\
& + \mathcal{P} \sum_{kl} h_{lkNi}^2 t_{NI}^1 t_{aNkj}^2 - \mathcal{P} \sum_k h_{NkNN}^2 t_{Ni}^1 t_{aNkj}^2 - \mathcal{P} \sum_k h_{bkNN}^2 t_{Ni}^1 t_{NNkj}^2 \\
& - \mathcal{P} \sum_{k,c \neq N} h_{bkcN}^2 t_{Ni}^1 t_{Nckj}^2 + 1/2 \mathcal{P} \sum_{kd} h_{lkNd}^2 t_{dNi}^2 t_{aNkj}^2 + 1/2 \mathcal{P} \sum_{kc \neq N} h_{lkcN}^2 t_{NNil}^2 t_{Nckj}^2 \\
& + 1/2 \mathcal{P} \sum_k h_{lkNN}^2 t_{Nbi}^2 t_{NNkj}^2 + 1/2 \mathcal{P} \sum_{k,c \neq N} h_{lkcN}^2 t_{Nbi}^2 t_{Nckj}^2 \tag{106}
\end{aligned}$$

$$\begin{aligned}
T_{13} = & -\mathcal{P} \sum_{kc} h_{akci}^2 t_{cNkj}^2 - \mathcal{P} \sum_k h_{NkNi}^2 t_{Nbkj}^2 \\
& + \mathcal{P} \sum_{kl} h_{lkNi}^2 t_{NI}^1 t_{NNkj}^2 + \mathcal{P} \sum_{kl} h_{lkNi}^2 t_{NI}^1 t_{Nbkj}^2 - \mathcal{P} \sum_{kc} h_{akcN}^2 t_{Ni}^1 t_{cNkj}^2 \\
& - \mathcal{P} \sum_k h_{NkNN}^2 t_{Ni}^1 t_{Nbkj}^2 + 1/2 \mathcal{P} \sum_{lc} h_{lkcN}^2 t_{NNil}^2 t_{cNkj}^2 + 1/2 \mathcal{P} \sum_{l,d \neq N} h_{lkNd}^2 t_{dNi}^2 t_{NNkj}^2 \\
& + 1/2 \mathcal{P} \sum_{ld} h_{lkNd}^2 t_{dNi}^2 t_{Nbkj}^2 + 1/2 \mathcal{P} \sum_{klc} h_{lkcN}^2 t_{Nail}^2 t_{cNkj}^2 \tag{107}
\end{aligned}$$

From the above expressions, it can be easily seen that the  $t^2$ -residual equation can be written as,

$$0 = \tilde{T}_{ij}^{aN} + \tilde{T}_{ij}^{Nb} \tag{108}$$

Here  $a, b, c, d \in \mathcal{V}, i, j, k, l \in \mathcal{O}$  where  $b \neq N \forall t_{bprs}^2$  &  $t_{pbrs}^2$  and,  $a \neq N \forall t_{pars}^2$  terms with  $p, r, s$  representing arbitrary molecular orbitals.

In order to compute these tensor operations on quantum circuits, we will layout the formalism in the next section

## 7 Quantum Circuits for Block encoding tensor operations

Let us consider a matrix (2-tensor)  $B$  of size  $M \times N$ . Here we will describe a circuit that allows us to encode this matrix and facilitate further processing. For our convenience, we will assume that  $M$  and  $N$  are of the form  $2^m$  and  $2^n$  respectively and  $\|B\| = 1$ .

Consider a quantum circuit with two multi-qubit registers labelled  $I, J$  of sizes  $m, n$  respectively and two single qubit registers  $A, D$  with the following ordering:

$$|\cdot\rangle_I |\cdot\rangle_J |\cdot\rangle_A |\cdot\rangle_D \quad (109)$$

Let the label  $a$  denote the state of the single qubit register  $A$ . We call the quantum circuit that loads our data onto a quantum circuit as a block-encoder. It is defined as follows:

$$V_{IJ}^a(A) = \left[ \sum_{j \in J; i \in I} |i, j, a\rangle \langle i, j, a| \otimes \left\{ (1-a) \left( A_{ij} I + i \sqrt{1 - A_{ij}^2} Y \right) + \right. \right. \quad (110)$$

$$\left. \left. a \left( (A_{ij}^T)' I + i \sqrt{1 - (A_{ij}^T)^2} Y \right) \right\} + |i, j, 1-a\rangle \langle i, j, 1-a| \otimes I_2 \right] \quad (111)$$

. We can read an element  $B_{ij}$  by evolving the state  $|i, j, a, 0\rangle$  as,

$$\langle i, j, a, 0 | V_{IJ}^a | i, j, a, 0 \rangle \quad (112)$$

Using the above operator together with superposed states, we can perform various tensor operations. The concept of multiplexed rotations<sup>72,73</sup> allows us to implement the above circuit using  $MN$  number of CX Gates, and  $MN$  single qubit rotations ( $RX, RY, RZ$  rotations). This is insufficient to capture the complexity of implementing it on fault tolerant quantum computers.

Fault tolerant quantum computing utilizes clifford + T basis ( $H, S, T, CX$ ) to represent

quantum gates. There are two well known methods of implementing single qubit rotations in this basis as described in the tables below.

Table 1: Analyzing T-depth for Single qubit rotations

Method	T-Count	Runtime
The Solovay-Kitaev Process <sup>74</sup>	$O(\log^{3.97} \frac{1}{\epsilon})$	$O(\log^{2.71} \frac{1}{\epsilon})$
Solving Diophantine Equations <sup>75</sup>	$3 \log \frac{1}{\epsilon} + O(\log \log \frac{1}{\epsilon})$	$O(\log \log \frac{1}{\epsilon})$

Thus, encoding a  $M \times N$  circuit can be performed with the below resources.

Table 2: Analyzing T-depth for Block Encoding Circuits

Method	T-Depth	Runtime
The Solovay-Kitaev Process <sup>74</sup>	$O(MN \log^{3.97} \frac{1}{\epsilon})$	$O(MN \log^{2.71} \frac{1}{\epsilon})$
Solving Diophantine Equations <sup>75</sup>	$3MN \log \frac{1}{\epsilon} + O(MN \log \log \frac{1}{\epsilon})$	$O(MN \log \log \frac{1}{\epsilon})$

## 7.1 Realizing Tensor Operations

In this section, we will perform various tensor operations on quantum circuits and utilize them to construct the downfolding expressions. For that, we present multiple theorems on matrix multiplication and tensor operations using quantum circuits.

### 7.1.1 Qubitization circuit for Matrix-Matrix multiplication with isometries

#### Theorem

If  $A$  and  $B$  are general rectangular matrices of dimensions  $dim(A) = (N, P)$  and  $dim(B) = (P, M)$  with  $N, M \geq 2$  then there is a unitary operation  $U(A, B)$  of dimension  $2^{n_q} \times 2^{n_q}$  that operates on a system of  $n_q = p + \max(m, n) + 2$  qubit registers :  $|\cdot\rangle_p |\cdot\rangle_{\max(m, n)} |\cdot\rangle_{a_1} |\cdot\rangle_{a_2}$  (where  $n = \lceil \log_2 N \rceil, m = \lceil \log_2 M \rceil, p = \lceil \log_2 P \rceil$ ) and block encodes the matrix multiplication of  $A$  and  $B$  s.t.

$$\langle 0|_p \langle i|_{\max(m, n)} \langle 0|_{a_1} \langle 0|_{a_2} U(A, B) |0\rangle_p |j\rangle_{\max(m, n)} |1\rangle_{a_1} |0\rangle_{a_2} = \frac{1}{P^2} \frac{\sum_k A_{ik} B_{kj}}{\|A\| \|B\|}.$$



*Proof-* Lets define an isometry  $T(A, B)$ ,

$$\begin{aligned}
T(A, B) &= \frac{1}{\sqrt{2 \max(N, M)}} \sum_{r,c} |c\rangle\langle c| \otimes |r\rangle \otimes \left[ \frac{A_{rc}}{\|A\|} |0, 0\rangle + \sqrt{1 - \left(\frac{A_{rc}}{\|A\|}\right)^2} |0, 1\rangle \right. \\
&\quad \left. + \frac{B_{cr}}{\|B\|} |r, 1, 0\rangle + \sqrt{1 - \left(\frac{B_{cr}}{\|B\|}\right)^2} |r, 1, 1\rangle \right]
\end{aligned} \tag{113}$$

The isometry  $T(A, B)$  has the property  $T^\dagger(A, B)T(A, B) = I_2^{\otimes p}$  this can be checked as follows,

$$\begin{aligned}
T^\dagger(A, B)T(A, B) &= \frac{1}{2 \max(N, M)} \sum_c |c\rangle\langle c| \otimes \left[ \sum_r (|A_{rc}|^2 + 1 - A_{rc}^2 + B_{cr}^2 + 1 - B_{cr}^2) \right] \\
&= \sum_c |c\rangle\langle c| = I_2^{\otimes p}
\end{aligned} \tag{114}$$

Utilizing the above property we can define a unitary operator  $W := W(A, B)$ ,

$$W(A, B) = 2T(A, B)T^\dagger(A, B) - 1 \tag{115}$$

The unitarity of  $W$  can be checked as follows,

$$\begin{aligned}
W^\dagger W &= WW^\dagger = I \\
&= (2T(A, B)T^\dagger(A, B) - 1)(2T(A, B)T^\dagger(A, B) - 1) \\
&= 4T(A, B)T^\dagger(A, B) - 4T(A, B)T^\dagger(A, B) + 1 = 1
\end{aligned} \tag{116}$$

To proceed further we normalizing the matrices  $A' := A/(\sqrt{2}\|A\|)$  and  $B' := B/(\sqrt{2}\|B\|)$ .

The form of the  $W$  matrix in terms of registers is as follows,

$$\begin{aligned}
W &= \sum_{c,r,r'} |c, r\rangle\langle c, r'| \otimes \left[ (4A'_{rc}A'_{r'c} - \delta_{rr'})|0, 0\rangle\langle 0, 0| + 4A'_{rc}\sqrt{1 - A'^2_{r'c}}|0, 0\rangle\langle 0, 1| \right. \\
&\quad \left. + 4\sqrt{1 - A'^2_{rc}A'_{r'c}}|0, 1\rangle\langle 0, 0| + (4\sqrt{(1 - A'^2_{rc})(1 - A'^2_{r'c})} - \delta_{rr'})|0, 1\rangle\langle 0, 1| \right]
\end{aligned}$$

$$\begin{aligned}
& + (4B'_{cr}B'_{cr'} - \delta_{rr'})|1,0\rangle\langle 1,0| + 4B'_{cr}\sqrt{1-B'^2_{cr'}}|1,0\rangle\langle 1,1| \\
& + 4\sqrt{1-B'^2_{cr'}}B'_{cr'}|1,1\rangle\langle 1,0| + (4\sqrt{(1-B'^2_{cr})(1-B'^2_{cr'})} - \delta_{rr'})|1,1\rangle\langle 1,1| \\
& + 4A'_{rc}B'_{cr'}|0,0\rangle\langle 1,0| + 4B'_{cr}A'_{r'c}|1,0\rangle\langle 0,0| + 4B'_{cr}\sqrt{1-A'^2_{r'c}}|1,0\rangle\langle 0,1| + 4\sqrt{1-A'^2_{rc}}B'_{cr'}|0,1\rangle\langle 1,0| \\
& + 4A'_{rc}\sqrt{1-B'^2_{cr'}}|0,0\rangle\langle 1,1| + 4\sqrt{1-B'^2_{cr'}}A'_{r'c}|1,1\rangle\langle 0,0| + 4\sqrt{(1-B'^2_{cr})(1-A'^2_{cr'})}|1,1\rangle\langle 0,1| \\
& + 4\sqrt{(1-B'^2_{cr})(1-A'^2_{cr'})}|0,1\rangle\langle 1,1| \Big] \tag{117}
\end{aligned}$$

Starting from an initial state with Hadamard on the column qubit registers we obtain,

$$H^{\otimes p}|0\rangle|j\rangle|1\rangle|0\rangle = \frac{1}{P} \sum_c |c\rangle|j\rangle|1\rangle|0\rangle. \tag{118}$$

Upon acting  $W$ ,

$$\begin{aligned}
WH^{\otimes p}|0\rangle|j\rangle|1\rangle|0\rangle & = \frac{1}{2P} \sum_{c,r} |c,r\rangle \left[ (2B'_{cr}B'_{cj} - \delta_{rj})|1,0\rangle + 2\sqrt{1-A'^2_{rc}}B'_{cj}|0,1\rangle \right. \\
& \left. + 2\sqrt{1-B'^2_{rc}}B'_{cj}|1,1\rangle + 2A'_{rc}B'_{cj}|0,0\rangle \right] \tag{119}
\end{aligned}$$

Taking overlap of  $WH^{\otimes p}|0\rangle|j\rangle|1\rangle|0\rangle$  with the state  $H^{\otimes p}|0\rangle|i\rangle|0\rangle|0\rangle$  we get,

$$\langle 0|0\rangle\langle i|\langle 0|H^{\otimes p}WH^{\otimes p}|0\rangle|j\rangle|1\rangle|0\rangle = \frac{4}{4P^2} \sum_k A'_{ik}B'_{kj} = \frac{4}{P^2} (A'B')_{ij} = \frac{(AB)_{ij}}{P^2||A||||B||} \tag{120}$$

By construction we have proved the existence of  $U(A, B)$ ,

$$U(A, B) = H^{\otimes p}(2T^\dagger(A, B)T(A, B) - 1)H^{\otimes p}. \tag{121}$$

### 7.1.2 Matrix-multiplication with Quantum circuits only with Unitary operators

#### Theorem

(Isometry free proof) If  $A$  and  $B$  are general rectangular matrices of dimensions  $\dim(A) = (N, P)$  and  $\dim(B) = (P, M)$  then there is a unitary operation  $U(A, B)$  of dimension  $2^{n_a} \times 2^{n_q}$

that operates on a system of  $n_q = p + \max(m, n) + 2$  qubit registers  $|\cdot\rangle_p|\cdot\rangle_{\max(m,n)}|\cdot\rangle_{a_1}|\cdot\rangle_{a_2}$  (where  $n = \lceil \log_2 N \rceil, m = \lceil \log_2 M \rceil, p = \lceil \log_2 P \rceil$ ) and block encodes the matrix multiplication of  $A$  and  $B$  s.t.

$$\langle 0|_p \langle i|_{\max(m,n)} \langle 0|_{a_1} \langle 0|_{a_2} U(A, B) |0\rangle_p |j\rangle_{\max(m,n)} |1\rangle_{a_1} |0\rangle_{a_2} = \frac{1}{\max(M, N)P} \frac{\sum_k A_{ik} B_{kj}}{\|A\| \|B\|}.$$

*Proof-* Let us take the normalized matrices  $A' = A/(\sqrt{2}\|A\|)$ ,  $B' = B/(\sqrt{2}\|B\|)$ . For these we define two unitary operators  $V(A), V(B)$ ,

$$\begin{aligned} V_A &= \sum_{c=0, r=0}^{2^p, 2^{\max(m,n)}} \left[ |c, r, 0\rangle \langle c, r, 0| \otimes \left( A'_{rc} I + i\sqrt{1 - A'^2_{rc}} Y \right) + |c, r, 1\rangle \langle c, r, 1| \otimes I_2 \right] \\ V_B &= \sum_{c=0, r=0}^{2^p, 2^{\max(m,n)}} \left[ |c, r, 0\rangle \langle c, r, 0| \otimes I_2 + |c, r, 1\rangle \langle c, r, 1| \otimes \left( B'_{cr} I + i\sqrt{1 - B'^2_{cr}} Y \right) \right] \end{aligned} \quad (122)$$

We load the classical data of the B matrix using the state preparation oracle  $V_B H^{\otimes p}$  on the initial state  $|0\rangle|j\rangle|1\rangle|0\rangle$ ,

$$|\Phi_B\rangle = V_B H^{\otimes p} |0\rangle|j\rangle|1\rangle|0\rangle = \frac{1}{\sqrt{P}} \sum_c \left[ B'_{cj} |c, j, 1, 0\rangle + \sqrt{1 - B'^2_{cj}} |c, j, 1, 1\rangle \right]. \quad (123)$$

We load the classical data of the A matrix using the state preparation oracle  $V_A H^{\otimes p}$ ,

$$|\Phi_A\rangle = V_A H^{\otimes p} |0\rangle|i\rangle|0\rangle|0\rangle = \frac{1}{\sqrt{P}} \sum_c \left[ A'_{ic} |c, i, 0, 0\rangle + \sqrt{1 - A'^2_{ic}} |c, i, 0, 1\rangle \right] \quad (124)$$

Note that the states  $|\Phi_A\rangle$  and  $|\Phi_B\rangle$  are orthogonal,

$$\langle \Phi_A | \Phi_B \rangle = 0 \quad (125)$$

Next we define diffusion operator  $R$  acting on the row registers and the ancillas  $a_1, a_2$ ,

$$R = I_2^{\otimes p} \otimes \left[ \left( H^{\otimes \max(m,n)} \otimes H \otimes I_2 \right) (2|0, 0, 0\rangle \langle 0, 0, 0| - 1) \left( H^{\otimes \max(m,n)} \otimes H \otimes I_2 \right) \right]$$

$$= I_2^{\otimes p} \otimes \left[ \sum_{k,l} 2 \frac{|k, +, 0\rangle\langle l, +, 0|}{\max(M, N)} - I \right] \quad (126)$$

Then the overlap between these two states  $|\Phi_A\rangle$  and  $R|\Phi_B\rangle$  is given by,

$$\begin{aligned} \langle \Phi_A | R | \Phi_B \rangle &= \langle 0, i, 0, 0 | H_c^{\otimes p} V_A^\dagger R V_B H_c^{\otimes p} | 0, j, 1, 0 \rangle \\ &= \frac{2 \sum_c A'_{ic} B'_{cj}}{\max(M, N) P} = \frac{\sum_c A_{ic} B_{cj}}{\max(M, N) P \|A\| \|B\|} \end{aligned} \quad (127)$$

By construction we have proved the existence of  $U(A, B)$  that can be defined without any isometry,

$$U(A, B) = H_c^{\otimes p} V_A^\dagger R V_B H_c^{\otimes p}. \quad (128)$$

### 7.1.3 Quantum Circuit for Tensor Product

#### Theorem

If  $A, B$  are rectangular matrices with shapes  $M \times R$  and  $N \times Q$  then there exists a Unitary  $U(A, B)$  of dimension  $8MNQR \times 8MNQR$  that operates on a system of  $n_m + n_r + n_q + m_n + 3$  qubit registers  $|\cdot\rangle_I |\cdot\rangle_J |\cdot\rangle_K |\cdot\rangle_L |\cdot\rangle_{\hat{A}} |\cdot\rangle_D$  with  $I, J, K, L, \hat{A}, D$  denoting the qubit-registers of size  $n_m, n_r, m_n, n_q, 1, 2$  (where  $n_m = \lceil \log_2 M \rceil$ ,  $n_N = \lceil \log_2 N \rceil$ ,  $n_q = \lceil \log_2 Q \rceil$ ,  $n_r = \lceil \log_2 R \rceil$ ) and block encodes the tensors  $A_{ij} B_{kl}$  such that

$$\langle i, j, k, l, 0, 0 | U(A, B) | 0, 0, 0, 0, 0, 0 \rangle = \frac{A_{ij} B_{kl}}{\sqrt{MNQR}} \quad (129)$$

#### Proof

We assume that  $A, B$  are normalized matrices, with  $\|A\| = 1, \|B\| = 1$ . Define the operator  $V_{IJAD_1}^a(A)$ , as below, acting on qubits in registers  $I, J, \hat{A}$  and the qubit 1 of register  $D$ . We

also have  $a$  denoting the state of the single qubit register  $\hat{A}$ .

$$V_{IJ\hat{A}D_1}^a(A) = \left[ \sum_{j \in J; i \in I} |i, j, a\rangle \langle i, j, a| \otimes \left\{ (1-a) \left( A_{ij}I + i\sqrt{1-A_{ij}^2}Y \right) + a \left( A_{ij}^T I + i\sqrt{1-(A_{ij}^T)^2}Y \right) \right\} + |i, j, 1-a\rangle \langle i, j, 1-a| \otimes I_2 \right] \quad (130)$$

Similarly, one can define the operator  $V_{KL\hat{A}D_2}^a(B)$ , as below, acting on qubits in registers  $K, L, \hat{A}$  and the qubit 2 of register  $D$ . We also have  $a$  denoting the state of the single qubit register  $\hat{A}$ .

$$V_{KL\hat{A}D_2}^a(B) = \left[ \sum_{k \in K; l \in L} |k, l, a\rangle \langle k, l, a| \otimes \left\{ (1-a) \left( B_{kl}I + i\sqrt{1-B_{kl}^2}Y \right) + a \left( B_{kl}^T I + i\sqrt{1-(B_{kl}^T)^2}Y \right) \right\} + |k, l, 1-a\rangle \langle k, l, 1-a| \otimes I_2 \right] \quad (131)$$

Then, one can observe that  $V_{IJ\hat{A}D_1}^a(A)V_{KL\hat{A}D_2}^a(B)H_I H_J H_K H_L$  satisfies

$$\langle i, j, k, l, 0, 0 | V_{IJ\hat{A}D_1}^a(A) V_{KL\hat{A}D_2}^a(B) | 0, 0, 0, 0, 0, 0 \rangle = \frac{A_{ij}B_{kl}}{\sqrt{MNQR}} \quad (132)$$

### Theorem

If  $A, B, C$  are rectangular matrices with shapes  $M \times R, N \times Q, P \times S$  then there exists a Unitary  $U(A, B, C)$  of dimension  $16MRNQPS \times 16MRNQPS$  that operates on a system of  $n_m + n_r + n_q + m_n + m_p + m_s + 4$  qubit registers  $|\cdot\rangle_I |\cdot\rangle_J |\cdot\rangle_K |\cdot\rangle_E |\cdot\rangle_F |\cdot\rangle_A |\cdot\rangle_D$  with  $I, J, K, L, E, F, A, D$  denoting the qubit-registers of size  $n_m, n_r, m_n, n_q, 1, 2$  (where  $n_m = \lceil \log_2 M \rceil$ ,  $n_N = \lceil \log_2 N \rceil$ ,  $n_q = \lceil \log_2 Q \rceil$ ,  $n_r = \lceil \log_2 R \rceil$ ,  $n_s = \lceil \log_2 S \rceil$ ,  $n_P = \lceil \log_2 P \rceil$  and block encodes the tensors  $A_{ij}B_{kl}C_{ef}$  such that

$$\langle i, j, k, l, e, f, 0, 0 | U(A, B, C) | 0, 0, 0, 0, 0, 0, 0, 0 \rangle = \frac{A_{ij}B_{kl}C_{ef}}{\sqrt{MNQRPS}} \quad (133)$$

### Proof

We assume that  $A, B, C$  are normalized matrices, with  $\|A\| = 1, \|B\| = 1, \|C\| = 1$ . Define the operator  $V_{IJ\hat{A}D_1}^a(A)$ , as below, acting on qubits in registers  $I, J, \hat{A}$  and the qubit 1 of register  $D$ . We also have  $a$  denoting the state of the single qubit register  $\hat{A}$ .

$$V_{IJ\hat{A}D_1}^a(A) = \left[ \sum_{j \in J; i \in I} |i, j, a\rangle \langle i, j, a| \otimes \left\{ (1-a) \left( A_{ij}I + i\sqrt{1-A_{ij}^2}Y \right) + a \left( (A_{ij}^T)'I + i\sqrt{1-(A_{ij}^T)^2}Y \right) \right\} + |i, j, 1-a\rangle \langle i, j, 1-a| \otimes I_2 \right] \quad (134)$$

Similarly, one can define the operator  $V_{KL\hat{A}D_2}^a(B)$ , as below, acting on qubits in registers,  $K, L, \hat{A}$  and the qubit 2 of register  $D$ . We also have  $a$  denoting the state of the single qubit register  $\hat{A}$ .

$$V_{KL\hat{A}D_2}^a(B) = \left[ \sum_{k \in K; l \in L} |k, l, a\rangle \langle k, l, a| \otimes \left\{ (1-a) \left( B_{kl}I + i\sqrt{1-B_{kl}^2}Y \right) + a \left( (B_{kl}^T)'I + i\sqrt{1-(B_{kl}^T)^2}Y \right) \right\} + |k, l, 1-a\rangle \langle k, l, 1-a| \otimes I_2 \right] \quad (135)$$

Similarly, one can define the operator  $V_{EF\hat{A}D_3}^a(C)$ , as below, acting on qubits in registers,  $E, F, \hat{A}$  and the qubit 3 of register  $D$ . We also have  $a$  denoting the state of the single qubit register  $\hat{A}$ .

$$V_{EF\hat{A}D_3}^a(C) = \left[ \sum_{e \in E; f \in F} |e, f, a\rangle \langle e, f, a| \otimes \left\{ (1-a) \left( C_{ef}I + i\sqrt{1-C_{ef}^2}Y \right) + a \left( (C_{ef}^T)'I + i\sqrt{1-(C_{ef}^T)^2}Y \right) \right\} + |e, f, 1-a\rangle \langle e, f, 1-a| \otimes I_2 \right] \quad (136)$$

Then, one can observe that  $V_{IJ\hat{A}D_1}^a(A)V_{KL\hat{A}D_2}^a(B)V_{EF\hat{A}D_3}^a(C)H_IH_JH_KH_LH_EH_F$  satisfies

$$\begin{aligned} \langle i, j, k, l, e, f, 0, 0 | V_{IJ\hat{A}D_1}^a(A)V_{KL\hat{A}D_2}^a(B)V_{EF\hat{A}D_3}^a(C)H_IH_JH_KH_LH_EH_F | 0, 0, 0, 0, 0, 0, 0, 0 \rangle \\ = \frac{A_{ij}B_{kl}C_{ef}}{\sqrt{MNQRPS}} \end{aligned} \quad (137)$$

### 7.1.4 Quantum Circuit for Tensor Contraction

#### Theorem

If  $A, B$  are rectangular matrices with shapes  $M \times R$  and  $M \times Q$  then there exists a Unitary  $U(A, B)$  of dimension  $2^{n_m+n_r+n_q+3} \times 2^{n_m+n_r+n_q+3}$  that operates on a system of  $n_m + n_r + n_q + 3$  qubit registers  $|\cdot\rangle_I |\cdot\rangle_J |\cdot\rangle_K |\cdot\rangle_A |\cdot\rangle_D$  with  $I, J, K, A, D$  denoting the qubit-registers of size  $n_m, n_r, n_q, 1, 2$  and block encodes the tensor contraction  $\sum_i A_{ij} B_{ik}$  such that

$$\langle 0, j, 0, 0, 0 | U(A, B) | 0, 0, 0, 0, 0 \rangle = \frac{\sum_i A_{ij} B_{ik}}{M\sqrt{QR}} \quad (138)$$

#### Proof

We assume that  $A, B$  are normalized matrices, with  $\|A\| = 1, \|B\| = 1$ . Define the operator  $V_{IJ\hat{A}D_1}^a(A)$ , as below, acting on qubits in registers  $I, J, \hat{A}$  and the qubit 1 of register  $D$ . We also have  $a$  denoting the state of the single qubit register  $\hat{A}$ .

$$V_{IJ\hat{A}D_1}^a(A) = \left[ \sum_{j \in J; i \in I} |i, j, a\rangle \langle i, j, a| \otimes \left\{ (1-a) \left( A_{ij} I + i\sqrt{1-A_{ij}^2} Y \right) + a \left( (A_{ij}^T)' I + i\sqrt{1-(A_{ij}^T)^2} Y \right) \right\} + |i, j, 1-a\rangle \langle i, j, 1-a| \otimes I_2 \right] \quad (139)$$

Similarly, one can define the operator  $V_{IK\hat{A}D_2}^a(B)$ , as below, acting on qubits in registers  $I, K, \hat{A}$  and the qubit 2 of register  $D$ . We also have  $a$  denoting the state of the single qubit register  $\hat{A}$ .

$$V_{IK\hat{A}D_2}^a(B) = \left[ \sum_{k \in K; i \in I} |i, k, a\rangle \langle i, k, a| \otimes \left\{ (1-a) \left( B_{ik} I + i\sqrt{1-B_{ik}^2} Y \right) + a \left( (B_{ik}^T)' I + i\sqrt{1-(B_{ik}^T)^2} Y \right) \right\} + |i, k, 1-a\rangle \langle i, k, 1-a| \otimes I_2 \right] \quad (140)$$

Then, one can observe that  $H_I V_{IJ\hat{A}D_1}^a(A) V_{IK\hat{A}D_2}^a(B) H_I H_J H_K$  satisfies

$$\langle 0, j, k, 0, 0 | H_I V_{IJ\hat{A}D_1}^a(A) V_{IK\hat{A}D_2}^a(B) H_I H_J H_K | 0, 0, 0, 0, 0 \rangle = \frac{\sum_i A_{ij} B_{ik}}{M\sqrt{QR}} \quad (141)$$

### Theorem

If  $A, B, C$  are rectangular matrices with shapes  $M \times R, M \times Q, M \times S$  then there exists a Unitary  $U(A, B, C)$  of dimesnion  $2^{n_m+n_r+n_q+m_n+m_p+m_s+4} \times 2^{n_m+n_r+n_q+m_n+m_p+m_s+4}$  that operates on a system of  $n_m+n_r+n_q+m_n+m_p+m_s+4$  qubit registers  $|\cdot\rangle_I |\cdot\rangle_J |\cdot\rangle_K |\cdot\rangle_L |\cdot\rangle_A |\cdot\rangle_D$  with  $I, J, K, L, A, D$  denoting the qubit-registers of size  $n_m, n_r, m_n, n_q, m_p, m_s, 1, 2$  and block encodes the tensor contraction  $\sum_i A_{ij} B_{ik} C_{il}$  such that

$$\langle 0, j, k, l, 0, 0 | U(A, B, C) | 0, 0, 0, 0, 0, 0 \rangle = \frac{\sum_i A_{ij} B_{ik} C_{il}}{M\sqrt{QRS}} \quad (142)$$

### Proof

We assume that  $A, B$  are normalized matrices, with  $\|A\| = 1, \|B\| = 1$ . Define the operator  $V_{IJ\hat{A}D_1}^a(A)$ , as below, acting on qubits in registers  $I, J, \hat{A}$  and the qubit 1 of register  $D$ . We also have  $a$  denoting the state of the single qubit register  $\hat{A}$ .

$$V_{IJ\hat{A}D_1}^a(A) = \left[ \sum_{j \in J; i \in I} |i, j, a\rangle \langle i, j, a| \otimes \left\{ (1-a) \left( A_{ij} I + i\sqrt{1-A_{ij}^2} Y \right) + a \left( (A_{ij}^T)' I + i\sqrt{1-(A_{ij}^T)^2} Y \right) \right\} + |i, j, 1-a\rangle \langle i, j, 1-a| \otimes I_2 \right] \quad (143)$$

Similarly, one can define the operator  $V_{IK\hat{A}D_2}^a(B)$ , as below, acting on qubits in registers  $I, K, \hat{A}$  and the qubit 2 of register  $D$ . We also have  $a$  denoting the state of the single qubit register  $\hat{A}$ .

$$V_{IK\hat{A}D_2}^a(B) = \left[ \sum_{k \in K; i \in I} |i, k, a\rangle \langle i, k, a| \otimes \left\{ (1-a) \left( B_{ik} I + i\sqrt{1-B_{ik}^2} Y \right) + \right. \right.$$



$$a \left( (B_{ik}^T)'I + i\sqrt{1 - (B_{ik}^T)^2Y} \right) \left. \vphantom{a} \right\} + |i, k, 1 - a\rangle\langle i, k, 1 - a| \otimes I_2 \left. \vphantom{a} \right] \quad (144)$$

Similarly, one can define the operator  $V_{IL\hat{A}D_3}^a(B)$ , as below, acting on qubits in registers  $I, L, \hat{A}$  and the qubit 3 of register  $D$ . We also have  $a$  denoting the state of the single qubit register  $\hat{A}$ .

$$V_{IL\hat{A}D_2}^a(C) = \left[ \sum_{l \in L; i \in I} |i, l, a\rangle\langle i, l, a| \otimes \left\{ (1 - a) \left( B_{il}I + i\sqrt{1 - B_{il}^2Y} \right) + a \left( (B_{il}^T)'I + i\sqrt{1 - (B_{il}^T)^2Y} \right) \right\} + |i, l, 1 - a\rangle\langle i, l, 1 - a| \otimes I_2 \right] \quad (145)$$

Then, one can observe that  $H_I V_{IJ\hat{A}D_1}^a(A) V_{IK\hat{A}D_2}^a(B) V_{IL\hat{A}D_2}^a(C) H_I H_J H_K H_L$  satisfies

$$\langle 0, j, k, l, 0, 0 | H_I V_{IJ\hat{A}D_1}^a(A) V_{IK\hat{A}D_2}^a(B) H_I H_J H_K | 0, 0, 0, 0, 0, 0 \rangle = \frac{\sum_i A_{ij} B_{ik} C_{il}}{M\sqrt{QRS}} \quad (146)$$

Using the theorems developed in the above subsection, we describe different operations.

### 7.1.5 Tensor Contraction

For the contraction  $c_{ij} = a_{ik} b_{kj}$ , consider a quantum circuit with the registers in order  $I, K, A, D$ . Let  $a, b$  be of size  $2^m \times 2^p, 2^p \times 2^n$  respectively. We can also assume that  $m > n$ . Let the registers be of size  $m, p$  respectively. We define the circuit as

$$H_J V_{IK}^0(A) R_K V_{IK}^1(B) H_J \quad (147)$$

The above circuit encodes the term  $\frac{c_{ij}}{2^{m+p}}$  in the  $|i, 0, 0, 0\rangle$  state of the circuit. Note that  $R$  is the reflector as defined in the multiplication theorems.

The T-depth for implementing this operation is:

$$O\left(2^{m+p} \log \frac{1}{\epsilon}\right) \quad (148)$$

### 7.1.6 Tensor Dot

For the operation  $d_{ij} = a_{ix}b_{jx}$ , we consider a quantum circuit with the registers in order  $I, J, K, A, D$ . Let the tensors  $a, b$  be of size  $2^m \times 2^x, 2^n \times 2^x$ . Note that we are considering these sizes, as these are the types of tensors, we would be dealing with. Although the result below holds for other arbitrary shapes as well.

Let the registers be of size  $m, n, x, 1, 2$  respectively. Then

$$H_K V_{IK}^0(A) V_{JK}^0(B) H_I H_J H_K \quad (149)$$

encodes the tensors  $\frac{d_{ij}}{\sqrt{2^{m+n+2x}}}$ .

This can be implemented with t-depth

$$O\left(2^{m+x} \log \frac{1}{\epsilon}\right) + O\left(2^{n+x} \log \frac{1}{\epsilon}\right) \quad (150)$$

### 7.1.7 Hadamard Product

For the operation  $c_{ix} = a_{ix}b_{ix}$ , we consider a quantum circuit with the registers in order  $I, X, A, D$ . Let the tensors  $a, b$  be of size  $2^m \times 2^x$  and the registers be of size  $m, x, 1, 2$  respectively. Then,

$$V_{IX}^0(A) V_{IX}^0(B) H_I H_X \quad (151)$$

encodes the tensors  $\frac{d_{ij}}{\sqrt{2^{m+x}}}$ .

This can be implemented in a quantum circuit of depth

$$2 * O\left(2^{m+x} \log \frac{1}{\epsilon}\right) \quad (152)$$

The above theorems on different tensor operations can be summarized as follows:

- Multiplication: Load matrices on different states and sandwich a reflector between them. Use Hadamard gates to generate whole columns.

- Tensor Product: Load matrices on different sets of qubits.
- Tensor Contraction: Load matrices on different sets of qubits for different indices. Indices to be contracted share registers. Sandwich the contracted registers between Hadamard gates.

## 7.2 Complexity Analysis of Single Reference Recursive Hamiltonian Downfolding(Singles Doubles)

From the explicit form of residual equations given above, we can obtain closed form expressions for the two RHD(SD) amplitude equations that directly correspond to our more general multireference RHD formulation. The singles residual equation takes the form,

$$r_i^{1,(N)} = A_i^{1,(N)} + \sum_j A_{ji}^{2,(N)} t_j^{1,(N)} + \sum_{jk} A_{jki}^{3,(N)} t_j^{1,(N)} t_k^{1,(N)} + \sum_{akl} A_{klia}^{4,(N)} t_{akl}^{2,(N)} + \sum_{klc} A_{klc}^{5,(N)} t_l^{1,(N)} t_{cik}^{2,(N)} \quad (153)$$

And the doubles residual equation looks like,

$$r_{aij}^{2,(N)} = h_{aNij}^{2,(N)} + \sum_{kl} B_{klj}^{1,(N)} t_{akl}^{2,(N)} + \sum_b B_{ab}^{2,(N)} t_{bij}^{2,(N)} + \sum_{akb} B_{akb}^{3,(N)} t_{bij}^{2,(N)} t_k^{1,(N)} + B_a^{4,(N)} t_i^{1,(N)} t_j^{1,(N)} + \sum_{klc} B_{klc}^{5,(N)} t_{cil}^{2,(N)} t_{akj}^{2,(N)} \quad (154)$$

The terms corresponding to the tensors,  $A^{2,(N)}$ ,  $A^{4,(N)}$ ,  $B^{1,(N)}$  and  $B^{2,(N)}$  originate from the class of terms,  $\eta PHP$  and  $QHQ\eta$ , of the Bloch equation eq.(6). Whereas,  $A^{3,(N)}$ ,  $A^{5,(N)}$ ,  $B^{3,(N)}$ ,  $B^{4,(N)}$  and  $B^{5,(N)}$  comes from the  $\eta PHQ\eta$  class of terms. The terms  $A^{1,(N)}$  and ERI-slice ( $h_{aNij}^{2,(N)}$ ) can be attributed to the  $QHP$  expressions.

The Cholesky Decomposition of the ERI is carried out with a density fitted auxiliary basis

set of size  $N_{aux}$ . The mathematical form of the Cholesky factorization is given by,

$$h_{abij}^{2,(N)} \rightarrow \sum_x L_{xai} L_{xbj} \quad (155)$$

where  $L$  is the 3-rank Cholesky factor and  $x$  is the auxiliary basis direction. For the downfolding residual equations we need only slices of the ERI which are obtained by setting index  $a$  or  $b$  to  $N$ . A further tensor decomposition of the Cholesky factors is carried out using Convex Polyadic Alternating Least Squares Decomposition (CPALSD),<sup>69</sup> and is represented as,

$$L_{xai} \rightarrow \sum_p X_{xp} Y_{ap} Z_{ip} \quad (156)$$

Here  $X, Y, Z$  are 2-rank tensor factors of a 3-rank Cholesky factor ( $L$ ) and  $p$  indexes the Tensor factorization(TF) based auxiliary basis direction. The size of this auxiliary basis set arising from the decomposition of Cholesky factors is  $N_{htf}$ . Within downfolding, the doubles cluster amplitude is a 3-rank tensor that can be initialized in its tensor factorized representation as,

$$t_{aij}^{2,(N)} = \sum_r T_{ar} U_{ir} V_{jr} \quad (157)$$

Here  $T, U, V$  are the tensor factors and  $r$  indexes the auxiliary basis direction associated with the decomposition of the doubles cluster amplitudes. The size of this auxiliary basis set is given by  $N_{ttf}$ .

To study the operational scaling complexity of solving the residual equations, we will consider representative tensor factorized forms for each of the terms in both the singles and the doubles residual equations. In this section we will use i,j,k,l indices for occupied orbitals; a,b,c,d for virtual orbitals; x for auxiliary basis sets associated with the Cholesky Decomposition of ERIs; p,q for auxiliary basis sets associated with the tensor factorization of those Cholesky

factors; and  $r,s$  for the auxiliary basis sets associated with the factorization of doubles cluster amplitudes. All summations over  $i,j,k,l$  will range from 1 to  $N_o$ ;  $a,b,c,d$  from 1 to  $N_v$ ;  $x$  from 1 to  $N_{aux}$ ;  $p,q$  from 1 to  $N_{htf}$ ; and  $r,s$  from 1 to  $N_{ttf}$ . The relationship between  $N_o$ ,  $N_v$ ,  $N_{aux}$ ,  $N_{htf}$  and  $N_{ttf}$  can be written as,

$$N_{htf} > N_{aux} > N_{ttf} > N_v > N_o \quad (158)$$

We will, for the entirety of our calculations, contract the tensor factorized terms of the residual equation to their irreducible representations. As the convergence of a Downfolding recursion happens completely in terms of these irreducible representations, the operational complexity of Downfolding recursion goes down to  $\mathcal{O}(N^3)$ . In subsequent sections we will study the tensor decompositions of the terms in the residual equation in detail.

### 7.3 Implementing Downfolding Expressions on Quantum Circuits

To generate the quantum circuits for our residual equation let us setup the relevant notations. Consider quantum registers  $\tilde{P}, \tilde{Q}, \tilde{R}, \tilde{S}, \tilde{I}, \tilde{J}, \tilde{K}, \tilde{L}, \tilde{A}, \tilde{B}, \tilde{C}, \tilde{D}, \hat{A}_1, \hat{D}_{\{i\}}, \tilde{X}$  as following:

$$\tilde{P}, \tilde{Q} \in [N_{htf}] \quad (159)$$

$$\tilde{R}, \tilde{S} \in [N_{ttf}] \quad (160)$$

$$\tilde{I}, \tilde{J}, \tilde{K}, \tilde{L} \in [N_o] \quad (161)$$

$$\tilde{A}, \tilde{B}, \tilde{C}, \tilde{D} \in [N_v] \quad (162)$$

$$\tilde{X} \in [N_{aux}] \quad (163)$$

$$\hat{A}_1 \in [1] \quad (164)$$

$$\hat{D} \in [12] \quad (165)$$

Here,

1.  $\tilde{I}, \tilde{J}, \tilde{K}, \tilde{L}$  are qubit registers of size  $\log_2 N_o$

2.  $\tilde{A}, \tilde{B}, \tilde{C}$  are qubit registers of size  $\log_2 N_v$
3.  $\tilde{X}$  is a qubit register of size  $\log_2 N_{aux}$
4.  $\tilde{P}, \tilde{Q}$  are qubit registers of size  $\log_2 N_{htf}$
5.  $\tilde{R}, \tilde{S}$  are qubit registers of size  $\log_2 N_{ttf}$
6.  $\hat{A}_1$  is a single qubit ancilla to facilitate contraction.
7.  $\hat{D}$  is a qubit register of size 12 num tensors.
8. For quantum circuit representation purposes (Fig.5), four of the tensor factorization direction quantum registers, P,Q,R,S, are clubbed into a single register category, TF, which in turn can be partitioned into 4 groups:
  - (a) Group-1:  $[1, \log_2(N_{htf})]$
  - (b) Group-2:  $[\log_2(N_{htf}) + 1, 2\log_2(N_{htf})]$
  - (c) Group-3:  $[2\log_2(N_{htf}) + 1, 2\log_2(N_{htf}) + \log_2(N_{ttf})]$
  - (d) Group-4:  $[2\log_2(N_{htf}) + \log_2(N_{ttf}) + 1, 2\log_2(N_{htf}) + 2\log_2(N_{ttf})]$
9. Each  $V(\cdot)$  gate acts on a unique  $D_i \in \hat{D}$ .
10. Corresponding to each term, the  $V(\cdot)$  gates acting with  $X, Y, Z$  as input operate on the qubits in Group-1 and Group-2 of TF.
11. The gates  $V(\cdot)$  acting with  $T, U, V$  as input operate on the qubits in Group-3 and Group-4 of TF.
12. For any arbitrary tensor  $G$ , we denote terms of the form  $V_{IJ}^0(G)$  acting on qubits of registers  $I, J$  and qubits  $A_1, D_i$  as  $V_{IJ,i}(G)$

### 7.3.1 Depth of a Quantum Circuit in S,CNOT,H,T basis that block encodes a two-rank tensor

For any arbitrary tensor  $G$  of shape  $N, M$ , the operation  $V_{IJ,i}(G)$  has a depth of

$$2NM \log_2 \left( \frac{1}{\epsilon} \right) \quad (166)$$

The starting and final Hadamard layers contribute to a depth of 2.

### 7.3.2 Expression 1

The first term of the singles residual equation (eq. 153) is generated from the  $QHP$  class of terms in the Bloch equation. It is given by the vector-projection of the fock matrix along the  $N$ th molecular orbital as,

$$A_i^{1,(N)} \rightarrow f_{Ni} \quad (167)$$

The Quantum Circuit for representing this tensor is given by,

$$V_{\bar{I},1}(X)H_{\bar{I}} \quad (168)$$

And the depth of this Quantum Circuit is,

$$2N_o \log_2(1/\epsilon) \quad (169)$$

### 7.3.3 Expression 2

The second term of singles residual equation (153) is generated from both the  $\eta PHP$  and  $QH Q \eta$  classes of terms in the Bloch equation. Also, there will be two separate forms for this term, one coming from the fock part of the Hamiltonian and other from the ERI. The

fock contribution can be written as,

$$\sum_j A_{ji}^{2,(N)} t_j^{1,(N)} \rightarrow \sum_k f_{ji}^{(N)} t_j^{1,(N)} \quad (170)$$

The order of complexity for contracting this term to its irreducible representation is  $\mathcal{O}(N_o^2)$ . The ERI contribution to this term in the residual equation can originate from different components of the ERI,  $h_{NjNi}^{2,(N)}$ ,  $h_{jNni}^{2,(N)}$ ,  $h_{NjiN}^{2,(N)}$ ,  $h_{jNiN}^{2,(N)}$ . Here we will show the  $h_{jNni}^{2,(N)}$  contribution in its tensor factorized form below,

$$\sum_j A_{ji}^{2,(N)} t_j^{1,(N)} \rightarrow \sum_j \sum_{xpq} X_{xp} Y_{jp} Z_{Np} X_{xq} Y_{Nq} Z_{iq} t_j^{1,(N)} \quad (171)$$

A similar factorization is performed for all four contributions from ERI. The diagrammatic representation of this decomposition is shown in figure 3a. The contraction path to an irreducible representation can be written as,

$$\begin{aligned} & \overbrace{xp, jp, p, xq, q, iq, j}^{\square} \quad \mathcal{O}(2N_{htf}N_o) \\ \rightarrow & \overbrace{p, iq, xp, p, xq}^{\square} \quad \mathcal{O}(N_{htf}) \\ \rightarrow & \overbrace{p, iq, xp, xq}^{\square} \quad \mathcal{O}(N_{htf}N_{aux}) \\ \rightarrow & \overbrace{x, iq, xq}^{\square} \quad \mathcal{O}(N_{htf}N_{aux}) \\ \rightarrow & \overbrace{q, iq}^{\square} \quad \mathcal{O}(N_{htf}N_o) \\ \rightarrow & i \end{aligned} \quad (172)$$

The complexity for this contraction is given by,

$$\mathcal{O}(2N_{htf}N_{aux} + 3N_{htf}N_o + N_{htf}) \quad (173)$$



The Quantum Circuit for representing this set of tensor operations is given by,

$$\begin{aligned}
& H_{\tilde{X}} H_{\tilde{P}} H_{\tilde{Q}} H_{\tilde{J}} V_{\tilde{X}\tilde{P},1}(X) V_{\tilde{J}\tilde{P},2}(Y) V_{\tilde{P},3}(Z) V_{\tilde{X}\tilde{Q},4}(X) V_{\tilde{Q},5}(Y) V_{\tilde{I}\tilde{Q},6}(Z) V_{\tilde{J},7}(T^{1,(N)}) \\
& H_{\tilde{I}} H_{\tilde{X}} H_{\tilde{P}} H_{\tilde{Q}} H_{\tilde{J}}
\end{aligned} \tag{174}$$

The diagrammatic representation of this circuit is given in figure 5a. The depth of this Quantum Circuit is,

$$2(2N_{aux}N_{htf} + 2N_oN_{htf} + 2N_{htf} + N_o)\log_2(1/\epsilon) \tag{175}$$

$$\tag{176}$$

### 7.3.4 Expression 3

The third term of singles residual equation (153) is generated from the  $\eta PHQ\eta$  class of terms in the Bloch equation. This term is generated from two different slices of the ERI tensor,  $h_{jkiN}^{2,(N)}$  and  $h_{jkNi}^{2,(N)}$ . We show the tensor factorized representation of the  $h_{jkiN}^{2,(N)}$  contribution below,

$$\sum_{jk} A_{jki}^{3,(N)} t_j^{1,(N)} t_k^{1,(N)} \rightarrow \sum_{jk} \sum_{xpq} X_{xp} Y_{jp} Z_{ip} X_{xq} Y_{kq} Z_{Nq} t_j^{1,(N)} t_k^{1,(N)} \tag{177}$$

The diagrammatic representation of this decomposition is shown in figure 3b. The contraction path to an irreducible representation is given by,

$$\begin{aligned}
& \overbrace{xp, jp, ip, xq, kq, q, j, k} \quad \mathcal{O}(2N_{htf}N_o) \\
\rightarrow & \overbrace{p, q, xp, ip, xq, q} \quad \mathcal{O}(N_{htf}N_o + N_{htf}) \\
\rightarrow & \overbrace{ip, q, xp, xq} \quad \mathcal{O}(N_{htf}N_{aux}) \\
\rightarrow & \overbrace{x, ip, xp} \quad \mathcal{O}(N_{htf}N_{aux}) \\
\rightarrow & \overbrace{p, ip} \quad \mathcal{O}(N_{htf}N_o)
\end{aligned}$$

$$\rightarrow i \quad (178)$$

The total complexity of this calculation is given by,

$$\mathcal{O}(2N_{htf}N_{aux} + 4N_{htf}N_o + N_{htf}) \quad (179)$$

The Quantum Circuit representing this set of tensor operations is given by,

$$\begin{aligned} & H_{\tilde{X}}H_{\tilde{P}}H_{\tilde{Q}}H_{\tilde{J}}H_{\tilde{K}}V_{\tilde{X}\tilde{P},1}(X)V_{\tilde{J}\tilde{P},2}(Y)V_{\tilde{I}\tilde{P},3}(Z)V_{\tilde{X}\tilde{Q},4}(X)V_{\tilde{K}\tilde{Q},5}(Y)V_{\tilde{Q},6}(Z)V_{\tilde{J},7}(T^{1,(N)})V_{\tilde{K},8}(T^{1,(N)}) \\ & H_{\tilde{I}}H_{\tilde{X}}H_{\tilde{P}}H_{\tilde{Q}}H_{\tilde{J}}H_{\tilde{K}} \end{aligned} \quad (180)$$

The diagrammatic representation of this circuit is given in figure 5b. The depth of this Quantum Circuit is,

$$2(2N_{aux}N_{htf} + 3N_oN_{htf} + N_{htf} + 2N_o)\log_2(1/\epsilon) \quad (181)$$

### 7.3.5 Expression 4

The fourth term of the singles residual equation(153) is generated from both the  $\eta PHP$  and  $QH Q\eta$  terms in the Bloch equation. This can be generated from four different slices of the ERI tensor,  $h_{klia}^{2,(N)}$ ,  $h_{klai}^{2,(N)}$ ,  $h_{lkia}^{2,(N)}$  and  $h_{lkai}^{2,(N)}$ . The tensor factorized representation of the  $h_{klia}^{2,(N)}$  contribution is given by,

$$\sum_{kla} A_{klia}^{4,(N)} t_{akl}^{2,(N)} \rightarrow \sum_{kla} \sum_{xpqr} X_{xp} Y_{kp} Z_{ip} X_{xq} Y_{lq} Z_{aq} T_{ar} U_{kr} V_{lr} \quad (182)$$

The diagrammatic representation of this decomposition is shown in figure 3c. The contraction path to an irreducible representation can be written as,

$$\overbrace{xp, kp, ip, xq, lq, aq, ar, kr, lr} \quad \mathcal{O}(2N_{htf}N_{ttf}N_o + N_{htf}N_{ttf}N_v)$$

$$\begin{aligned}
&\rightarrow \overbrace{pr, qr, qr, xp, ip, xq} \quad \mathcal{O}(N_{htf}N_{ttf}) \\
&\rightarrow \overbrace{qr, pr, xp, ip, xq} \quad \mathcal{O}(N_{htf}N_{ttf}N_{aux}) \\
&\rightarrow \overbrace{xr, pr, xp, ip} \quad \mathcal{O}(N_{htf}N_{ttf}N_{aux}) \\
&\rightarrow \overbrace{xp, xp, ip} \quad \mathcal{O}(N_{htf}N_{aux}) \\
&\rightarrow \overbrace{p, ip} \quad \mathcal{O}(N_{htf}N_o) \\
&\rightarrow i
\end{aligned} \tag{183}$$

The total complexity of this calculation is given by,

$$\mathcal{O}(2N_{htf}N_{ttf}N_{aux} + 2N_{htf}N_{ttf}N_o + N_{htf}N_{ttf}N_v + N_{htf}N_{aux} + N_{htf}N_{ttf} + N_{htf}N_o) \tag{184}$$

The Quantum Circuit representing this set of tensor operations is given by,

$$\begin{aligned}
&H_{\tilde{X}}H_{\tilde{P}}H_{\tilde{Q}}H_{\tilde{R}}H_{\tilde{K}}H_{\tilde{L}}H_{\tilde{A}}V_{\tilde{X}\tilde{P},1}(X)V_{\tilde{K}\tilde{P},2}(Y)V_{\tilde{I}\tilde{P},3}(Z)V_{\tilde{X}\tilde{Q},4}(X)V_{\tilde{L}\tilde{Q},5}(Y)V_{\tilde{A}\tilde{Q},6}(Z) \\
&V_{\tilde{A}\tilde{R},7}(T)V_{\tilde{K}\tilde{R},8}(U)V_{\tilde{L}\tilde{R},9}(V)H_{\tilde{I}}H_{\tilde{X}}H_{\tilde{P}}H_{\tilde{Q}}H_{\tilde{R}}H_{\tilde{K}}H_{\tilde{L}}H_{\tilde{A}}
\end{aligned} \tag{185}$$

The diagrammatic representation of this circuit is given in figure 5c. The depth of this Quantum Circuit is,

$$2(2N_{aux}N_{htf} + 3N_oN_{htf} + N_vN_{htf} + 2N_oN_{ttf} + N_vN_{ttf})\log_2(1/\epsilon) \tag{186}$$

### 7.3.6 Expression 5

The fifth term of the singles residual equation(153) is generated from the  $\eta PHQ\eta$  class of terms in the Bloch equation. It contains contributions from four different slices of the ERI tensor,  $h_{klcN}^{2,(N)}$ ,  $h_{klNc}^{2,(N)}$ ,  $h_{lkcN}^{2,(N)}$  and  $h_{lkNc}^{2,(N)}$ . And, for all the ERI slices, there will be contributions from two different forms of the doubles cluster amplitudes,  $t_{cik}^{2,(N)}$  and  $t_{cki}^{2,(N)}$ . The tensor factorized representation of the contribution from a combination of  $h_{klcN}^{2,(N)}$  and  $t_{cik}^{2,(N)}$  is given

by,

$$\sum_{klc} A_{klc}^{5,(N)} t_l^{1,(N)} t_{cik}^{2,(N)} \rightarrow \sum_{klc} \sum_{xpqr} X_{xp} Y_{kp} Z_{cp} X_{xq} Y_{lq} Z_{Nq} t_l^{1,(N)} T_{cr} U_{ir} V_{kr} \quad (187)$$

The diagrammatic representation of this decomposition is shown in figure 3d. The contraction path to an irreducible representation can be written as,

$$\begin{aligned} & \overbrace{xp, kp, cp, xq, lq, q, l, cr, ir, kr} \quad \mathcal{O}(N_{htf} N_{ttf} N_o + N_{htf} N_{ttf} N_v + N_{htf} N_o) \\ \rightarrow & \overbrace{pr, pr, q, xp, xq, q, ir} \quad \mathcal{O}(N_{htf} N_{ttf} + N_{htf}) \\ \rightarrow & \overbrace{pr, q, xp, xq, ir} \quad \mathcal{O}(N_{htf} N_{aux}) \\ \rightarrow & \overbrace{x, pr, xp, ir} \quad \mathcal{O}(N_{htf} N_{aux}) \\ \rightarrow & \overbrace{p, pr, ir} \quad \mathcal{O}(N_{htf} N_{ttf}) \\ \rightarrow & \overbrace{r, ir} \quad \mathcal{O}(N_{ttf} N_o) \\ \rightarrow & i \end{aligned} \quad (188)$$

The total complexity of this calculation is given by,

$$\mathcal{O}(N_{htf} N_{ttf} N_o + N_{htf} N_{ttf} N_v + N_{htf} N_o + 2N_{htf} N_{ttf} + 2N_{htf} N_{aux} + N_{ttf} N_o + N_{htf}) \quad (189)$$

The Quantum Circuit representing this set of tensor operations is given by,

$$\begin{aligned} & H_{\tilde{X}} H_{\tilde{P}} H_{\tilde{Q}} H_{\tilde{R}} H_{\tilde{K}} H_{\tilde{L}} H_{\tilde{C}} V_{\tilde{X}\tilde{P},1}(X) V_{\tilde{K}\tilde{P},2}(Y) V_{\tilde{C}\tilde{P},3}(Z) V_{\tilde{X}\tilde{Q},4}(X) V_{\tilde{L}\tilde{Q},5}(Y) V_{\tilde{Q},6}(Z) V_{\tilde{L},7}(T^{1,(N)}) \\ & V_{\tilde{C}\tilde{R},8}(T) V_{\tilde{I}\tilde{R},9}(U) V_{\tilde{K}\tilde{R},10}(V) H_{\tilde{I}} H_{\tilde{X}} H_{\tilde{P}} H_{\tilde{Q}} H_{\tilde{R}} H_{\tilde{K}} H_{\tilde{L}} H_{\tilde{C}} \end{aligned} \quad (190)$$

The diagrammatic representation of this circuit is given in figure 5d. The depth of this Quantum Circuit is,

$$2(2N_{aux} N_{htf} + 2N_o N_{htf} + N_v N_{htf} + N_{htf} + N_o + 2N_o N_{ttf} + N_v N_{ttf}) \log_2(1/\epsilon) \quad (191)$$

### 7.3.7 Expression 6

The first term of the doubles residual equation(154) is generated from the *QHP* class of terms in the Bloch equation. It is generated from an ERI tensor slice along the direction of the *N*th molecular orbital,  $h_{aNij}^{2,(N)}$ . The tensor factorized representation of this term is given by,

$$h_{aNij}^{2,(N)} \rightarrow \sum_{xpq} X_{xp} Y_{ap} Z_{ip} X_{xq} Y_{Nq} Z_{jq} \quad (192)$$

The diagrammatic representation of this decomposition is shown in figure 4a. The contraction path to an irreducible representation can be written as,

$$\begin{aligned} & xp, ap, ip, xq, \overline{q}, \overline{jq} \quad \mathcal{O}(N_{htf}N_o) \\ \rightarrow & \overline{jq}, xp, ap, ip, xq \quad \mathcal{O}(N_{htf}N_{aux}N_o) \\ \rightarrow & \overline{jx}, xp, ap, ip \quad \mathcal{O}(N_{htf}N_{aux}N_o) \\ \rightarrow & jp, ap, ip \end{aligned} \quad (193)$$

The total complexity of this calculation is given by,

$$\mathcal{O}(2N_{htf}N_{aux}N_o + N_{htf}N_o) \quad (194)$$

The Quantum Circuit representing this set of tensor operations is given by,

$$H_{\tilde{X}} H_{\tilde{P}} H_{\tilde{Q}} V_{\tilde{X}\tilde{P},1}(X) V_{\tilde{A}\tilde{P},2}(Y) V_{\tilde{I}\tilde{P},3}(Z) V_{\tilde{X}\tilde{Q},4}(X) V_{\tilde{Q},5}(Y) V_{\tilde{J}\tilde{Q},6}(Z) H_{\tilde{A}} H_{\tilde{I}} H_{\tilde{J}} H_{\tilde{X}} H_{\tilde{P}} H_{\tilde{Q}} \quad (195)$$

The diagrammatic representation of this circuit is given in figure 5e. The depth of this Quantum Circuit is,

$$2(2N_{aux}N_{htf} + 2N_oN_{htf} + N_vN_{htf} + N_{htf})\log_2(1/\epsilon) \quad (196)$$

### 7.3.8 Expression 7

The second term of the doubles residual equation(154) is generated from contributions from both  $\eta PHP$  and  $QHQ\eta$  classes of terms in the Bloch equation. There will be contributions from two different slices of the ERI tensor,  $h_{kl ij}^{2,(N)}$  and  $h_{lk ij}^{2,(N)}$ . The tensor factorized representation of the  $h_{kl ij}^{2,(N)}$  can be written as,

$$\sum_{kl} B_{kl ij}^{1,(N)} t_{akl}^{2,(N)} \rightarrow \sum_{kl} \sum_{x p q r} X_{xp} Y_{kp} Z_{ip} X_{xq} Y_{lq} Z_{jq} T_{ar} U_{kr} V_{lr} \quad (197)$$

The diagrammatic representation of this decomposition is shown in figure 4b. The contraction path to an irreducible representation can be written as,

$$\begin{array}{l} \overbrace{xp, kp, ip, xq, lq, jq, ar, kr, lr} \\ \rightarrow pq, pr, qr, ip, jq, ar \end{array} \quad \mathcal{O}(N_{htf} N_{ttf} N_{aux} + 2N_{htf} N_{ttf} N_o) \quad (198)$$

The total complexity of this calculation is given by,

$$\mathcal{O}(N_{htf} N_{ttf} N_{aux} + 2N_{htf} N_{ttf} N_o) \quad (199)$$

The Quantum Circuit representing this set of tensor operations is given by,

$$\begin{array}{l} H_{\tilde{X}} H_{\tilde{P}} H_{\tilde{Q}} H_{\tilde{R}} H_{\tilde{K}} H_{\tilde{L}} V_{\tilde{X}\tilde{P},1}(X) V_{\tilde{K}\tilde{P},2}(Y) V_{\tilde{I}\tilde{P},3}(Z) V_{\tilde{X}\tilde{Q},4}(X) V_{\tilde{L}\tilde{Q},5}(Y) V_{\tilde{J}\tilde{Q},6}(Z) \\ V_{\tilde{A}\tilde{R},7}(T) V_{\tilde{K}\tilde{R},8}(U) V_{\tilde{L}\tilde{R},9}(V) H_{\tilde{A}} H_{\tilde{I}} H_{\tilde{J}} H_{\tilde{X}} H_{\tilde{P}} H_{\tilde{Q}} H_{\tilde{R}} H_{\tilde{K}} H_{\tilde{L}} \end{array} \quad (200)$$

The diagrammatic representation of this circuit is given in figure 5f. The depth of this Quantum Circuit is,

$$2(2N_{aux} N_{htf} + 4N_o N_{htf} + 2N_o N_{ttf} + N_v N_{ttf}) \log_2(1/\epsilon) \quad (201)$$

### 7.3.9 Expression 8

The third term of the doubles residual equation(154) is generated from both  $\eta PHP$  and  $QH Q\eta$  classes of terms in the Bloch equation. There will be contributions from both the fock and the ERI components of the second quantized Hamiltonian. The fock contribution can be represented as,

$$\sum_b B_{ab}^{2,(N)} t_{bij}^{2,(N)} \rightarrow \sum_b \sum_r f_{ab}^{(N)} T_{br} U_{ir} V_{jr} \quad (202)$$

The contraction path towards an irreducible tensor decomposed form is given by,

$$\begin{aligned} & \overline{ab, br, ir, jr} \quad \mathcal{O}(N_{ttf} N_v^2) \\ & \rightarrow ar, ir, jr \end{aligned} \quad (203)$$

The more complex contributions arise from different slices of the ERI tensor,  $h_{aNbN}^{2,(N)}$  and  $h_{aNNb}^{2,(N)}$ . The tensor representation of the  $h_{aNNb}^{2,(N)}$  contribution is given by,

$$\sum_b B_{ab}^{2,(N)} t_{bij}^{2,(N)} \rightarrow \sum_b \sum_{xpqr} X_{xp} Y_{ap} Z_{Np} X_{xq} Y_{Nq} Z_{bq} T_{br} U_{ir} V_{jr} \quad (204)$$

The diagrammatic representation of this decomposition is shown in figure 4c. The contraction path to an irreducible representation can be written as,

$$\begin{aligned} & xp, \overline{ap, p}, \overline{xq, q}, bq, br, ir, jr \quad \mathcal{O}(2N_{htf} N_v) \\ & \rightarrow \overline{ap, bq, xp, xq}, br, ir, jr \quad \mathcal{O}(2N_{htf} N_{aux} N_v) \\ & \rightarrow \overline{ax, bx}, br, ir, jr \quad \mathcal{O}(N_{aux} N_v^2) \\ & \rightarrow \overline{ab, br}, ir, jr \quad \mathcal{O}(N_{ttf} N_v^2) \\ & \rightarrow ar, ir, jr \end{aligned} \quad (205)$$

The total complexity of this calculation is given by,

$$\mathcal{O}(2N_{htf}N_{aux}N_v + N_{aux}N_v^2 + N_{ttf}N_v^2 + 2N_{htf}N_v) \quad (206)$$

The Quantum Circuit representing this set of tensor operations is given by,

$$\begin{aligned} & H_{\tilde{X}}H_{\tilde{P}}H_{\tilde{Q}}H_{\tilde{R}}H_{\tilde{B}}V_{\tilde{X}\tilde{P},1}(X)V_{\tilde{A}\tilde{P},2}(Y)V_{\tilde{P},3}(Z)V_{\tilde{X}\tilde{Q},4}(X)V_{\tilde{Q},5}(Y)V_{\tilde{B}\tilde{Q},6}(Z) \\ & V_{\tilde{B}\tilde{R},7}(T)V_{\tilde{I}\tilde{R},8}(U)V_{\tilde{J}\tilde{R},9}(V)H_{\tilde{A}}H_{\tilde{I}}H_{\tilde{J}}H_{\tilde{X}}H_{\tilde{P}}H_{\tilde{Q}}H_{\tilde{R}}H_{\tilde{B}} \end{aligned} \quad (207)$$

The diagrammatic representation of this circuit is given in figure 5g. The depth of this Quantum Circuit is,

$$2(2N_{aux}N_{htf} + 2N_vN_{htf} + 2N_{htf} + 2N_oN_{ttf} + N_vN_{ttf})\log_2(1/\epsilon) \quad (208)$$

### 7.3.10 Expression 9

The fourth term of the doubles residual equation(154) is generated from the  $\eta PHQ\eta$  class of terms in the Bloch equation. It contains contributions from two different slices of the ERI tensor,  $h_{akbN}^{2,(N)}$  and  $h_{akNb}^{2,(N)}$ . The tensor factorized representation of the  $h_{akbN}^{2,(N)}$  contribution is given by,

$$\sum_{kb} B_{akb}^{3,(N)} t_{bij}^{2,(N)} t_k^{1,(N)} \rightarrow \sum_{kb} \sum_{xpqr} X_{xp} Y_{ap} Z_{bp} X_{xq} Y_{kq} Z_{Nq} T_{br} U_{ir} V_{jr} t_k^{1,(N)} \quad (209)$$

The diagrammatic representation of this decomposition is shown in figure 4d. The contraction path to an irreducible representation can be written as,

$$\begin{aligned} & \overbrace{xp, ap, bp, xq, kq, q, br, ir, jr, k} \quad \mathcal{O}(N_{htf}N_{ttf}N_v + N_{htf}N_o) \\ \rightarrow & \overbrace{pr, q, xp, ap, xq, q, ir, jr} \quad \mathcal{O}(N_v) \\ \rightarrow & \overbrace{q, pr, xp, ap, xq, ir, jr} \quad \mathcal{O}(N_{htf}N_{aux}) \end{aligned}$$



$$\begin{aligned}
&\rightarrow \overbrace{x, pr, xp, ap, ir, jr} \quad \mathcal{O}(N_{htf}N_{aux}) \\
&\rightarrow \overbrace{p, pr, ap, ir, jr} \quad \mathcal{O}(N_{htf}N_v) \\
&\rightarrow \overbrace{ap, pr, ir, jr} \quad \mathcal{O}(N_{htf}N_{ttf}N_v) \\
&\rightarrow ar, ir, jr
\end{aligned} \tag{210}$$

The total complexity of this calculation is given by,

$$\mathcal{O}(2N_{htf}N_{ttf}N_v + 2N_{htf}N_{aux} + N_{htf}N_v + N_{htf}N_o + N_v) \tag{211}$$

The Quantum Circuit representing this set of tensor operations is given by,

$$\begin{aligned}
&H_{\tilde{X}}H_{\tilde{P}}H_{\tilde{Q}}H_{\tilde{R}}H_{\tilde{K}}H_{\tilde{B}}V_{\tilde{X}\tilde{P},1}(X)V_{\tilde{A}\tilde{P},2}(Y)V_{\tilde{B}\tilde{P},3}(Z)V_{\tilde{X}\tilde{Q},4}(X)V_{\tilde{K}\tilde{Q},5}(Y)V_{\tilde{Q},6}(Z)V_{\tilde{B}\tilde{R},7}(T) \\
&V_{\tilde{I}\tilde{R},8}(U)V_{\tilde{J}\tilde{R},9}(V)V_{\tilde{K},10}(T^{1,(N)})H_{\tilde{A}}H_{\tilde{I}}H_{\tilde{J}}H_{\tilde{X}}H_{\tilde{P}}H_{\tilde{Q}}H_{\tilde{R}}H_{\tilde{K}}H_{\tilde{B}}
\end{aligned} \tag{212}$$

The diagrammatic representation of this circuit is given in figure 5h. The depth of this Quantum Circuit is,

$$2(2N_{aux}N_{htf} + 2N_vN_{htf} + N_{htf}N_o + N_{htf} + N_o + 2N_oN_{ttf} + N_vN_{ttf})\log_2(1/\epsilon) \tag{213}$$

### 7.3.11 Expression 10

The fifth term of the doubles residual equation(154) is generated from the  $\eta PHQ\eta$  class of terms in the Bloch equation. It contains contributions from both the fock and the ERI components of the Hamiltonian. The fock contribution is directly in its tensor decomposed form given by,

$$B_a^{4,(N)}t_i^{1,(N)}t_j^{1,(N)} \rightarrow f_{aN}^{(N)}t_i^{1,(N)}t_j^{1,(N)} \tag{214}$$

A more complex ERI contribution comes from two different slices of ERI,  $h_{NaNN}^{2,(N)}$  and  $h_{aNNN}^{2,(N)}$ . The  $h_{aNNN}^{2,(N)}$  contribution is given by,

$$B_a^{4,(N)} t_i^{1,(N)} t_j^{1,(N)} \rightarrow \sum_{xpq} X_{xp} Y_{ap} Z_{Np} X_{xq} Y_{Nq} Z_{Nq} t_i^{1,(N)} t_j^{1,(N)} \quad (215)$$

The diagrammatic representation of this decomposition is shown in figure 4e. The contraction path to an irreducible representation can be written as,

$$\begin{aligned} & xp, \overbrace{ap, p}, \overbrace{xq, q}, q, i, j \quad \mathcal{O}(N_{htf} N_v + N_{htf}) \\ \rightarrow & \overbrace{ap, q, xp, xq}, i, j \quad \mathcal{O}(N_{htf} N_{aux}) \\ \rightarrow & \overbrace{x, ap, xp}, i, j \quad \mathcal{O}(N_{htf} N_{aux}) \\ \rightarrow & \overbrace{p, ap}, i, j \quad \mathcal{O}(N_{htf} N_v) \\ \rightarrow & a, i, j \end{aligned} \quad (216)$$

The total complexity of this calculation is given by,

$$\mathcal{O}(2N_{htf} N_v + 2N_{htf} N_{aux} + N_{htf}) \quad (217)$$

The Quantum Circuit representing this set of tensor operations is given by,

$$\begin{aligned} & H_{\tilde{X}} H_{\tilde{P}} H_{\tilde{Q}} V_{\tilde{X}\tilde{P},1}(X) V_{\tilde{A}\tilde{P},2}(Y) V_{\tilde{P},3}(Z) V_{\tilde{X}\tilde{Q},4}(X) V_{\tilde{Q},5}(Y) V_{\tilde{Q},6}(Z) V_{\tilde{I},7}(T^{1,(N)}) V_{\tilde{J},8}(T^{1,(N)}) \\ & H_{\tilde{A}} H_{\tilde{I}} H_{\tilde{J}} H_{\tilde{X}} H_{\tilde{P}} H_{\tilde{Q}} \end{aligned} \quad (218)$$

The diagrammatic representation of this circuit is given in figure 5i. The depth of this Quantum Circuit is,

$$2(2N_{aux} N_{htf} + N_v N_{htf} + 2N_{htf} + 2N_o) \log_2(1/\epsilon) \quad (219)$$

### 7.3.12 Expression 11

The sixth term of the doubles residual equation(154) is generated from  $\eta PHQ\eta$  class of terms in the Bloch Equation. It contains contributions from two different slices of ERI,  $h_{klcN}^{2,(N)}$  and  $h_{klNc}^{2,(N)}$ . The tensor factorized form of the  $h_{klcN}^{2,(N)}$  contribution is given by,

$$\sum_{klc} B_{klc}^{5,(N)} t_{cil}^{2,(N)} t_{akj}^{2,(N)} \rightarrow \sum_{klc} \sum_{xpqrs} X_{xp} Y_{kp} Z_{cp} X_{xq} Y_{lq} Z_{Nq} T_{cr} U_{ir} V_{lr} T_{as} U_{ks} V_{js} \quad (220)$$

The diagrammatic representation of this decomposition is shown in figure 4f. The contraction path to an irreducible representation can be written as,

$$\begin{aligned} & \overbrace{xp, kp, cp, xq, lq, q, cr, ir, lr, as, ks, js} \quad \mathcal{O}(N_{htf}N_{ttf}N_o + N_{htf}N_{ttf}N_v + N_{htf}N_o) \\ \rightarrow & \overbrace{ps, pr, lq, xp, xq, ir, lr, as, js} \quad \mathcal{O}(N_{htf}N_{ttf}N_o) \\ \rightarrow & \overbrace{qr, ps, pr, xp, xq, ir, as, js} \quad \mathcal{O}(N_{htf}N_{ttf}N_{aux}) \\ \rightarrow & \overbrace{xr, ps, pr, xp, ir, as, js} \quad \mathcal{O}(N_{htf}N_{ttf}N_{aux}) \\ \rightarrow & \overbrace{pr, ps, pr, ir, as, js} \quad \mathcal{O}(N_{htf}N_{ttf}) \\ \rightarrow & \overbrace{pr, ps, ir, as, js} \quad \mathcal{O}(N_{htf}N_{ttf}N_o) \\ \rightarrow & \overbrace{pi, ps, as, js} \quad \mathcal{O}(N_{htf}N_{ttf}N_o) \\ \rightarrow & is, as, js \end{aligned} \quad (221)$$

The total complexity of this calculation is given by,

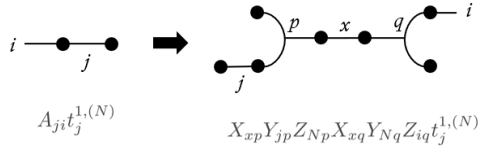
$$\mathcal{O}(2N_{htf}N_{ttf}N_{aux} + N_{htf}N_{ttf}N_v + 4N_{htf}N_{ttf}N_o + N_{htf}N_{ttf} + N_{htf}N_o) \quad (222)$$

The Quantum Circuit representing this set of tensor operations is given by,

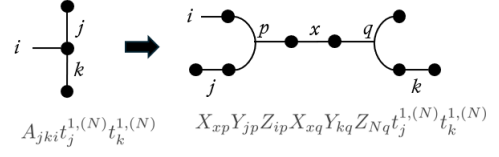
$$\begin{aligned} & H_{\tilde{X}} H_{\tilde{P}} H_{\tilde{Q}} H_{\tilde{R}} H_{\tilde{K}} H_{\tilde{L}} H_{\tilde{C}} V_{\tilde{X}\tilde{P},1}(X) V_{\tilde{K}\tilde{P},2}(Y) V_{\tilde{C}\tilde{P},3}(Z) V_{\tilde{X}\tilde{Q},4}(X) V_{\tilde{L}\tilde{Q},5}(Y) V_{\tilde{Q},6}(Z) V_{\tilde{C}\tilde{R},7}(T) \\ & V_{\tilde{I}\tilde{R},8}(U) V_{\tilde{L}\tilde{R},9}(V) V_{\tilde{A}\tilde{S},10}(T) V_{\tilde{K}\tilde{S},11}(U) V_{\tilde{J}\tilde{S},12}(V) H_{\tilde{A}} H_{\tilde{I}} H_{\tilde{J}} H_{\tilde{X}} H_{\tilde{P}} H_{\tilde{Q}} H_{\tilde{R}} H_{\tilde{K}} H_{\tilde{L}} H_{\tilde{C}} \end{aligned} \quad (223)$$

The diagrammatic representation of this circuit is given in figure 5j. The depth of this Quantum Circuit is,

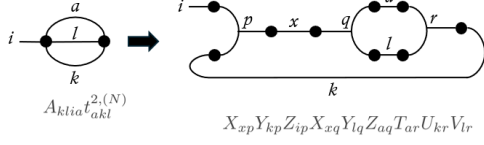
$$2(2N_{aux}N_{htf} + 2N_oN_{htf} + N_vN_{htf} + N_{htf} + 4N_oN_{ttf} + 2N_vN_{ttf})\log_2(1/\epsilon) \quad (224)$$



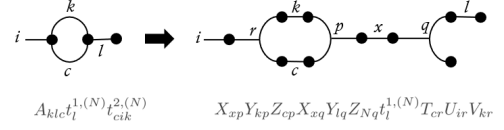
(a) Expression 2



(b) Expression 3

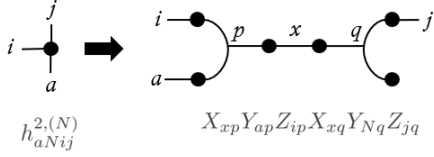


(c) Expression 4

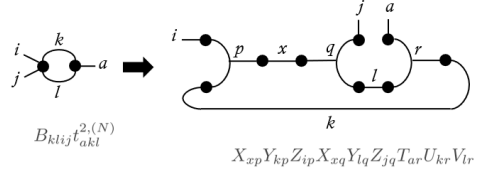


(d) Expression 5

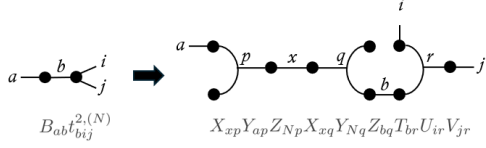
Figure 3: Tensor Factorized Representation of terms in Singles Residual Equation



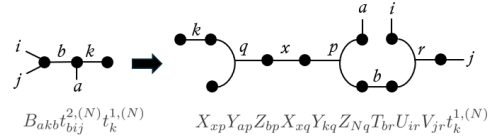
(a) Expression 6



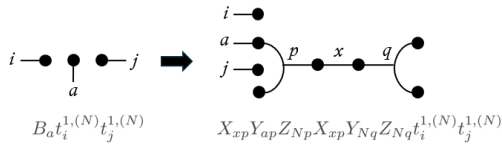
(b) Expression 7



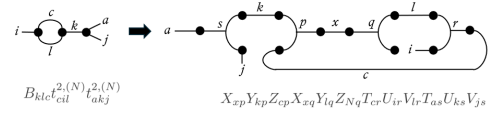
(c) Expression 8



(d) Expression 9

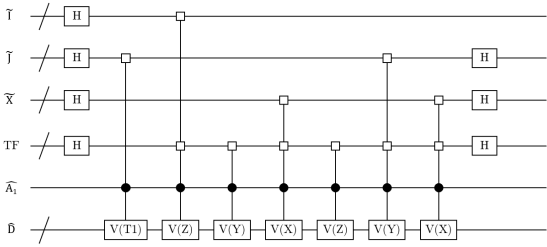


(e) Expression 10

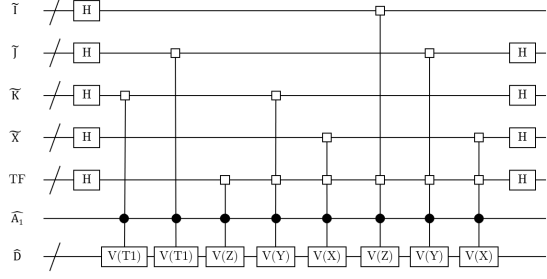


(f) Expression 11

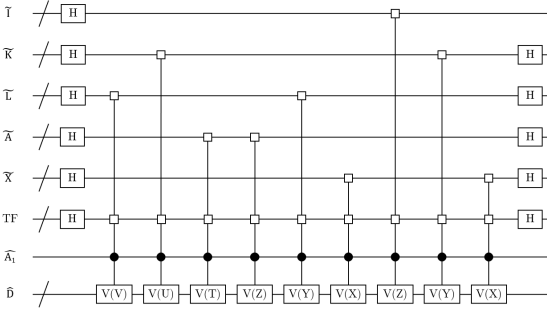
Figure 4: Tensor Factorized Representation of terms in Doubles Residual Equation



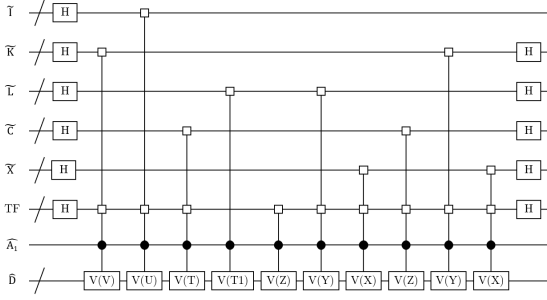
(a) Circuit for Expression 2



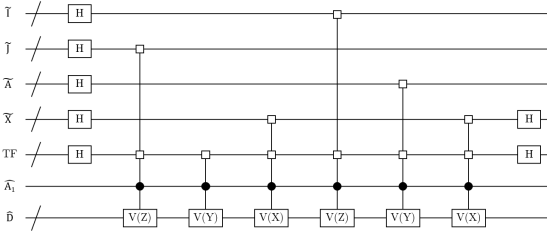
(b) Circuit for Expression 3



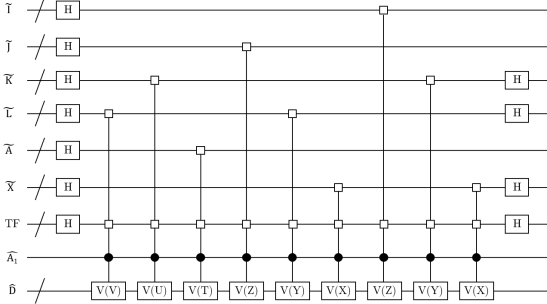
(c) Circuit for Expression 4



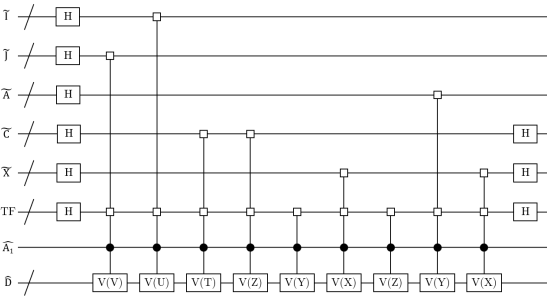
(d) Circuit for Expression 5



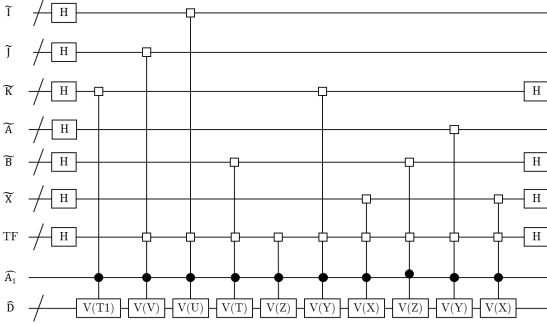
(e) Circuit for Expression 6



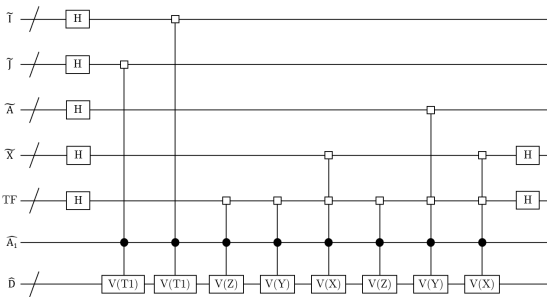
(f) Circuit for Expression 7



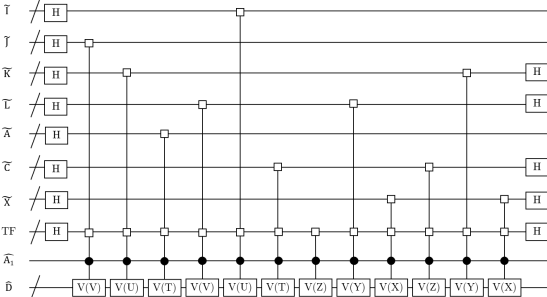
(g) Circuit for Expression 8



(h) Circuit for Expression 9



(i) Circuit for Expression 10



(j) Circuit for Expression 11

## 7.4 Error from Quantum Phase Estimation and Downfolding

When considering state of the art methods in Quantum Phase Estimation (QPE) based algorithms for quantum chemistry, we refer to.<sup>57</sup> The sources of error in this approach are largely due to two sources.

1. Discretization and Preparation of the Hamiltonian ( $\epsilon_{THC}$ )
2. Phase Estimation ( $\epsilon_{PEA}$ )

The former arises out of approximating given's rotations, state-preparation, tensor hyper-contraction, and the choice of basis functions used in approximating the Hamiltonian, The latter is due to the process of phase estimation. We can write this expression as

$$\epsilon = \epsilon_{PEA} + \epsilon_{THC} + \epsilon_{basis} \quad (225)$$

$$\epsilon_{THC} = \epsilon_{rot} + \epsilon_{TF} \quad (226)$$

The errors in our approach are largely influenced by the approximation of rotations used in state preparation, and the error in tensor factorization.

## 7.5 Benchmarking

Table 3: Citric Acid Conformer Ranking with downfolding- Single Point energies computed from downfolding with 6-31g basis incorporating singles and doubles clusters starting from single reference state. In 6-31g basis the Cholesky is of dimension  $N_{tf} = 2000$  tensor factors,  $N_{aux} = 1094$  density fitting vectors,  $N_o = 50$  occupied orbitals.  $N_v = 83$  virtual orbitals. The rankings of conformers obtained are as follows- SCF:(4,8,1,10,3,2,5,7,9,6), RMP2:(4,8,10,1,3,2,5,7,9,6), CCSD:(4,8,10,1,3,2,5,7,9,6), DOWNFOLDING:(4,8,1,10,2,3,5,7,9,6)

Citric Acid Conformers	Level of theory (basis: 6-31g)			
	SCF	RMP2	CCSD	DOWNFOLDING
Conformer 1	-755.5702231	-756.9940412	-757.0249044	-757.0179777
Conformer 2	-755.5555467	-756.9852885	-757.0148742	-757.0054337
Conformer 3	-755.5602742	-756.9853357	-757.0160611	-757.0019248
Conformer 4	-755.5803311	-757.0023419	-757.0336214	-757.0219172
Conformer 5	-755.5551208	-756.9811494	-757.0114966	-757.0002892
Conformer 6	-755.5355274	-756.96786	-756.9965834	-756.9900533
Conformer 7	-755.5495943	-756.9768728	-757.0071598	-756.9979194
Conformer 8	-755.5750486	-756.998113	-757.0292071	-757.0207515
Conformer 9	-755.5432721	-756.9720897	-757.0014425	-756.9920599
Conformer 10	-755.570067	-756.9956409	-757.0261098	-757.0162994

Table 4: Citric Acid Conformer Ranking with downfolding- Single Point energies computed from downfolding with def2-svp basis incorporating singles and doubles clusters starting from single reference state. In def2-svp basis the Cholesky is of dimension  $N_{tf} = 2200$  tensor factors,  $N_{aux} = 1133$  density fitting vectors,  $N_o = 50$  occupied orbitals.  $N_v = 172$  virtual orbitals. The rankings of conformers obtained are as follows- SCF:(4,8,1,10,3,2,5,7,9,6), RMP2:(4,8,10,1,2,3,5,7,9,6), CCSD:(4,8,10,1,3,2,5,7,9,6), DOWNFOLDING:(4,8,10,1,3,2,5,7,9,6)

Citric Acid Conformers	Level of theory (basis: def2-svp)			
	SCF	RMP2	CCSD	DOWNFOLDING
Conformer 1	-755.3570971	-757.4731958	-757.5214172	-757.4868588
Conformer 2	-755.342948	-757.4673823	-757.5135503	-757.4779496
Conformer 3	-755.3480262	-757.4673686	-757.5148784	-757.4795734
Conformer 4	-755.3655959	-757.480623	-757.5290297	-757.4909161
Conformer 5	-755.3409242	-757.4621949	-757.5091232	-757.4722697
Conformer 6	-755.3199347	-757.4487587	-757.4936955	-757.4620916
Conformer 7	-755.3385779	-757.458564	-757.5060326	-757.4705519
Conformer 8	-755.3613695	-757.4776596	-757.525767	-757.4902219
Conformer 9	-755.3291166	-757.4525266	-757.4987229	-757.4662678
Conformer 10	-755.3568708	-757.475352	-757.5228783	-757.4890177



Table 5: Citric Acid Conformer Ranking with downfolding- Single Point energies computed from downfolding with ccpvdz basis incorporating singles and doubles clusters starting from single reference state. In ccpvdz basis the Cholesky is of dimension  $N_{tf} = 2200$  tensor factors,  $N_{aux} = 1094$  density fitting vectors,  $N_o = 50$  occupied orbitals.  $N_v = 172$  virtual orbitals. The rankings of conformers obtained are as follows- SCF:(4,8,1,10,3,2,5,7,9,6), RMP2:(4,8,10,1,2,3,5,7,9,6), CCSD: (4,8,10,1,3,2,5,7,9,6), DOWNFOLDING:(4,8,10,1,3,2,5,7,9,6)

Citric Acid Conformers	Level of theory (basis: ccpvdz)			
	SCF	RMP2	CCSD	DOWNFOLDING
Conformer 1	-756.0040102	-758.1216979	-758.169231	-758.1288886
Conformer 2	-755.9907601	-758.1162632	-758.1618224	-758.1221673
Conformer 3	-755.9950628	-758.1156926	-758.1625198	-758.123187
Conformer 4	-756.0121186	-758.1287919	-758.1764974	-758.1352263
Conformer 5	-755.9881586	-758.1109601	-758.15714	-758.118457
Conformer 6	-755.9671993	-758.0970568	-758.1413555	-758.1042623
Conformer 7	-755.9859496	-758.1075671	-758.1543593	-758.1138361
Conformer 8	-756.0080427	-758.1258409	-758.1732388	-758.134931
Conformer 9	-755.9765094	-758.101256	-758.1468017	-758.1088486
Conformer 10	-756.0035965	-758.1233642	-758.1702097	-758.1323347

Table 6: Aspirin Conformer Ranking with downfolding- Single Point energies computed from downfolding with 6-31g basis incorporating singles and doubles clusters starting from single reference state. In 6-31g basis the Cholesky is of dimension  $N_{tf} = 2200$  tensor factors,  $N_{aux} = 1094$  density fitting vectors,  $N_o = 47$  occupied orbitals.  $N_v = 86$  virtual orbitals. The rankings of conformers obtained are as follows- SCF:(1,4,8,3,10,2,6,9,5,7), MP2:(1,4,3,8,10,6,2,7,9,5), CCSD:(1,4,3,8,10,2,9,5,6,7), DOWNFOLDING:(1,4,8,10,3,6,2,7,9,5)

Aspirin Conformers	Level of Theory (basis: 6-31g)			
	SCF	RMP2	CCSD	DOWNFOLDING
Conformer 1	-644.6610982	-645.9585356	-646.0036644	-645.9924406
Conformer 2	-644.6389322	-645.9373075	-645.9826633	-645.9714558
Conformer 3	-644.6423715	-645.9449257	-645.9897701	-645.9770809
Conformer 4	-644.6581017	-645.9553979	-646.0005532	-645.9893473
Conformer 5	-644.631892	-645.9364658	-645.9811905	-645.966734
Conformer 6	-644.6331812	-645.9373469	-645.9808511	-645.9719798
Conformer 7	-644.6300114	-645.9366897	-645.9805286	-645.9686558
Conformer 8	-644.645868	-645.9439862	-645.9895043	-645.9782853
Conformer 9	-644.6319342	-645.936523	-645.9812477	-645.9667718
Conformer 10	-644.6418289	-645.9415013	-645.9862054	-645.9771029

Table 7: Aspirin Conformer Ranking with downfolding- Single Point energies computed from downfolding with def2-svp basis incorporating singles and doubles clusters starting from single reference state. In def2-svp basis the Cholesky is of dimension  $N_{tf} = 2200$  tensor factors,  $N_{aux} = 1127$  density fitting vectors,  $N_o = 47$  occupied orbitals.  $N_v = 175$  virtual orbitals. The rankings of conformers obtained are as follows- SCF:(1,4,8,10,3,2,9,5,6,7), RMP2:(1,4,3,8,10,6,9,5,7,2), CCSD:(1,4,3,8,10,2,6,9,5,7), DOWNFOLDING:(1,4,3,8,10,6,7,2,9,5).

Aspirin Conformers	Level of Theory (basis: def2-svp)			
	SCF	RMP2	CCSD	DOWNFOLDING
Conformer 1	-644.4563718	-646.3873246	-646.4372907	-646.4186128
Conformer 2	-644.434291	-646.3662881	-646.4163628	-646.3961012
Conformer 3	-644.4373907	-646.3732314	-646.4225723	-646.4036205
Conformer 4	-644.4528848	-646.3840958	-646.4339928	-646.4134617
Conformer 5	-644.4279823	-646.3672113	-646.4160287	-646.3949031
Conformer 6	-644.4271181	-646.3691688	-646.4163438	-646.3975334
Conformer 7	-644.4264025	-646.3671135	-646.4151305	-646.3969465
Conformer 8	-644.4406671	-646.3722646	-646.4225624	-646.4029735
Conformer 9	-644.4280075	-646.3672411	-646.4160588	-646.3949112
Conformer 10	-644.437574	-646.3715154	-646.420843	-646.3999801

Table 8: Aspirin Conformer Ranking with downfolding- Single Point energies computed from downfolding with ccpvdz basis incorporating singles and doubles clusters starting from single reference state. In ccpvdz basis the Cholesky is of dimension  $N_{tf} = 2200$  tensor factors,  $N_{aux} = 1094$  density fitting vectors,  $N_o = 47$  occupied orbitals.  $N_v = 175$  virtual orbitals. The rankings of conformers obtained are as follows- SCF:(1,4,8,10,3,2,9,5,6,7), RMP2:(1,4,3,8,10,6,9,7,5,2), CCSD:(1,4,8,3,10,6,2,9,5,7), DOWNFOLDING:(1,4,8,3,10,2,7,6,9,5).

Aspirin Conformers	Level of Theory (basis: ccpvdz)			
	SCF	RMP2	CCSD	DOWNFOLDING
Conformer 1	-644.9997392	-646.9318783	-646.9805528	-646.9555228
Conformer 2	-644.9778063	-646.9109991	-646.9597428	-646.936159
Conformer 3	-644.9806198	-646.917197	-646.9652798	-646.9410966
Conformer 4	-644.9963784	-646.928845	-646.9774418	-646.9527424
Conformer 5	-644.9713608	-646.9110801	-646.9586147	-646.9339922
Conformer 6	-644.9706391	-646.914223	-646.959752	-646.9343443
Conformer 7	-644.9698768	-646.9110831	-646.957796	-646.9350735
Conformer 8	-644.9839666	-646.9168041	-646.965791	-646.9417124
Conformer 9	-644.9713855	-646.9111134	-646.9586482	-646.934041
Conformer 10	-644.98115	-646.9163835	-646.9642987	-646.9396566

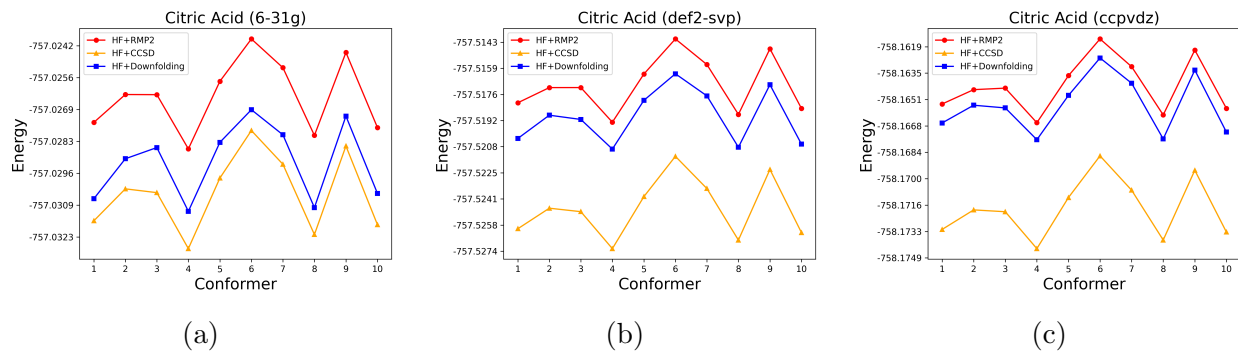


Figure 6: Energy Calculations in different basis sets for Citric Acid Conformers

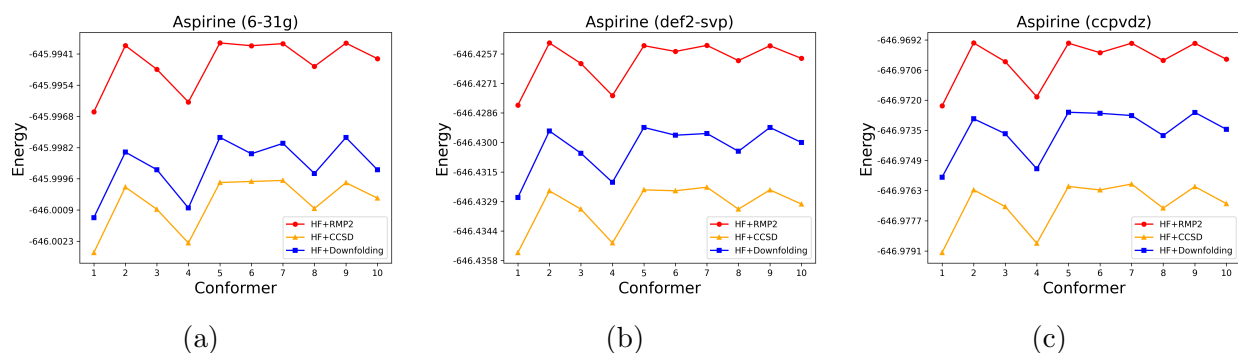


Figure 7: Energy Calculations in different basis sets for Aspirin Conformers

Table 9: The table represents the calculated correlation energies of molecules 1  $\rightarrow$  1,3-hexadiene, 2  $\rightarrow$  1-heptyne, 3  $\rightarrow$  benzene, 4  $\rightarrow$  NaBr, 5  $\rightarrow$  NaCl, 6  $\rightarrow$  propyne in the basis: 6-31g, ccpvdz and def2-tzvp for the methods: MP2, RHD(Downfolding) and CCSD

#	Correlation Energy (6-31g)			Correlation Energy (ccpvdz)			Correlation Energy (def2-tzvp)		
	MP2	RHD(SD)	CCSD	MP2	RHD(SD)	CCSD	MP2	RHD(SD)	CCSD
1	-0.5429	-0.5904	-0.6090	-0.8374	-0.8843	-0.9068	-1.0795	-1.1285	-1.1437
2	-0.6437	-0.6886	-0.7154	-0.9868	-1.0337	-1.0657	-1.2705	-1.3188	-1.3441
3	-0.5236	-0.5546	-0.5667	-0.7986	-0.8300	-0.8370	-1.0416	-1.0787	-1.0739
4	N/A			-0.1530	-0.1612	-0.1632	-0.5395	-0.5427	-0.5380
5	-0.0516	-0.0592	-0.0616	-0.1637	-0.1775	-0.1785	-0.4908	-0.5088	-0.5065
6	-0.2729	-0.3033	-0.2988	-0.4034	-0.4361	-0.4323	-0.5236	-0.5595	-0.5499

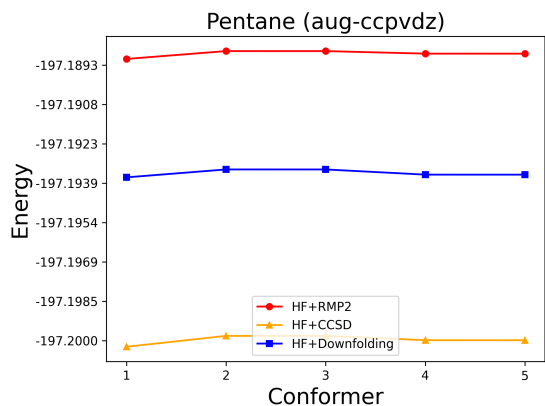


Figure 8: Energy Calculations for Pentane Conformers in highly diffuse basis

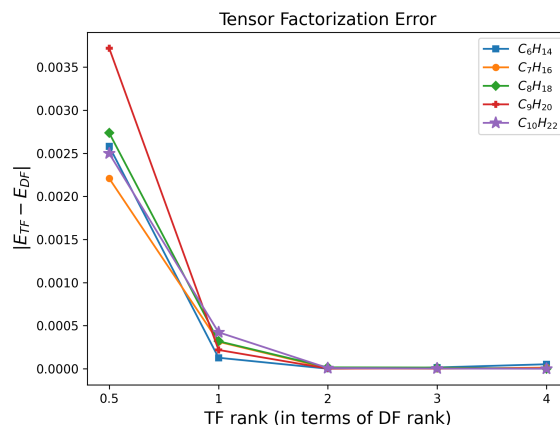


Figure 9: Plot of Tensor factorization errors in Energy Calculations with tf-rank

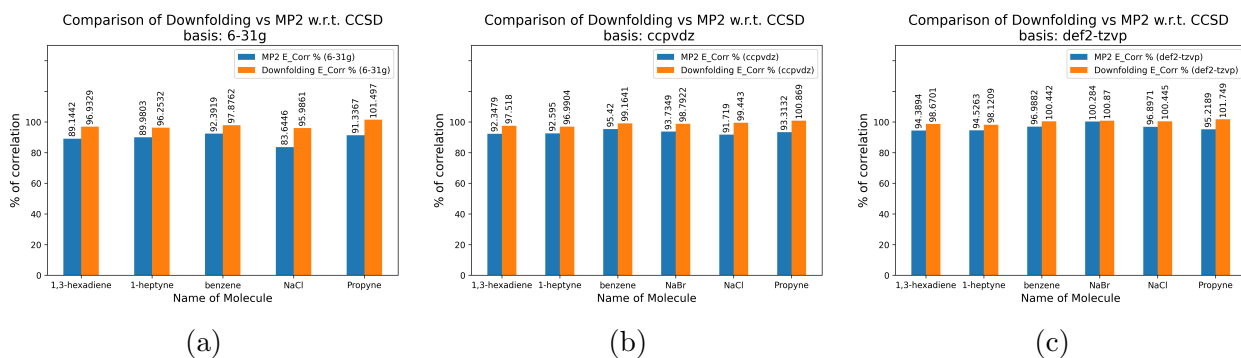


Figure 10: Energy Calculations in different basis sets for different molecules

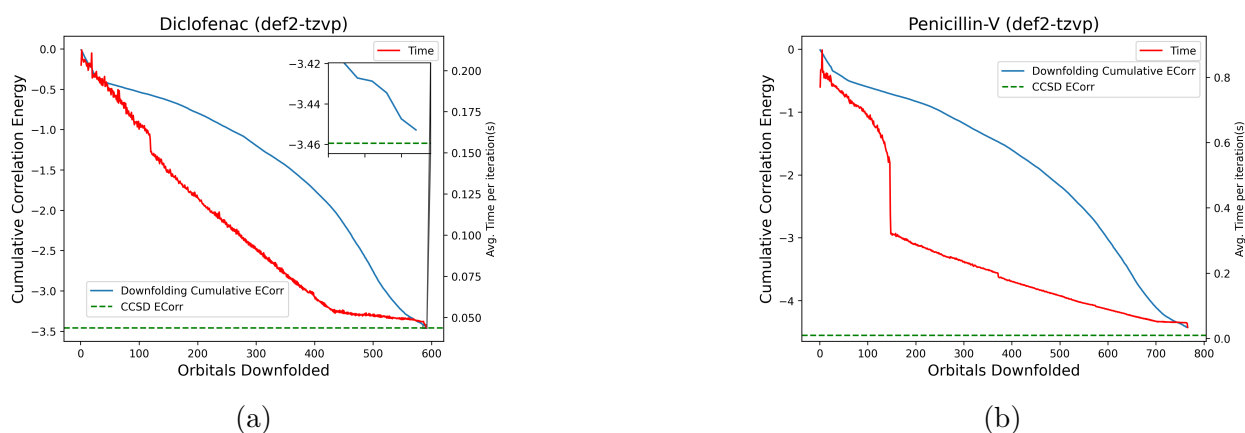


Figure 11: Downfolding Cumulative Correlation energy and iteration time with recursion steps for Diclofenac and Penicillin V

Table 10: Pentane Conformer Ranking with downfolding- Single Point energies computed from downfolding with ccpvdz basis incorporating singles and doubles clusters starting from single reference state. In ccpvdz basis the Cholesky is of dimension  $N_{tf} = 2200$  tensor factors,  $N_{aux} = 814$  density fitting vectors,  $N_{occ} = 21$  occupied orbitals.  $N_{virt} = 202$  virtual orbitals. The rankings of conformers obtained are as follows- SCF:(1,5,4,2,3), RMP2:(1,5,4,3,2), CCSD:(1,5,4,3,2), DOWNFOLDING:(1,5,4,3,2)

Pentane Conformers	Level of theory (basis: aug-ccpvdz)			
	SCF	RMP2	CCSD	DOWNFOLDING
Conformer 1	-196.3530103	-197.1284168	-197.2015472	-197.1585037
Conformer 2	-196.3475753	-197.126418	-197.1987854	-197.1564927
Conformer 3	-196.3475749	-197.1264208	-197.1987886	-197.1564972
Conformer 4	-196.3501434	-197.1270664	-197.1998807	-197.1578099
Conformer 5	-196.3501481	-197.1270735	-197.1998892	-197.1578173

Table 11: Single point energies are computed from downfolding at the level of 6-31g basis for different alkane molecules with 1 to 10 carbon atoms using tensor factorization approximation at varying ranks:  $N_{tf} = 0.5N_{aux}$ ,  $N_{tf} = N_{aux}$ ,  $N_{tf} = 2N_{aux}$ ,  $N_{tf} = 3N_{aux}$ ,  $N_{tf} = 4N_{aux}$  with  $N_{aux}$  being the density fitting auxiliary basis rank. The energy values obtained using the density fitting recursive Hamiltonian downfolding for the corresponding molecules is also presented for comparison

Alkane	Level of Approximation (basis: 6-31g)					
	DF	TF-0.5DF	TF-1DF	TF-2DF	TF-3DF	TF-4DF
1	-38.43259267	-38.43215632	-38.43259267	-38.43259267	-38.43259267	-38.43259267
2	-79.40927911	-79.40844159	-79.40922995	-79.40927911	-79.40927911	-79.40927911
3	-118.5268271	-118.5268112	-118.526724	-118.5268378	-118.5268271	-118.5268271
4	-157.6403285	-157.6393513	-157.6401943	-157.6403458	-157.6403307	-157.6403285
5	-196.7550323	-196.7539008	-196.7549078	-196.7550365	-196.7550666	-196.7550323
6	-235.8671152	-235.8645352	-235.8669872	-235.8671161	-235.8671307	-235.8671678
7	-274.9818615	-274.9796533	-274.9815484	-274.9818699	-274.9818612	-274.9818751
8	-314.0939191	-314.0911834	-314.0935996	-314.0939026	-314.0939334	-314.0939195
9	-353.2063983	-353.2026801	-353.2061796	-353.206401	-353.2064015	-353.2064029
10	-392.3185959	-392.3160985	-392.3181725	-392.3186047	-392.3185993	-392.318597

Table 12: A comparison of times taken for running calculations using CCSD and Downfolding techniques is listed below. Alkanes with 1 to 18 carbon atoms are considered. In a Nvidia V-100 GPU, the calculations were executed. GPU4PySCF implementation of CCSD couldn't perform calculations for alkanes with more than 13 carbon atoms due to storage constraints. For alkanes with more than 18 carbon atoms, the scf didn't converge under the same convergence criterion as for the rest of the molecules; hence downfolding data has not been provided for those molecules in this comparison

Basis: 6-31g Alkanes	Time taken (s)	
	CCSD	DOWNFOLDING
1	10.49121623	28.33036164
2	1.83537627	20.23007961
3	2.350443989	28.49350869
4	5.125217073	37.14023147
5	7.213134691	40.32105076
6	13.12267528	43.23324662
7	23.01328656	54.20392644
8	30.59317699	64.25860699
9	76.35492604	67.0198999
10	94.40636803	74.4054365
11	112.6176385	81.65810721
12	186.0039043	87.60531043
13	347.5013103	96.58040202
14	-	100.6939708
15	-	119.8199068
16	-	121.2039495
17	-	136.8925819
18	-	165.9558665

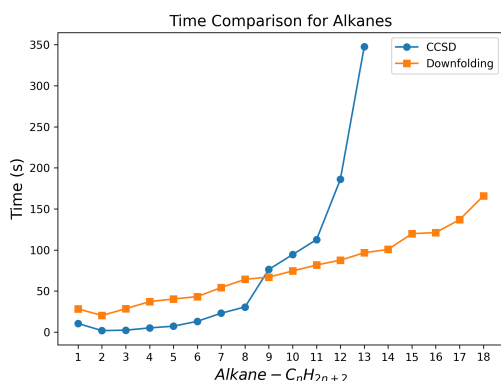


Figure 12: Comparative runtimes of Downfolding and CCSD for different alkanes

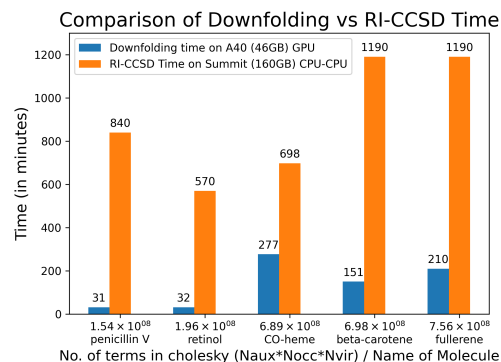


Figure 13: Comparative runtimes of Downfolding and RI-CCSD for different molecules

Table 13: Table for Downfolding energies runtimes and memory usage for molecules 1: $\beta$ -Carotene, 2:Retinol, 3:  $C_{60}$ , 4: CO-Heme, 5: Penicillin-V, 6:Diclofenac on Intel Xeon , A40 Nvidia GPU 46 GB GPU, 75 GB RAM and comparison to state of the art. Electronic integrals for Molecules is represented in basis/aux-basis 1 in A (cc-pVDZ/aug-cc-pVTZ-RI),2 in B (def2-TZVPP/def2-TZVPP-RI), 3 in (cc-pVDZ/aug-cc-pvdz-RI),4 in C (Fe and five nitrogens around it is def2-tzvp and rest in def2-SVP and the auxilliary basis is def2-TZVP-RI), 5 and 6 in E,F (def2-tzvp/def2-tzvp-RI).The Time-1 and Mem-1 represents the state of the art times (in minutes) and memory requirements for RI-CCSD(T) implementation on Polaris supercomputer where two Nvidia A100 GPUs of total 80 GB GPU is being used.<sup>16</sup> The Time-1 is estimated assuming 100 iterations of CC, per CC iteration time is presented in ref.<sup>16</sup> The Time represents the downfolding time (in minutes)

Mol	Rep.	$N_O$	$N_V$	$N_{aux}$	Downfolding	Time	Mem	Time-1	Mem-1
1	A	148	692	6816	-1552.42171499	151.28	(8/16)GB	1190	64 GB
2	B	79	992	2496	-853.61229138	31.8	(4/10)GB	570	32 GB
3	C	180	660	6360	-2278.79962753	210.16	(8.44/16)GB	1190	64GB
4	D	185	840	4431	-3428.60238789	277.35	10/40GB	698	80 GB
5	E	92	766	2191	-1501.94189954	30.71	6.1/24.2GB	141.9	68.1 GB
6	F	76	591	1735	-1663.48077496	10.05	2.9GB/15.3 GB	165.14	74.41 GB

Table 14: The table represents resource estimates i.e. Number of Qubits and Depth in the Clifford+T basis for emulating downfolding on Quantum Circuits for molecules: 1  $\rightarrow$   $\beta$ -Carotene, 2  $\rightarrow$  Retinol, 3  $\rightarrow$   $C_{60}$ , 4  $\rightarrow$  CO-Heme. The plots shows variations of resources for different tensor factors and different precision of representing the integrals and the cluster amplitudes on the Quantum Circuit.

Mol	norbs	# TF	Error	# Qubits	Depth(S,CNOT,H,T) for Precision			
					1E-02	1E-03	1E-04	1E-05
1	840	6816	$3.48 \times 10^{-4}$	117	$6.71 \times 10^8$	$1.01 \times 10^9$	$1.34 \times 10^9$	$1.67 \times 10^9$
		10224	$3.5 \times 10^{-4}$	121	$1.01 \times 10^9$	$1.51 \times 10^9$	$2.01 \times 10^9$	$2.51 \times 10^9$
		13632	$3.5 \times 10^{-4}$	121	$1.34 \times 10^9$	$2.01 \times 10^9$	$2.68 \times 10^9$	$3.35 \times 10^9$
		17040	-	125	$1.67 \times 10^9$	$2.52 \times 10^9$	$3.35 \times 10^9$	$4.2 \times 10^9$
2	1071	2496	$7.43 \times 10^{-4}$	108	$1.17 \times 10^8$	$1.75 \times 10^8$	$2.34 \times 10^8$	$2.92 \times 10^9$
		3744	$7.1 \times 10^{-4}$	108	$1.75 \times 10^8$	$2.63 \times 10^8$	$3.51 \times 10^8$	$4.38 \times 10^8$
		4992	$7.58 \times 10^{-4}$	112	$2.34 \times 10^8$	$3.51 \times 10^8$	$4.68 \times 10^8$	$5.85 \times 10^8$
		6240	$7.51 \times 10^{-4}$	112	$2.92 \times 10^8$	$4.38 \times 10^8$	$5.85 \times 10^8$	$7.31 \times 10^8$
3	840	6360	$2.29 \times 10^{-4}$	117	$5.89 \times 10^8$	$8.84 \times 10^8$	$1.18 \times 10^9$	$1.47 \times 10^9$
		9540	$2.52 \times 10^{-4}$	121	$8.84 \times 10^8$	$1.32 \times 10^9$	$1.76 \times 10^9$	$2.21 \times 10^9$
		12720	$2.55 \times 10^{-4}$	121	$1.18 \times 10^9$	$1.77 \times 10^9$	$2.36 \times 10^9$	$2.95 \times 10^9$
		15900	$2.54 \times 10^{-4}$	121	$1.47 \times 10^9$	$2.21 \times 10^9$	$2.94 \times 10^9$	$3.68 \times 10^9$
4	1025	4431	-	117	$3.1 \times 10^8$	$4.65 \times 10^8$	$6.2 \times 10^8$	$7.75 \times 10^8$
		6646	-	117	$4.65 \times 10^8$	$6.97 \times 10^8$	$9.3 \times 10^8$	$1.16 \times 10^9$
		8862	-	121	$6.2 \times 10^8$	$9.3 \times 10^8$	$1.24 \times 10^9$	$1.55 \times 10^9$
		11077	-	121	$7.75 \times 10^8$	$1.16 \times 10^9$	$1.55 \times 10^9$	$1.93 \times 10^9$

Table 15: The table represents the Number of Toffoli's and Number of Qubits for the quantum phase estimation circuits for different molecules for different sizes of tensor factors

Molecule	# TF's	# Toffoli's in QPE	# Qubits in QPE
retinol	2496	5.79566E+13	23756
	3744	6.42007E+13	23757
	4992	6.84462E+13	23762
	6240	7.40703E+13	23763
$\beta$ -carotene	6816	2.3614E+13	40748
	10224	2.77809E+13	42800
$C_{60}$ Fullerene	6360	3.25465E+13	40750
	9540	3.8797E+13	42802
	12720	4.57649E+13	42804
	15900	5.15462E+13	83763
CO-bound Heme	4431	4.67249E+13	22748
	6646	5.84054E+13	41120
	8862	5.90529E+13	43172
	11077	6.51382E+13	43172



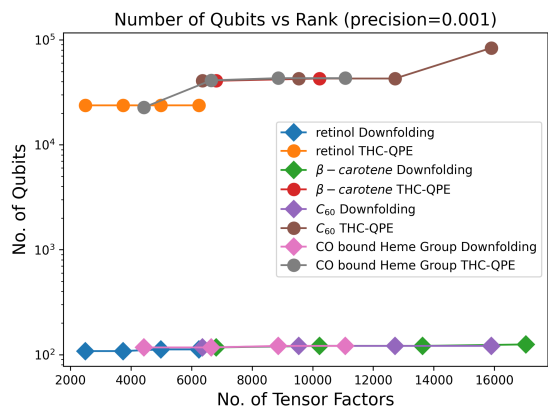


Figure 14: Plot for Number of Qubits vs Rank

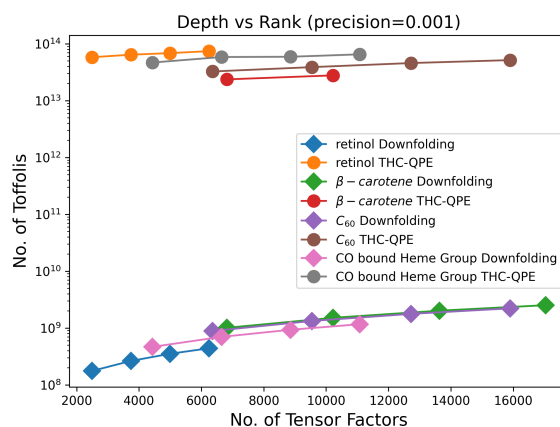
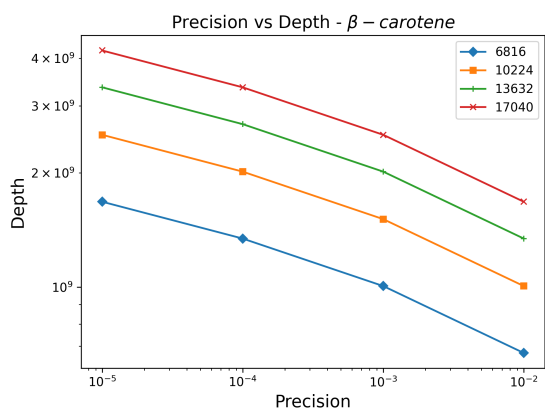
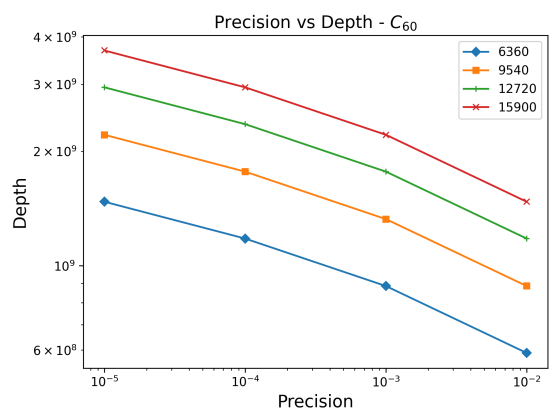


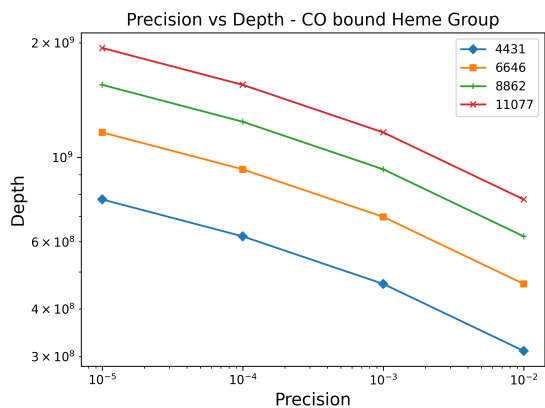
Figure 15: Plot for Depth vs Rank



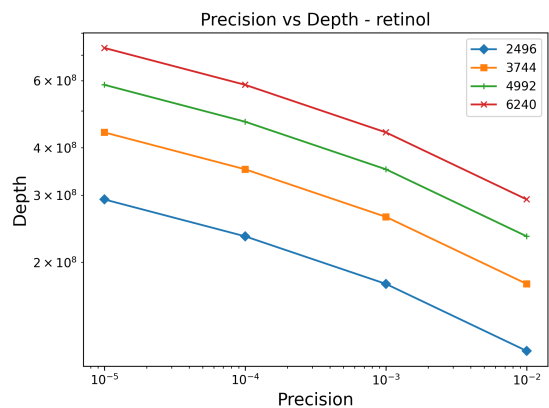
(a)



(b)



(c)



(d)

Figure 16: Number of Qubits vs Rank of Tensor factors for different molecules

## 8 Results and Discussion

We have distributed the results into three components the first component of the result deals with determining the computational complexity of the optimized quantum chemistry calculations resulting from downfolding the single reference CC, MRCC and the general full configuration calculations. The downfolding calculations are carried out in a tensor factorized representation. We also prove a bunch of theorems that enable porting this tensor factorized computations onto quantum circuits using the block-encoding formalism. The second component of our results deal with constructing the tensor networks Fig3, Fig4 to showcase pictorially how the complexity is curbed on the classical computers. We also build the Quantum circuits Fig5 for implementing the tensor network operation arising from downfolding on Quantum computers. The third component of our results deals with getting bench-marking data that demonstrate the accuracy towards ranking conformers, accuracy of energy values with respect to CCSD and MP2, time and memory requirements for determining post-HF correlation energy from downfolding for medium to large molecules and or chemical complexes. Comparison of energies to state-of-the-art. We then also present a variety of data on the Quantum circuit resources for large molecules, the variation of the number of qubits and variation of the depth of the quantum circuit in the Clifford+T basis with the number of tensor factors. The accuracy towards approximating the electronic integrals in the tensor factorized representation. We provide comparisons to the state-of-the-art Qubitized Phase estimation in the tensor hyper-contraction representation of.<sup>57</sup> We also demonstrate two cases of downfolding (i) closed form expression for the unitary variant of the downfolding similarity transformation for the coupled cluster singles and doubles case Sec5 and (ii) we demonstrate a family of downfolding similarity transformation for singles and paired doubles where the renormalized Hamiltonian within the two electron interaction regime remains self-similar Sec4. Below we discuss the results for all the three components we just discussed.

In the approach of recursive Hamiltonian Downfolding at every step one orbital is decou-

pled, i.e. all the interactions terms coupling the one-orbital via one-particle, two-particle and higher order terms become zero. This is requirement of the Bloch equation with the form of generator of similarity transformation  $\eta$  eq.(7). With a tensor factorized representation of the generator  $\eta$  and the electronic integrals eq. (2) and the general expression for ordering fermionic strings(strings of creation and annihilation operators) into irreducible representations the Bloch equation can be reduced to hierarchy of families of cluster equations that is given by eq.(14). From the computation of the order of complexity eq.(18), generic tensor operation diagram Fig.1 and the tensor factorized form of the Hamiltonian we conclude that all the Multiconfigurational Quantum Chemistry calculations have a cubic complexity.

For single configuration downfolding with singles and doubles for small molecules we present the benchmarking results below. All the calculations performed below are done on Nvidia V100 32 GB GPU. The results showcase the overall correlation capture efficacy of downfolding compared to MP2 and also efficacy towards conformer ranking. In tables 6,7, 8 and figure 7 we show that for different Aspirin conformers downfolding captures more than 98% correlation energy of CCSD for all three basis sets, 6-31g, def2-svp and ccpvdz. On the other-hand for both the molecules- Citric acid and Aspirin MP2 reproduces the electronic correlation  $> 97\%$  of CCSD correlations). So we conclude that for small organic molecules with H, C, O downfolding captures more correlations than MP2.

Importantly also for both Citric acid and Aspirin conformers, for all basis sets studied as seen from figures Fig.7, Fig.6 downfolding reproduces the energy rankings accurately with small deviations. However, the shape of the energy curves agree with CCSD showcasing the robustness of the downfolding protocol. The deviations between the aforementioned curves can be attributed to the differential capture of electronic correlations via recursive downfolding compared to one the one-shot similarity transformation in CCSD that decouples the HF state from its excitations.

The result below demonstrates the efficiency towards conformer ranking with increasing basis set size for MP2 and downfolding compared to CCSD. We show that for pentane with

a large basis set, aug-ccpvdz, (table 10 and figure 8) the energy rankings is same for all three methods: MP2, CCSD and downfolding. These captures the accuracy of the downfolding technique for the cases where also both MP2 and CCSD accurately captures the conformer rankings. This shows that for highly correlated basis sets downfolding, CCSD and MP2 captures differential rankings between n-alkane chain conformers in the same way.

*Differential capture of electronic correlations:* Below we demonstrate cases where downfolding captures significantly more correlations than MP2 compared to CCSD. In table 9 and figure 10 we study a variety of molecules where MP2 cannot accurately calculate the electronic correlations due to presence of one or more of the following: strong electrovalent bonds, delocalization of electrons, triple bonds, etc. For 6-31g basis sets, downfolding reproduces more than 95.9% of CCSD correlations for all molecules studied, whereas MP2 could capture 83.7%–89.1% correlations. For larger basis sets(ccpvdz, def2-tzvp) downfolding consistently captures more correlations than MP2. In some cases downfolding shows higher correlation energies(magnitudes) than CCSD. This is again owing to the way downfolding captures correlation differently from CCSD.

*Accuracy of TF:* In table 11 and figure 9 we provide a detailed description of how the size of auxiliary basis sets for tensor factorization affect downfolding energies. For different n-alkanes with carbon atoms, 1 to 10, we show a drastic reduction of error in the total energy by increasing the size of the the auxiliary basis set. For basis set sizes more than  $N_{aux}$ , the auxiliary basis set size for Cholesky Decomposition, Tensor factorization gives errors of less than 1 mHa in the energy values. For auxiliary basis sizes of  $2N_{aux}$  and more, the tensor factorization error is negligible.

*Comparative Timings:* Downfolding is inherently faster than CCSD due to its reduced operational scaling complexity. Also orders of magnitude reduction in storage complexities allow for much greater parallelization which in turn, increases the speed of this formalism drastically than CCSD. In figure 11, we study two molecules, Penicillin V and Diclofenac and show how the downfolding correlation energy accumulates recursively to give the total

correlation energy. Here we can see how the average run time for each iteration step reduces significantly as we downfold orbitals one by one, as a result of a reduction in dimension of the effective Hamiltonian. From table 12 and figure 12, it is evident how downfolding provides a significant advantage in run-time speeds of high accuracy quantum chemistry calculations than CCSD. From table 13 we can see the comparison of downfolding with RI-CCSD(T) with respect to speedup and memory usage. For this calculations of the big molecules we used the A40 46 GB GPU. We can also see that CCSD goes out of memory where as downfolding can work on much smaller storage requirements.

*Quantum Resources*-The Quantum Circuit results in table14, table15 and figures Fig.14, Fig.15, Fig.16 demonstrate that our qubitized-block encoding based Hamiltonian downfolding approach offers a substantial improvement over the quantum phase estimation.<sup>57</sup> In QPE, achieving high precision requires repeated applications of controlled-unitary operations that scale exponentially as  $O(1/\epsilon)$ , where  $\epsilon$  is the desired precision in phase estimation. Moreover, QPE requires a register of  $O(\log(1/\epsilon))$  ancilla qubits to store phase information.

Our results show that for a target precision of  $10^{-5}$  the circuit depth in QPE is of the magnitude of  $10^{13}$  while our approach achieves similar precision with depths of  $10^8 - 10^9$  even for molecules, representing a nearly  $10000x$  reduction in circuit depth. A key factor accounting for this drastic reduction is due to the block-encoding scheme in our approach, where the scaling with precision is only  $O(\log(1/\epsilon))$ .<sup>75,76</sup> By directly encoding the Hamiltonian onto the circuit we eliminate the need for repeated controlled-unitary operations, a major bottleneck in QPE.<sup>54</sup>

Furthermore, our approach requires significantly fewer qubits. For example the number of qubits needed for complex systems like the Heme bound CO complex is in the range of 100-150 qubits, while QPE requires upwards of 40,000 qubits Fig16 for the same system. The reduction in logical qubit count further emphasizes the feasibility of our approach on near-term fault tolerant quantum devices.

## 9 Future Directions

In this work we have presented the recursive Hamiltonian Downfolding that is efficiently implemented in tensor factorized representation on GPUs and can be implemented on future Quantum Computers. Future work will be pursued to in one hand develop computational chemistry packages that incorporate tensor factorization and multi-configuration effects where downfolding is used to speedup those calculations and alongside further benchmarks for d-orbital block systems will be provided. Further integrating Hamiltonian downfolding with tree tensor networks (TTNs)<sup>25,77</sup> and density matrices presents a fresh avenue to scaling Quantum Chemistry computations for molecules at cheaper computational cost.

## A Lowdin Decomposition of The Hamiltonian $H$ For Primary Space ( $P$ ) and Secondary Space ( $Q$ )

For decoupling the  $N$ th Molecular Orbital where  $N \in \mathcal{V}$  the projection operator for primary space  $P$  and secondary space  $Q$  are given by,

$$P_{(N)} = (1 - \hat{n}_{N\uparrow})(1 - \hat{n}_{N\downarrow}), Q_{(N)} = \hat{n}_{N\uparrow}(1 - \hat{n}_{N\downarrow}) + \hat{n}_{N\downarrow}(1 - \hat{n}_{N\uparrow}) + \hat{n}_{N\uparrow}\hat{n}_{N\downarrow} \quad (227)$$

With this definition we can compute the Lowdin decomposition of the Hamiltonian as,

$$Q_{(N)}H_{(N)}P_{(N)} = \sum_{j\sigma} h_{Nj}^{1,\sigma}(1 - \hat{n}_{N-\sigma})f_{N\sigma}^\dagger f_{j\sigma} + \sum_{jkl,\sigma\sigma'} h_{Nklj}^{2,\sigma\sigma'}(1 - \hat{n}_{N-\sigma})f_{N\sigma}^\dagger f_{j\sigma} f_{k\sigma'}^\dagger f_{l\sigma'} + \sum_{kl} h_{NNkl}^2 f_{N\uparrow}^\dagger f_{N\downarrow}^\dagger f_{k\downarrow} f_{l\uparrow} \quad (228)$$

$$Q_{(N)}H_{(N)}Q_{(N)} = H_{(N)}^Q + h_N^2 \hat{n}_{N\uparrow}\hat{n}_{N\downarrow} + \sum_{j\sigma} \hat{n}_{N-\sigma} h_N^{1,\sigma} (f_{j\sigma}^\dagger f_{N\sigma} + h.c.) + \sum_{\sigma} h_{NN}^{1,\sigma} \hat{n}_{N\sigma} + \sum_{jkl\sigma\sigma'} \hat{n}_{N-\sigma} h_{Njkl}^{2,\sigma\sigma'} (f_{N\sigma}^\dagger f_{j\sigma'}^\dagger f_{k\sigma'} f_{l\sigma} + h.c.). \quad (229)$$

To derive the analytical expression from the operator Bloch equation eq.(6) we normal order the fermionic operators and obtain the criteria for every normal ordered fermionic term to be zero. And  $P_{(N)}H_{(N)}P_{(N)}$  has the same form as  $H$  with orbital indices running from  $1 \rightarrow N$ .

## A.1 Normal Ordering $\eta_{(N)}P_{(N)}HQ_{(N)}\eta_{(N)}$

The Bloch equation eq.(6) can be equivalently written as,

$$\begin{aligned} Q_{(N)}S_{(N)}^{-1}H_{(N)}S_{(N)}P_{(N)} &= Q_{(N)}H_{(N)}P_{(N)} - \eta_{(N)}P_{(N)}H_{(N)}P_{(N)} \\ &+ Q_{(N)}H_{(N)}Q_{(N)}\eta_{(N)} - \eta_{(N)}P_{(N)}H_{(N)}Q_{(N)}\eta_{(N)} \end{aligned} \quad (230)$$

For the electronic Hamiltonian eq.(1) and the transformation generator eq.(7) we first list down all the different Fermionic operator products comprising,

$$\eta_{(N)}P_{(N)}HQ_{(N)}\eta_{(N)} = \sum_{i=1}^{12} T_i, \quad (231)$$

where the  $T_i$ 's are given as,

$$\begin{aligned} T_1 &= \sum_{\substack{ijk, \\ \sigma\mu\nu}} t_i^{1,\sigma} h_{jN}^{1,\mu} t_k^{1,\nu} (1 - \hat{n}_{N-\sigma}) f_{N\sigma}^\dagger f_{i\sigma} (1 - \hat{n}_{N-\mu}) f_{j\mu}^\dagger f_{N\mu} (1 - \hat{n}_{N-\nu}) f_{N\nu}^\dagger f_{k\nu} \\ T_2 &= \sum_{\substack{ijklm, \\ \sigma\mu\nu\rho}} t_i^{1,\sigma} h_{jklN}^{2,\mu\nu} t_m^{1,\rho} (1 - \hat{n}_{N-\sigma}) f_{N\sigma}^\dagger f_{i\sigma} (1 - \hat{n}_{N-\mu}) f_{j\mu}^\dagger f_{k\nu}^\dagger f_{l\nu} f_{N\mu} (1 - \hat{n}_{N-\rho}) f_{N\rho}^\dagger f_{m\rho} \\ T_3 &= \sum_{\substack{ijkl, \\ \sigma\nu}} t_i^{1,\sigma} h_{jk}^{2,\mu\nu} t_l^{1,\nu} (1 - \hat{n}_{N-\sigma}) f_{N\sigma}^\dagger f_{i\sigma} f_{j\uparrow}^\dagger f_{k\downarrow}^\dagger f_{N\downarrow} f_{N\uparrow} (1 - \hat{n}_{N-\nu}) f_{N\nu}^\dagger f_{l\nu} \\ T_4 &= \sum_{\substack{ijkl, \\ \sigma\mu}} t_i^{1,\sigma} h_{jN}^{1,\mu} t_{kl}^2 (1 - \hat{n}_{N-\sigma}) f_{N\sigma}^\dagger f_{i\sigma} (1 - \hat{n}_{N-\mu}) f_{j\mu}^\dagger f_{N\mu} f_{N\uparrow}^\dagger f_{N\downarrow}^\dagger f_{k\downarrow} f_{l\uparrow} \\ T_5 &= \sum_{\substack{ijklmn, \\ \sigma\mu\nu}} t_i^{1,\sigma} h_{jklN}^{2,\mu\nu} t_{mn}^2 (1 - \hat{n}_{N-\sigma}) f_{N\sigma}^\dagger f_{i\sigma} (1 - \hat{n}_{N-\mu}) f_{j\mu}^\dagger f_{k\nu}^\dagger f_{l\nu} f_{N\mu} f_{N\uparrow}^\dagger f_{N\downarrow}^\dagger f_{m\downarrow} f_{n\uparrow} \\ T_6 &= \sum_{\substack{ijklm, \\ \sigma}} t_i^{1,\sigma} h_{jkNN}^2 t_{lm}^2 (1 - \hat{n}_{N-\sigma}) f_{N\sigma}^\dagger f_{i\sigma} f_{j\uparrow}^\dagger f_{k\downarrow}^\dagger f_{N\downarrow} f_{N\uparrow}^\dagger f_{N\downarrow}^\dagger f_{l\downarrow} f_{m\uparrow} \end{aligned}$$

$$\begin{aligned}
T_7 &= \sum_{\substack{ijkl, \\ \sigma\mu}} t_{ij}^2 h_{kN}^{1,\sigma} t_l^{1,\mu} f_{N\uparrow}^\dagger f_{N\downarrow}^\dagger f_{i\downarrow} f_{j\uparrow} (1 - \hat{n}_{N-\sigma}) f_{k\sigma}^\dagger f_{N\sigma} (1 - \hat{n}_{N-\mu}) f_{N\mu}^\dagger f_{l\mu} \\
T_8 &= \sum_{\substack{ijklmn, \\ \sigma\mu\nu}} t_{ij}^2 h_{klmN}^{2,\sigma\mu} t_n^{1,\nu} f_{N\uparrow}^\dagger f_{N\downarrow}^\dagger f_{i\downarrow} f_{j\uparrow} (1 - \hat{n}_{N-\sigma}) f_{k\sigma}^\dagger f_{l\mu}^\dagger f_{m\mu} f_{N\sigma} (1 - \hat{n}_{N-\nu}) f_{N\nu}^\dagger f_{n\nu} \\
T_9 &= \sum_{\substack{ijklm, \\ \mu}} t_{ij}^2 h_{klNN}^2 t_m^{1,\mu} f_{N\uparrow}^\dagger f_{N\downarrow}^\dagger f_{i\downarrow} f_{j\uparrow} f_{k\uparrow}^\dagger f_{l\downarrow}^\dagger f_{N\downarrow} f_{N\uparrow} (1 - \hat{n}_{N-\mu}) f_{N\mu}^\dagger f_{m\mu} \\
T_{10} &= \sum_{\substack{ijklm, \\ \sigma}} t_{ij}^2 h_{kN}^{1,\sigma} t_{lm}^2 f_{N\uparrow}^\dagger f_{N\downarrow}^\dagger f_{i\downarrow} f_{j\uparrow} f_{k\sigma}^\dagger f_{N\sigma} f_{N\uparrow}^\dagger f_{N\downarrow}^\dagger f_{l\downarrow} f_{m\uparrow} \\
T_{11} &= \sum_{\substack{ijklmno, \\ \sigma\mu}} t_{ij}^2 h_{klmN}^{2,\sigma\mu} t_{no}^2 f_{N\uparrow}^\dagger f_{N\downarrow}^\dagger f_{i\downarrow} f_{j\uparrow} f_{k\sigma}^\dagger f_{l\mu}^\dagger f_{m\mu} f_{N\sigma} f_{N\uparrow}^\dagger f_{N\downarrow}^\dagger f_{n\downarrow} f_{o\uparrow} \\
T_{12} &= \sum_{ijklmn} t_{ij}^2 h_{klNN}^2 t_{mn}^2 f_{N\uparrow}^\dagger f_{N\downarrow}^\dagger f_{i\downarrow} f_{j\uparrow} f_{k\uparrow}^\dagger f_{l\downarrow}^\dagger f_{N\downarrow} f_{N\uparrow}^\dagger f_{N\downarrow}^\dagger f_{m\downarrow} f_{n\uparrow} \tag{232}
\end{aligned}$$

From the Pauli blockade conditions i.e.,  $(f_{N\sigma}^\dagger)^2 = 0$ ,  $(f_{N\sigma})^2 = 0$  the terms  $T_3, T_4, T_5$  and  $T_9, T_{10}, T_{11}$  have zero contribution and are eliminated. As a next step we normal order(N.O.) the fermionic operators (denoted as  $::$ ) within the remaining six terms in eqs.(232), in the process of doing we use the Pauli-blockade conditions to balance the expressions,

$$\begin{aligned}
:T_1: &= \sum_{\substack{ijk, \\ \sigma\mu\nu}} t_i^{1,\sigma} h_{jN}^{1,\mu} t_k^{1,\nu} \delta_{\mu\nu} \left( \delta_{ij} \delta_{\sigma\mu} (1 - \hat{n}_{N-\sigma}) f_{N\sigma}^\dagger (1 - \hat{n}_{N-\mu}) (1 - \hat{n}_{N-\nu}) f_{k\nu} \right. \\
&\quad \left. + (1 - \hat{n}_{N-\sigma}) f_{N\sigma}^\dagger (1 - \hat{n}_{N-\mu}) f_{j\mu}^\dagger f_{k\nu} f_{i\sigma} \right) \\
:T_2: &= \sum_{\substack{ijklm, \\ \sigma\mu\nu\rho}} t_i^{1,\sigma} h_{jklN}^{2,\mu\nu} \left( (1 - \hat{n}_{N-\sigma}) (1 - \hat{n}_{N-\mu}) (1 - \hat{n}_{N-\rho}) \delta_{ij} \delta_{\sigma\mu} \delta_{\mu\rho} f_{N\sigma}^\dagger f_{k\nu}^\dagger f_{l\nu} f_{m\rho} \right. \\
&\quad \left. - (1 - \hat{n}_{N-\sigma}) \delta_{ik} \delta_{\sigma\nu} \delta_{\mu\rho} f_{N\sigma}^\dagger f_{j\mu}^\dagger (1 - \hat{n}_{N-\mu}) f_{l\sigma} (1 - \hat{n}_{N-\rho}) f_{m\mu} + (1 - \hat{n}_{N-\sigma}) \delta_{\mu\rho} f_{N\sigma}^\dagger f_{j\mu}^\dagger f_{k\nu}^\dagger f_{l\nu} f_{m\rho} f_{i\sigma} \right) \\
:T_6: &= \sum_{\substack{ijklm, \\ \sigma}} t_i^{1,\sigma} h_{jkNN}^2 t_{lm}^2 \left( \delta_{ij} \delta_{\sigma\uparrow} (1 - \hat{n}_{N-\sigma}) f_{N\sigma}^\dagger f_{k\downarrow}^\dagger f_{l\downarrow} f_{m\uparrow} + \delta_{ik} \delta_{\sigma\downarrow} (1 - \hat{n}_{N-\sigma}) f_{N\sigma}^\dagger f_{j\uparrow}^\dagger f_{m\uparrow} f_{l\downarrow} \right. \\
&\quad \left. + (1 - \hat{n}_{N-\sigma}) f_{N\sigma}^\dagger f_{j\uparrow}^\dagger f_{k\downarrow}^\dagger f_{l\downarrow} f_{m\uparrow} f_{i\sigma} \right) \\
:T_7: &= \sum_{\substack{ijkl, \\ \sigma\mu}} t_{ij}^2 h_{kN}^{1,\sigma} t_l^{1,\mu} \left( \delta_{jk} \delta_{\sigma\uparrow} \delta_{\mu\sigma} f_{N\uparrow}^\dagger f_{N\downarrow}^\dagger f_{i\downarrow} f_{l\mu} + \delta_{ik} \delta_{\sigma\downarrow} \delta_{\mu\sigma} f_{N\uparrow}^\dagger f_{N\downarrow}^\dagger f_{l\mu} f_{j\uparrow} + \delta_{\mu\sigma} f_{k\sigma}^\dagger f_{N\uparrow}^\dagger f_{N\downarrow}^\dagger f_{i\downarrow} f_{j\uparrow} f_{l\sigma} \right)
\end{aligned}$$



$$\begin{aligned}
:T_8: &= \sum_{\substack{ijklmn, \\ \sigma\mu\nu}} t_{ij}^2 h_{klmN}^{2,\sigma\mu} t_n^{1,\nu} \left( \delta_{\sigma\nu} \delta_{jk} \delta_{\sigma\uparrow} \delta_{il} \delta_{\mu\downarrow} f_{N\uparrow}^\dagger f_{N\downarrow}^\dagger f_{m\downarrow} f_{n\uparrow} + \delta_{\sigma\nu} \delta_{jk} \delta_{\sigma\uparrow} f_{N\uparrow}^\dagger f_{N\downarrow}^\dagger f_{l\mu}^\dagger f_{m\mu} f_{i\downarrow} f_{n\uparrow} \right. \\
&+ \delta_{\sigma\nu} \delta_{ik} \delta_{\sigma\downarrow} \delta_{jl} \delta_{\mu\uparrow} f_{N\uparrow}^\dagger f_{N\downarrow}^\dagger f_{n\downarrow} f_{m\uparrow} + \delta_{\sigma\nu} \delta_{ik} \delta_{\sigma\downarrow} f_{N\uparrow}^\dagger f_{N\downarrow}^\dagger f_{l\mu}^\dagger f_{m\mu} f_{n\downarrow} f_{j\uparrow} + \delta_{jl} \delta_{\mu\uparrow} \delta_{\sigma\nu} f_{N\uparrow}^\dagger f_{N\downarrow}^\dagger f_{k\sigma}^\dagger f_{n\sigma} f_{i\downarrow} f_{m\uparrow} \\
&\left. + \delta_{il} \delta_{\mu\downarrow} \delta_{\sigma\nu} f_{N\uparrow}^\dagger f_{N\downarrow}^\dagger f_{k\sigma}^\dagger f_{n\sigma} f_{m\downarrow} f_{j\uparrow} + \delta_{\sigma\nu} f_{N\uparrow}^\dagger f_{N\downarrow}^\dagger f_{k\sigma}^\dagger f_{l\mu}^\dagger f_{m\mu} f_{n\sigma} f_{i\downarrow} f_{j\uparrow} \right) \\
:T_{12}: &= \sum_{ijklmn} t_{ij}^2 h_{klmN}^2 t_{mn}^2 \left( \delta_{il} \delta_{jk} f_{N\uparrow}^\dagger f_{N\downarrow}^\dagger f_{m\downarrow} f_{n\uparrow} + \delta_{jk} f_{N\uparrow}^\dagger f_{N\downarrow}^\dagger f_{l\downarrow}^\dagger f_{m\downarrow} f_{i\downarrow} f_{n\uparrow} - \delta_{il} f_{N\uparrow}^\dagger f_{N\downarrow}^\dagger f_{k\uparrow}^\dagger f_{j\uparrow} f_{m\downarrow} f_{n\uparrow} \right. \\
&\left. + f_{N\uparrow}^\dagger f_{N\downarrow}^\dagger f_{k\uparrow}^\dagger f_{l\downarrow}^\dagger f_{i\downarrow} f_{j\uparrow} f_{m\downarrow} f_{n\uparrow} \right) \tag{233}
\end{aligned}$$

## B Normal ordering $\eta_{(N)} P_{(N)} H P_{(N)}$

We carry out the term multiplications within  $\eta_{(N)} P_{(N)} H P_{(N)} = V_1 + V_2 + V_3 + V_4$  and write down the fermionic terms,

$$\begin{aligned}
V_1 &= \sum_{ijk\sigma\nu} t_i^{1,\sigma} h_{jk}^{1,\nu} (1 - \hat{n}_{N-\sigma}) f_{N\sigma}^\dagger f_{i\sigma} f_{j\nu}^\dagger f_{k\nu} \\
V_2 &= \sum_{\substack{ijkl \\ \sigma}} t_{ij}^2 h_{kl}^{1,\sigma} f_{N\uparrow}^\dagger f_{N\downarrow}^\dagger f_{i\downarrow} f_{j\uparrow} f_{k\sigma}^\dagger f_{l\sigma} \\
V_3 &= \sum_{\substack{ijklm \\ \sigma\nu\rho}} t_i^{1,\sigma} h_{jklm}^{2,\nu\rho} (1 - \hat{n}_{N-\sigma}) f_{N\sigma}^\dagger f_{i\sigma} f_{j\nu}^\dagger f_{k\rho}^\dagger f_{l\rho} f_{m\nu} \\
V_4 &= \sum_{\substack{ijklmn, \\ \sigma\nu}} t_{ij}^2 h_{klmn}^{2,\sigma\nu} f_{N\uparrow}^\dagger f_{N\downarrow}^\dagger f_{i\downarrow} f_{j\uparrow} f_{k\sigma}^\dagger f_{l\nu}^\dagger f_{m\nu} f_{n\sigma} \tag{234}
\end{aligned}$$

Upon normal ordering the eqs.(234) we get,

$$\begin{aligned}
:V_1: &= \sum_{ijk\sigma\nu} \sum_{ijk\sigma\nu} t_i^{1,\sigma} h_{jk}^{1,\nu} \left( (1 - \hat{n}_{N-\sigma}) \delta_{ij} \delta_{\sigma\nu} f_{N\sigma}^\dagger f_{k\sigma} + (1 - \hat{n}_{N-\sigma}) f_{N\sigma}^\dagger f_{j\nu}^\dagger f_{k\nu} f_{i\sigma} \right) \\
:V_2: &= \sum_{\substack{ijkl \\ \sigma}} t_{ij}^2 h_{kl}^{1,\sigma} \left( \delta_{jk} \delta_{\sigma\uparrow} f_{N\uparrow}^\dagger f_{N\downarrow}^\dagger f_{i\downarrow} f_{l\uparrow} + \delta_{ik} \delta_{\sigma\downarrow} f_{N\uparrow}^\dagger f_{N\downarrow}^\dagger f_{l\downarrow} f_{j\uparrow} + f_{N\uparrow}^\dagger f_{N\downarrow}^\dagger f_{k\sigma}^\dagger f_{l\sigma} f_{i\downarrow} f_{j\uparrow} \right) \\
:V_3: &= \sum_{\substack{ijklm \\ \sigma\nu\rho}} t_i^{1,\sigma} h_{jklm}^{2,\nu\rho} \left( \delta_{ij} \delta_{\sigma\nu} (1 - \hat{n}_{N-\sigma}) f_{N\sigma}^\dagger f_{k\rho}^\dagger f_{l\rho} f_{m\nu} + \delta_{ik} \delta_{\sigma\rho} (1 - \hat{n}_{N-\sigma}) f_{N\sigma}^\dagger f_{j\nu}^\dagger f_{m\nu} f_{l\sigma} \right. \\
&\left. + (1 - \hat{n}_{N-\sigma}) f_{N\sigma}^\dagger f_{j\nu}^\dagger f_{k\rho}^\dagger f_{l\rho} f_{m\nu} f_{i\sigma} \right)
\end{aligned}$$

$$\begin{aligned}
:V_4: &= \sum_{\substack{ijklmn, \\ \sigma\nu}} t_{ij}^2 h_{klmn}^{2,\sigma\nu} \left( \delta_{il}\delta_{\nu\downarrow}\delta_{jk}\delta_{\sigma\uparrow}f_{N\uparrow}^\dagger f_{N\downarrow}^\dagger f_{m\nu}f_{n\sigma} + \delta_{jk}\delta_{\sigma\uparrow}f_{N\uparrow}^\dagger f_{N\downarrow}^\dagger f_{l\nu}^\dagger f_{m\nu}f_{i\downarrow}f_{n\uparrow} \right. \\
&+ \delta_{ik}\delta_{\sigma\downarrow}\delta_{jl}\delta_{\nu\uparrow}f_{N\uparrow}^\dagger f_{N\downarrow}^\dagger f_{n\downarrow}f_{m\uparrow} + \delta_{ik}\delta_{\sigma\downarrow}f_{N\uparrow}^\dagger f_{N\downarrow}^\dagger f_{l\nu}^\dagger f_{m\nu}f_{n\downarrow}f_{j\uparrow} + \delta_{jl}\delta_{\nu\uparrow}f_{N\uparrow}^\dagger f_{N\downarrow}^\dagger f_{k\sigma}^\dagger f_{n\sigma}f_{i\downarrow}f_{m\uparrow} \\
&\left. + \delta_{il}\delta_{\nu\downarrow}f_{N\uparrow}^\dagger f_{N\downarrow}^\dagger f_{k\sigma}^\dagger f_{n\sigma}f_{m\downarrow}f_{j\uparrow} + f_{N\uparrow}^\dagger f_{N\downarrow}^\dagger f_{k\sigma}^\dagger f_{l\nu}^\dagger f_{m\nu}f_{n\sigma}f_{i\downarrow}f_{j\uparrow} \right) \quad (235)
\end{aligned}$$

## C Normal ordering $Q_{(N)}HQ_{(N)}\eta_{(N)}$

We carry out the term multiplications and write down the fermionic terms comprising

$$Q_{(N)}HQ_{(N)}\eta_{(N)} = \sum_{i=1}^{15} W_i,$$

$$W_1 = \sum_{ij\sigma\nu} \hat{n}_{N-\sigma} h_{iN}^{1,\sigma} t_j^{1,\nu} f_{i\sigma}^\dagger f_{N\sigma} (1 - \hat{n}_{N-\nu}) f_{N\nu}^\dagger f_{j\nu}$$

$$W_2 = \sum_{ij\sigma\nu} \hat{n}_{N-\sigma} h_{iN}^{1,\sigma} t_j^{1,\nu} f_{N\sigma}^\dagger f_{i\sigma} (1 - \hat{n}_{N-\nu}) f_{N\nu}^\dagger f_{j\nu}$$

$$W_3 = \sum_{ijk\sigma} \hat{n}_{N-\sigma} h_{iN}^{1,\sigma} t_{jk}^2 f_{i\sigma}^\dagger f_{N\sigma} f_{N\uparrow}^\dagger f_{N\downarrow}^\dagger f_{j\downarrow} f_{k\uparrow}$$

$$W_4 = \sum_{ijk\sigma} \hat{n}_{N-\sigma} h_{iN}^{1,\sigma} t_{jk}^2 f_{N\sigma}^\dagger f_{i\sigma} f_{N\uparrow}^\dagger f_{N\downarrow}^\dagger f_{j\downarrow} f_{k\uparrow}$$

$$W_5 = \sum_{i\sigma} h_{NNNN}^2 t_i^{1,\sigma} \hat{n}_{N\uparrow} \hat{n}_{N\downarrow} (1 - \hat{n}_{N-\sigma}) f_{N\sigma}^\dagger f_{i\sigma}$$

$$W_6 = \sum_{ij} h_{NNNN}^2 t_{ij}^2 \hat{n}_{N\uparrow} \hat{n}_{N\downarrow} f_{N\uparrow}^\dagger f_{N\downarrow}^\dagger f_{i\downarrow} f_{j\uparrow}$$

$$W_7 = \sum_{\substack{ijkl, \\ \sigma\nu\rho}} \hat{n}_{N-\sigma} h_{Nijk}^{2,\sigma\nu} t_l^{1,\rho} f_{N\sigma}^\dagger f_{i\nu}^\dagger f_{j\nu} f_{k\sigma} (1 - \hat{n}_{N-\rho}) f_{N\rho}^\dagger f_{l\rho}$$

$$W_8 = \sum_{\substack{ijkl, \\ \sigma\nu\rho}} \hat{n}_{N-\sigma} h_{Nkji}^{2,\sigma\nu} t_l^{1,\rho} f_{i\sigma}^\dagger f_{j\nu}^\dagger f_{k\nu} f_{N\sigma} (1 - \hat{n}_{N-\rho}) f_{N\rho}^\dagger f_{l\rho}$$

$$W_9 = \sum_{\substack{ijklm, \\ \sigma\nu}} \hat{n}_{N-\sigma} h_{Nijk}^{2,\sigma\nu} t_{lm}^2 f_{N\sigma}^\dagger f_{i\nu}^\dagger f_{j\nu} f_{k\sigma} f_{N\uparrow}^\dagger f_{N\downarrow}^\dagger f_{l\downarrow} f_{m\uparrow}$$

$$W_{10} = \sum_{\substack{ijklm, \\ \sigma\nu}} \hat{n}_{N-\sigma} h_{Nijk}^{2,\sigma\nu} t_{lm}^2 f_{k\sigma}^\dagger f_{j\nu}^\dagger f_{i\nu} f_{N\sigma} f_{N\uparrow}^\dagger f_{N\downarrow}^\dagger f_{l\downarrow} f_{m\uparrow}$$

$$\begin{aligned}
W_{11} &= \sum_{i\sigma} h_{NN}^{1,\sigma} t_i^{1,\sigma} f_{N\sigma}^\dagger f_{i\sigma} + \sum_{ij\sigma} h_{NN}^{1,\sigma} t_{ij}^2 f_{N\uparrow}^\dagger f_{N\downarrow}^\dagger f_{i\downarrow} f_{j\uparrow} \\
W_{12} &= \sum_{ijk\sigma\nu} h_{ij}^{1,\nu} t_k^{1,\sigma} (1 - \hat{n}_{N-\sigma}) f_{N\sigma}^\dagger f_{i\nu}^\dagger f_{j\nu} f_{k\sigma} \\
W_{13} &= \sum_{ijkl, \sigma} h_{ij}^{1,\sigma} t_{kl}^2 f_{N\uparrow}^\dagger f_{N\downarrow}^\dagger f_{i\sigma}^\dagger f_{j\sigma} f_{k\downarrow} f_{l\uparrow} \\
W_{14} &= \sum_{ijklm, \sigma\nu\rho} h_{ijkl}^{2,\nu\rho} t_m^{1,\sigma} (1 - \hat{n}_{N-\rho}) f_{N\sigma}^\dagger f_{i\nu}^\dagger f_{j\rho}^\dagger f_{k\rho} f_{l\nu} f_{m\sigma} \\
W_{15} &= \sum_{ijklmn, \sigma\nu} h_{ijkl}^{2,\sigma\nu} t_{mn}^2 f_{N\uparrow}^\dagger f_{N\downarrow}^\dagger f_{i\sigma}^\dagger f_{j\nu}^\dagger f_{k\nu} f_{l\sigma} f_{m\downarrow} f_{n\uparrow}
\end{aligned} \tag{236}$$

From the Pauli blockade conditions the terms  $W_1, W_4, W_5$  and  $W_8, W_9$  have zero contribution and are eliminated. Also note that expressions  $W_6, W_{11}, W_{12}, W_{13}, W_{14}, W_{15}$  are already normal ordered. Next we normal order(N.O.) eqs.(236) the fermionic operators within the remaining four terms,

$$\begin{aligned}
:W_2: &= \sum_{ij\sigma\nu} h_{iN}^{1,\sigma} t_j^{1,\nu} \left( \delta_{\sigma\uparrow} \delta_{\nu\downarrow} f_{N\uparrow}^\dagger f_{N\downarrow}^\dagger f_{j\downarrow} f_{i\uparrow} + \delta_{\sigma\downarrow} \delta_{\nu\uparrow} f_{N\uparrow}^\dagger f_{N\downarrow}^\dagger f_{i\downarrow} f_{j\uparrow} \right) \\
:W_3: &= \sum_{ijk\sigma} h_{iN}^{1,\sigma} t_{jk}^2 \left( \delta_{\sigma\uparrow} f_{N\downarrow}^\dagger f_{i\uparrow}^\dagger f_{k\uparrow} f_{j\downarrow} + \delta_{\sigma\uparrow} f_{N\uparrow}^\dagger f_{i\downarrow}^\dagger f_{j\downarrow} f_{k\uparrow} \right) \\
:W_7: &= \sum_{ijkl, \sigma\nu\rho} h_{Nijk}^{2,\sigma\nu} t_l^{1,\rho} \left( \delta_{\sigma\uparrow} \delta_{\rho\downarrow} f_{N\uparrow}^\dagger f_{N\downarrow}^\dagger f_{i\nu}^\dagger f_{j\nu} f_{l\downarrow} f_{k\uparrow} + \delta_{\sigma\downarrow} \delta_{\rho\uparrow} f_{N\uparrow}^\dagger f_{N\downarrow}^\dagger f_{i\nu}^\dagger f_{j\nu} f_{k\downarrow} f_{l\uparrow} \right), \\
:W_{10}: &= \sum_{ijklm, \sigma\nu} h_{Nijk}^{2,\sigma\nu} t_{lm}^2 \left( \delta_{\sigma\uparrow} f_{N\downarrow}^\dagger f_{k\uparrow}^\dagger f_{j\nu}^\dagger f_{i\nu} f_{m\uparrow} f_{l\downarrow} + \delta_{\sigma\downarrow} f_{N\uparrow}^\dagger f_{k\downarrow}^\dagger f_{j\nu}^\dagger f_{i\nu} f_{l\downarrow} f_{m\uparrow} \right. \\
&\quad \left. + f_{N\uparrow}^\dagger f_{N\downarrow}^\dagger f_{k\sigma}^\dagger f_{j\nu}^\dagger f_{i\nu} f_{N\sigma} f_{l\downarrow} f_{m\uparrow} \right)
\end{aligned} \tag{237}$$

## C.1 Algebraic Downfolding equations Deduced From Bloch Equation

Starting from the Bloch equation eq.(230) we used the normal ordered expressions for,

$$: \eta_{(N)} P_{(N)} H_{(N)} Q_{(N)} \eta_{(N)} : \text{ eqs.(233)}, \quad : \eta_{(N)} P_{(N)} H_{(N)} P_{(N)} : \text{ eqs.(235)}, \quad : Q_{(N)} H_{(N)} Q_{(N)} \eta_{(N)} :$$

eqs.(237) to obtain the N.O. Bloch equation,

$$\begin{aligned}
: Q_{(N)} S_{(N)}^{-1} H_{(N)} S_{(N)} P_{(N)} : &= \sum_i A_i^{(N),\sigma} f_{N\sigma}^\dagger f_{i\sigma} + \sum_{ijk} B_{ijk}^{(N),\sigma\nu} f_{N\sigma}^\dagger f_{i\nu}^\dagger f_{j\nu} f_{k\sigma} + \sum_{ij} C_{ij}^{(N)} f_{N\uparrow}^\dagger f_{N\downarrow}^\dagger f_{i\downarrow} f_{j\uparrow} \\
&+ \sum_{ijkl\sigma} D_{ijkl}^{(N),\sigma} f_{N\uparrow}^\dagger f_{N\downarrow}^\dagger f_{i\sigma}^\dagger f_{j\sigma} f_{k\downarrow} f_{l\uparrow} + \sum_{ijklm, \sigma\mu\nu} E_{ijklm}^{(N),\sigma\nu\rho} f_{N\sigma}^\dagger f_{i\nu}^\dagger f_{j\rho}^\dagger f_{k\rho} f_{l\nu} f_{m\sigma} \\
&+ \sum_{ijklmn, \sigma\nu} F_{ijklm}^{(N),\sigma\nu\rho} f_{N\uparrow}^\dagger f_{N\downarrow}^\dagger f_{i\sigma}^\dagger f_{j\nu}^\dagger f_{k\nu} f_{l\sigma} f_{m\downarrow} f_{n\uparrow}
\end{aligned} \tag{238}$$

where  $\mathbf{A}^{(N),\sigma}$  constitute the N.O. single-particle excitations contribution to the downfolding Bloch equation. Here  $\mathbf{B}^{(N),\sigma\nu}$  represents the N.O. contribution of doubles excitation involving one of the downfolding spin-orbital ( $N\sigma$ ),  $\mathbf{B}^{(N),\sigma\nu}$ . The coefficient  $\mathbf{C}^{(N)}$  represents the contribution of paired doubles excitation corresponding to the downfolding orbital. Coefficient  $\mathbf{D}^\sigma$  constitutes the contribution from triples excitations containing paired doubles.  $\mathbf{E}^{(N),\sigma\nu\rho}$  and  $\mathbf{F}^{(N),\sigma\nu\rho}$  are the triples and quadruples contribution to the Bloch equation,

$$A_i^{(N),\sigma} = \sum_k t_k^{1,\sigma} \left( h_{kN}^{1,\sigma} t_i^{1,\sigma} + h_{ki}^{1,\sigma} \right) - h_{NN}^{1,\sigma} t_i^{1,\sigma} - h_{iN}^{1,\sigma} = 0 \tag{239}$$

$$\begin{aligned}
B_{ijk}^{(N),\sigma\nu} &= t_k^{1,\sigma} h_{iN}^{1,\nu} t_j^{1,\nu} + \sum_n t_n^{1,\sigma} \left( h_{nijN}^{2,\sigma\nu} t_k^{1,\sigma} + h_{inkN}^{2,\nu\sigma} t_j^{1,\nu} + \delta_{\nu,-\sigma} h_{niNN}^2 t_{jk}^2 + h_{nijk}^{2,\sigma\nu} + h_{inkj}^{2,\nu\sigma} \right) \\
&- \delta_{\nu,-\sigma} \left( \delta_{\sigma\downarrow} h_{iN}^{1,\sigma} t_{kj}^2 + \delta_{\sigma\uparrow} h_{iN}^{1,\sigma} t_{jk}^2 \right) - h_{Nijk}^{2,\sigma\nu} = 0
\end{aligned} \tag{240}$$

$$\begin{aligned}
C_{ij}^{(N)} &= \sum_n \left( t_{in}^2 \left( h_{nN}^{1,\uparrow} t_j^{1,\uparrow} + h_{nj}^{1,\uparrow} \right) + t_{nj}^2 \left( h_{nN}^{1,\downarrow} t_i^{1,\downarrow} + h_{ni}^{1,\downarrow} \right) \right) - \left( h_{jN}^{1,\uparrow} t_i^{1,\downarrow} + h_{iN}^{1,\downarrow} t_j^{1,\uparrow} \right) - \left( h_{NN}^{1,\uparrow} + h_{NN}^{1,\downarrow} \right) t_{ij}^2 \\
&+ \sum_{mn} t_{mn}^2 \left( h_{nmiN}^{2,\uparrow\downarrow} t_j^{1,\uparrow} + h_{mnjN}^{2,\downarrow\uparrow} t_i^{1,\downarrow} + h_{nmi}^{2,\uparrow\downarrow} + h_{mnji}^{2,\downarrow\uparrow} + h_{mnNN}^2 t_{ij}^2 \right) - h_{NNNN}^2 t_{ij}^2 - h_{NNij}^2
\end{aligned} \tag{241}$$

$$\begin{aligned}
D_{ijkl}^\sigma &= t_{kl}^2 \left( h_{iN}^{1,\sigma} t_j^{1,\sigma} + h_{ij}^{1,\sigma} \right) + \sum_n \left( t_{kn}^2 h_{nijN}^{2,\uparrow\sigma} t_l^{1,\uparrow} + t_{nl}^2 h_{nijN}^{2,\downarrow\sigma} t_k^{1,\downarrow} + t_{nl}^2 h_{inkN}^{2,\sigma\downarrow} t_j^{1,\sigma} + t_{kn}^2 h_{inlN}^{2,\sigma\uparrow} t_j^{1,\sigma} \right) \\
&+ \sum_n \left( \delta_{\sigma\downarrow} t_{kn}^2 h_{niNN}^2 t_{jl}^2 - \delta_{\sigma\uparrow} t_{nk}^2 h_{niNN}^2 t_{jl}^2 \right) + \sum_n \left( t_{kn}^2 \left( h_{nijl}^{2,\uparrow\sigma} + h_{inlj}^{2,\sigma\uparrow} \right) + t_{nl}^2 \left( h_{nijN}^{2,\downarrow\sigma} t_k^{1,\downarrow} + h_{inkN}^{2,\sigma\downarrow} t_j^{1,\sigma} \right) \right) \\
&- \left( h_{Nijl}^{2,\uparrow\sigma} t_k^{1,\downarrow} + h_{Nijk}^{2,\downarrow\sigma} t_l^{1,\uparrow} \right) - h_{ij}^{1,\sigma} t_{kl}^2
\end{aligned} \tag{242}$$

$$\mathbf{E}^{(N),\sigma\nu} = \mathbf{t}^{1,\sigma} \otimes \mathbf{h}_N^{2,\mu\nu} \otimes \mathbf{t}^{1,\mu} + \delta_{\sigma,-\nu} \mathbf{h}_{NN}^2 \otimes \mathbf{t}^2 \otimes \mathbf{t}^{1,\sigma} - \delta_{\sigma\downarrow} \left( \mathbf{h}_N^{2,\uparrow\nu} \otimes \mathbf{t}^2 \right)_{32154} - \delta_{\sigma\downarrow} \left( \mathbf{h}_N^{2,\downarrow\nu} \otimes \mathbf{t}^2 \right)_{32154} \tag{243}$$

$$\mathbf{F}^{(N),\sigma\nu\rho} = \mathbf{h}_N^{2,\sigma\mu} \otimes \mathbf{t}^{1,\sigma} \otimes \mathbf{t}^2 + \mathbf{h}_{NN}^2 \otimes \mathbf{t}^2 \otimes \mathbf{t}^2 \tag{244}$$

In the above expressions  $\mathbf{h}^{2,\sigma\nu}_{abcd}$  represents a permutation of indexes of the tensor for e.g.  $((\mathbf{h}^{2,\sigma\nu})_{3124})_{ijkl} = (\mathbf{h}^{2,\sigma\nu})_{kijl}$ . Here  $(\otimes)$  represents tensor product and  $(\cdot)$  represents tensor contraction. In order to satisfy the Bloch equation we need the contributions  $\mathbf{A}$  to  $\mathbf{D}$  to become zero. This corresponds to a quadratic polynomial system. In the next section we will evaluate its Jacobian.

## C.2 Tensor Factorization of three rank tensors-Convex Polyadic decomposition of three rank tensors

A detailed step-wise description is presented below.

1. We want to find a decomposition of the three rank tensor A in terms of two rank tensor factors X,Y,Z. The number of indices in a tensor is the rank. Each index can run over the sequence of integers starting from 1 to N, this running index is to be referred as direction in the later steps.

$$A_{ijk} = \sum_a X_{ia} Y_{ja} Z_{ka} \quad (245)$$

2. Randomly initialize tensors X and Y and multiply the transposition of X (call it XT), along the first direction of the tensor A. This leads to a matrix B. This matrix B also has three directions.

$$B_{bjk} = \sum_i X_{bi} A_{ijk} \quad (246)$$

3. This matrix B is now multiplied with the transposition of Y (call it YT) along the

second direction. This leads to matrix C. The matrix C has two directions now.

$$C_{bk} = \sum_i Y_{bj} B_{bjk} \quad (247)$$

4. Now we do the matrix multiplications XT with X call V and YT with Y call it W.

$$V = X^T X \quad (248)$$

$$W = Y^T Y \quad (249)$$

5. And then we perform Hadamard product of the matrices V and W leading to P.

$$P = VW \quad (250)$$

6. Finally we invert P and multiply it to C leading to solution for Z

$$Z = P^{-1}C \quad (251)$$

7. We repeat steps 3 to step 6 by now randomly initializing Y and taking the Z computed in step 6 to compute X

8. We repeat steps 3 to step 6 by taking the Z and X computed in step 7 to compute Y.

9. We start with the three factors X,Y,Z obtained from steps 1 to steps 8 and compute the error between the factorized representation and the original tensor

$$E = \sum_{ijk} |A_{ijk} - \sum_a X_{ia} Y_{ja} Z_{ka}|^2 \quad (252)$$

10. If error is above threshold we start with the X,Y,Z computed from last step and then repeat steps 1 to 8.

### C.3 Qubitization circuit for Matrix-Matrix multiplication with isometries

#### Theorem

If  $A$  and  $B$  are general rectangular matrices of dimensions  $\dim(A) = (N, P)$  and  $\dim(B) = (P, M)$  with  $N, M \geq 2$  then there is a unitary operation  $U(A, B)$  of dimension  $2^{n_q} \times 2^{n_q}$  that operates on a system of  $n_q = p + \max(m, n) + 2$  qubit registers :  $|\cdot\rangle_p |\cdot\rangle_{\max(m,n)} |\cdot\rangle_{a_1} |\cdot\rangle_{a_2}$  (where  $n = \lceil \log_2 N \rceil, m = \lceil \log_2 M \rceil, p = \lceil \log_2 P \rceil$ ) and block encodes the matrix multiplication of  $A$  and  $B$  s.t.

$$\langle 0|_p \langle i|_{\max(m,n)} \langle 0|_{a_1} \langle 0|_{a_2} U(A, B) |0\rangle_p |j\rangle_{\max(m,n)} |1\rangle_{a_1} |0\rangle_{a_2} = \frac{1}{P^2} \frac{\sum_k A_{ik} B_{kj}}{\|A\| \|B\|}.$$

*Proof-* Lets define an isometry  $T(A, B)$ ,

$$\begin{aligned} T(A, B) &= \frac{1}{\sqrt{2 \max(N, M)}} \sum_{r,c} |c\rangle \langle c| \otimes |r\rangle \otimes \left[ \frac{A_{rc}}{\|A\|} |0, 0\rangle + \sqrt{1 - \left(\frac{A_{rc}}{\|A\|}\right)^2} |0, 1\rangle \right. \\ &\quad \left. + \frac{B_{cr}}{\|B\|} |r, 1, 0\rangle + \sqrt{1 - \left(\frac{B_{cr}}{\|B\|}\right)^2} |r, 1, 1\rangle \right] \end{aligned} \quad (253)$$

The isometry  $T(A, B)$  has the property  $T^\dagger(A, B)T(A, B) = I_2^{\otimes p}$  this can be checked as follows,

$$\begin{aligned} T^\dagger(A, B)T(A, B) &= \frac{1}{2 \max(N, M)} \sum_c |c\rangle \langle c| \otimes \left[ \sum_r (|A_{rc}|^2 + 1 - A_{rc}^2 + B_{cr}^2 + 1 - B_{cr}^2) \right] \\ &= \sum_c |c\rangle \langle c| = I_2^{\otimes p} \end{aligned} \quad (254)$$

Utilizing the above property we can define a unitary operator  $W := W(A, B)$ ,

$$W(A, B) = 2T(A, B)T^\dagger(A, B) - 1 \quad (255)$$

The unitarity of  $W$  can be checked as follows,

$$\begin{aligned}
W^\dagger W &= WW^\dagger = I \\
&= (2T(A, B)T^\dagger(A, B) - 1)(2T(A, B)T^\dagger(A, B) - 1) \\
&= 4T(A, B)T^\dagger(A, B) - 4T(A, B)T^\dagger(A, B) + 1 = 1
\end{aligned} \tag{256}$$

To proceed further we normalizing the matrices  $A' := A/(\sqrt{2}\|A\|)$  and  $B' := B/(\sqrt{2}\|B\|)$ .

The form of the  $W$  matrix in terms of registers is as follows,

$$\begin{aligned}
W &= \sum_{c,r,r'} |c, r\rangle\langle c, r'| \otimes \left[ (4A'_{rc}A'_{r'c} - \delta_{rr'})|0, 0\rangle\langle 0, 0| + 4A'_{rc}\sqrt{1 - A'^2_{r'c}}|0, 0\rangle\langle 0, 1| \right. \\
&+ 4\sqrt{1 - A'^2_{rc}}A'_{r'c}|0, 1\rangle\langle 0, 0| + (4\sqrt{(1 - A'^2_{rc})(1 - A'^2_{r'c})} - \delta_{rr'})|0, 1\rangle\langle 0, 1| \\
&+ (4B'_{cr}B'_{cr'} - \delta_{rr'})|1, 0\rangle\langle 1, 0| + 4B'_{cr}\sqrt{1 - B'^2_{cr'}}|1, 0\rangle\langle 1, 1| \\
&+ 4\sqrt{1 - B'^2_{cr}}B'_{cr'}|1, 1\rangle\langle 1, 0| + (4\sqrt{(1 - B'^2_{cr})(1 - B'^2_{cr'})} - \delta_{rr'})|1, 1\rangle\langle 1, 1| \\
&+ 4A'_{rc}B'_{cr'}|0, 0\rangle\langle 1, 0| + 4B'_{cr}A'_{r'c}|1, 0\rangle\langle 0, 0| + 4B'_{cr}\sqrt{1 - A'^2_{r'c}}|1, 0\rangle\langle 0, 1| + 4\sqrt{1 - A'^2_{rc}}B'_{cr'}|0, 1\rangle\langle 1, 0| \\
&+ 4A'_{rc}\sqrt{1 - B'^2_{cr'}}|0, 0\rangle\langle 1, 1| + 4\sqrt{1 - B'^2_{cr}}A'_{r'c}|1, 1\rangle\langle 0, 0| + 4\sqrt{(1 - B'^2_{cr})(1 - A'^2_{cr'})}|1, 1\rangle\langle 0, 1| \\
&\left. + 4\sqrt{(1 - B'^2_{cr'})(1 - A'^2_{cr})}|0, 1\rangle\langle 1, 1| \right]
\end{aligned} \tag{257}$$

Starting from an initial state with Hadamard on the column qubit registers we obtain,

$$H^{\otimes p}|0\rangle|j\rangle|1\rangle|0\rangle = \frac{1}{P} \sum_c |c\rangle|j\rangle|1\rangle|0\rangle. \tag{258}$$

Upon acting  $W$ ,

$$\begin{aligned}
WH^{\otimes p}|0\rangle|j\rangle|1\rangle|0\rangle &= \frac{1}{2P} \sum_{c,r} |c, r\rangle \left[ (2B'_{cr}B'_{cj} - \delta_{rj})|1, 0\rangle + 2\sqrt{1 - A'^2_{rc}}B'_{cj}|0, 1\rangle \right. \\
&\left. + 2\sqrt{1 - B'^2_{rc}}B'_{cj}|1, 1\rangle + 2A'_{rc}B'_{cj}|0, 0\rangle \right]
\end{aligned} \tag{259}$$



Taking overlap of  $WH^{\otimes p}|0\rangle|j\rangle|1\rangle|0\rangle$  with the state  $H^{\otimes p}|0\rangle|i\rangle|0\rangle|0\rangle$  we get,

$$\langle 0| \langle 0| \langle i| \langle 0| H^{\otimes p} W H^{\otimes p} |0\rangle |j\rangle |1\rangle |0\rangle = \frac{4}{4P^2} \sum_k A'_{ik} B'_{kj} = \frac{4}{P^2} (A'B')_{ij} = \frac{(AB)_{ij}}{P^2 \|A\| \|B\|} \quad (260)$$

By construction we have proved the existence of  $U(A, B)$ ,

$$U(A, B) = H^{\otimes p} (2T^\dagger(A, B)T(A, B) - 1) H^{\otimes p}. \quad (261)$$

## C.4 Matrix-multiplication with Quantum circuits only with Unitary operators

### Theorem

(Isometry free proof) If  $A$  and  $B$  are general rectangular matrices of dimensions  $\dim(A) = (N, P)$  and  $\dim(B) = (P, M)$  then there is a unitary operation  $U(A, B)$  of dimension  $2^{n_q} \times 2^{n_q}$  that operates on a system of  $n_q = p + \max(m, n) + 2$  qubit registers  $|\cdot\rangle_p |\cdot\rangle_{\max(m,n)} |\cdot\rangle_{a_1} |\cdot\rangle_{a_2}$  (where  $n = \lceil \log_2 N \rceil, m = \lceil \log_2 M \rceil, p = \lceil \log_2 P \rceil$ ) and block encodes the matrix multiplication of  $A$  and  $B$  s.t.

$$\langle 0|_p \langle i|_{\max(m,n)} \langle 0|_{a_1} \langle 0|_{a_2} U(A, B) |0\rangle_p |j\rangle_{\max(m,n)} |1\rangle_{a_1} |0\rangle_{a_2} = \frac{1}{\max(M, N)P} \frac{\sum_k A_{ik} B_{kj}}{\|A\| \|B\|}.$$

*Proof-* Let us take the normalized matrices  $A' = A/(\sqrt{2}\|A\|)$ ,  $B' = B/(\sqrt{2}\|B\|)$ . For these we define two unitary operators  $V(A), V(B)$ ,

$$\begin{aligned} V_A &= \sum_{c=0, r=0}^{2^p, 2^{\max(m,n)}} \left[ |c, r, 0\rangle \langle c, r, 0| \otimes \left( A'_{rc} I + i\sqrt{1 - A'^2_{rc}} Y \right) + |c, r, 1\rangle \langle c, r, 1| \otimes I_2 \right] \\ V_B &= \sum_{c=0, r=0}^{2^p, 2^{\max(m,n)}} \left[ |c, r, 0\rangle \langle c, r, 0| \otimes I_2 + |c, r, 1\rangle \langle c, r, 1| \otimes \left( B'_{cr} I + i\sqrt{1 - B'^2_{cr}} Y \right) \right] \end{aligned} \quad (262)$$

We load the classical data of the B matrix using the state preparation oracle  $V_B H^{\otimes p}$  on the initial state  $|0\rangle|j\rangle|1\rangle|0\rangle$ ,

$$|\Phi_B\rangle = V_B H^{\otimes p} |0\rangle|j\rangle|1\rangle|0\rangle = \frac{1}{\sqrt{P}} \sum_c \left[ B'_{cj} |c, j, 1, 0\rangle + \sqrt{1 - B'_{cj}{}^2} |c, j, 1, 1\rangle \right]. \quad (263)$$

We load the classical data of the A matrix using the state preparation oracle  $V_A H^{\otimes p}$ ,

$$|\Phi_A\rangle = V_A H^{\otimes p} |0\rangle|i\rangle|0\rangle|0\rangle = \frac{1}{\sqrt{P}} \sum_c \left[ A'_{ic} |c, i, 0, 0\rangle + \sqrt{1 - A'_{ic}{}^2} |c, i, 0, 1\rangle \right] \quad (264)$$

Note that the states  $|\Phi_A\rangle$  and  $|\Phi_B\rangle$  are orthogonal,

$$\langle \Phi_A | \Phi_B \rangle = 0 \quad (265)$$

Next we define diffusion operator  $R$  acting on the row registers and the ancillas  $a_1, a_2$ ,

$$\begin{aligned} R &= I_2^{\otimes p} \otimes \left[ (H^{\otimes \max(m,n)} \otimes H \otimes I_2) (2|0, 0, 0\rangle\langle 0, 0, 0| - I) (H^{\otimes \max(m,n)} \otimes H \otimes I_2) \right] \\ &= I_2^{\otimes p} \otimes \left[ \sum_{k,l} 2 \frac{|k, +, 0\rangle\langle l, +, 0|}{\max(M, N)} - I \right] \end{aligned} \quad (266)$$

Then the overlap between these two states  $|\Phi_A\rangle$  and  $R|\Phi_B\rangle$  is given by,

$$\begin{aligned} \langle \Phi_A | R | \Phi_B \rangle &= \langle 0, i, 0, 0 | H_c^{\otimes p} V_A^\dagger R V_B H_c^{\otimes p} | 0, j, 1, 0 \rangle \\ &= \frac{2 \sum_c A'_{ic} B'_{cj}}{\max(M, N) P} = \frac{\sum_c A_{ic} B_{cj}}{\max(M, N) P \|A\| \|B\|} \end{aligned} \quad (267)$$

By construction we have proved the existence of  $U(A, B)$  that can be defined without any isometry,

$$U(A, B) = H_c^{\otimes p} V_A^\dagger R V_B H_c^{\otimes p}. \quad (268)$$

## Acknowledgement

The authors would like to thank his colleageaus Anil Sharma, Manoj Nambiar, Geetha Thiagarajan, Sriram Goverpet Srinivasan from TCS for their constructive feedback and support.

## Declaration

This work is based on two patents US patent No-20240202561 and Indian patent No. 202421039027.

## References

- (16) Datta, D.; Gordon, M. S. Accelerating coupled-cluster calculations with GPUs: An implementation of the density-fitted CCSD (T) approach for heterogeneous computing architectures using OpenMP directives. *Journal of Chemical Theory and Computation* **2023**, *19*, 7640–7657.
- (2) Datta, D.; Gordon, M. S. A massively parallel implementation of the CCSD (T) method using the resolution-of-the-identity approximation and a hybrid distributed/shared memory parallelization model. *Journal of Chemical Theory and Computation* **2021**, *17*, 4799–4822.
- (3) Lam, Y.-h.; Abramov, Y.; Ananthula, R. S.; Elward, J. M.; Hilden, L. R.; Nilsson Lill, S. O.; Norrby, P.-O.; Ramirez, A.; Sherer, E. C.; Mustakis, J., et al. Applications of quantum chemistry in pharmaceutical process development: Current state and opportunities. *Organic Process Research & Development* **2020**, *24*, 1496–1507.
- (4) Kostal, J.; Voutchkova-Kostal, A. Quantum-mechanical approach to predicting the carcinogenic potency of N-nitroso impurities in pharmaceuticals. *Chemical Research in Toxicology* **2023**, *36*, 291–304.

- (5) Bauer, B.; Bravyi, S.; Motta, M.; Chan, G. K.-L. Quantum algorithms for quantum chemistry and quantum materials science. *Chemical Reviews* **2020**, *120*, 12685–12717.
- (6) Head-Gordon, M. Quantum chemistry and molecular processes. *The Journal of Physical Chemistry* **1996**, *100*, 13213–13225.
- (7) Bartlett, R. J.; Musiał, M. Coupled-cluster theory in quantum chemistry. *Rev. Mod. Phys.* **2007**, *79*, 291.
- (8) Riplinger, C.; Neese, F. An efficient and near linear scaling pair natural orbital based local coupled cluster method. *The Journal of chemical physics* **2013**, *138*.
- (9) Hohenstein, E. G.; Fales, B. S.; Parrish, R. M.; Martínez, T. J. Rank-reduced coupled-cluster. III. Tensor hypercontraction of the doubles amplitudes. *The Journal of Chemical Physics* **2022**, *156*.
- (10) Shavitt, I.; Bartlett, R. J. *Many-body methods in chemistry and physics: MBPT and coupled-cluster theory*; Cambridge university press, 2009.
- (11) Sherrill, C. D.; Schaefer III, H. F. *Advances in quantum chemistry*; Elsevier, 1999; Vol. 34; pp 143–269.
- (12) Mahapatra, U. S.; Datta, B.; Mukherjee, D. A size-consistent state-specific multireference coupled cluster theory: Formal developments and molecular applications. *The Journal of chemical physics* **1999**, *110*, 6171–6188.
- (13) Ivanov, V. V.; Lyakh, D. I.; Adamowicz, L. Multireference state-specific coupled-cluster methods. State-of-the-art and perspectives. *Physical Chemistry Chemical Physics* **2009**, *11*, 2355–2370.
- (14) Musiał, M.; Perera, A.; Bartlett, R. J. Multireference coupled-cluster theory: The easy way. *The Journal of Chemical Physics* **2011**, *134*.

- (15) Evangelista, F. A. Perspective: Multireference coupled cluster theories of dynamical electron correlation. *The Journal of Chemical Physics* **2018**, *149*.
- (16) Datta, D.; Gordon, M. S. Accelerating coupled-cluster calculations with GPUs: An implementation of the density-fitted CCSD (T) approach for heterogeneous computing architectures using OpenMP directives. *Journal of Chemical Theory and Computation* **2023**, *19*, 7640–7657.
- (17) Knizia, G.; Chan, G. K.-L. Density matrix embedding: A simple alternative to dynamical mean-field theory. *Physical review letters* **2012**, *109*, 186404.
- (18) Knizia, G.; Chan, G. K.-L. Density matrix embedding: A strong-coupling quantum embedding theory. *Journal of chemical theory and computation* **2013**, *9*, 1428–1432.
- (19) Kotliar, G.; Savrasov, S. Y.; Haule, K.; Oudovenko, V. S.; Parcollet, O.; Marianetti, C. Electronic structure calculations with dynamical mean-field theory. *RMP* **2006**, *78*, 865.
- (20) Park, H.; Haule, K.; Kotliar, G. Cluster dynamical mean field theory of the Mott transition. *PRL* **2008**, *101*, 186403.
- (21) Pižorn, I.; Verstraete, F. Variational Numerical Renormalization Group: Bridging the Gap between NRG and Density Matrix Renormalization Group. *Phys. Rev. Lett.* **2012**, *108*, 067202.
- (22) White, S. R. Density matrix formulation for quantum renormalization groups. *Physical review letters* **1992**, *69*, 2863.
- (23) Verstraete, F.; Cirac, J. I. Renormalization algorithms for quantum-many body systems in two and higher dimensions. *arXiv preprint cond-mat/0407066* **2004**,
- (24) Vidal, G. Class of quantum many-body states that can be efficiently simulated. *Physical review letters* **2008**, *101*, 110501.

- (25) Murg, V.; Verstraete, F.; Schneider, R.; Nagy, P. R.; Legeza, O. Tree tensor network state with variable tensor order: An efficient multireference method for strongly correlated systems. *Journal of Chemical Theory and Computation* **2015**, *11*, 1027–1036.
- (26) Sachdev, S. Quantum Phase Transitions. 2007; <https://doi.org/10.1002/9780470022184.hmm108>.
- (27) Hirayama, M.; Yamaji, Y.; Misawa, T.; Imada, M. Ab initio effective Hamiltonians for cuprate superconductors. *Phys. Rev. B* **2018**, *98*, 134501.
- (28) Mukherjee, A.; Lal, S. Scaling theory for Mott–Hubbard transitions: I.  $T = 0$  phase diagram of the 1/2-filled Hubbard model. *New Journal of Physics* **2020**, *22*, 063007.
- (29) Mukherjee, A.; Lal, S. Scaling theory for Mott–Hubbard transitions-II: quantum criticality of the doped Mott insulator. *New Journal of Physics* **2020**, *22*, 063008.
- (30) Clementi, E. Effective Hamiltonian and density functionals in computational chemistry. **1996**,
- (31) Pokhilko, P.; Krylov, A. I. Effective Hamiltonians derived from equation-of-motion coupled-cluster wave functions: Theory and application to the Hubbard and Heisenberg Hamiltonians. *The Journal of Chemical Physics* **2020**, *152*, 094108.
- (32) Skomorowski, W.; Krylov, A. I. Feshbach–Fano approach for calculation of Auger decay rates using equation-of-motion coupled-cluster wave functions. II. Numerical examples and benchmarks. *The Journal of Chemical Physics* **2021**, *154*, 084125.
- (33) Ng, B.; Newman, D. J. Many-body perturbation theory for effective Hamiltonians using nonorthogonal basis sets. *The Journal of Chemical Physics* **1985**, *83*, 1758–1768.
- (34) Domcke, W. Theory of resonance and threshold effects in electron-molecule collisions: The projection-operator approach. *Physics Reports* **1991**, *208*, 97–188.

- (35) Capuzzi, F.; Mahaux, C. Projection Operator Approach to the Self-Energy. *Annals of Physics* **1996**, *245*, 147–208.
- (36) Schrieffer, J. R.; Wolff, P. A. Relation between the Anderson and Kondo Hamiltonians. *Phys. Rev.* **1966**, *149*, 491–492.
- (37) Suzuki, K.; Lee, S. Y. Convergent theory for effective interaction in nuclei. *Progress of Theoretical Physics* **1980**, *64*, 2091–2106.
- (38) Suzuki, K.; Okamoto, R. Degenerate perturbation theory in quantum mechanics. *Progress of Theoretical Physics* **1983**, *70*, 439–451.
- (39) Bravyi, S.; DiVincenzo, D. P.; Loss, D. Schrieffer–Wolff transformation for quantum many-body systems. *Annals of Physics* **2011**, *326*, 2793–2826.
- (40) Cohen, T.; Farnsworth, K.; Houtz, R.; Luty, M. A. Hamiltonian Truncation Effective Theory. 2021.
- (41) Chaudhuri, R. K.; Freed, K. F.; Hose, G.; Piecuch, P.; Kowalski, K.; Włoch, M.; Chattopadhyay, S.; Mukherjee, D.; Rolik, Z.; Szabados, Á.; Tóth, G.; Surján, P. R. Comparison of low-order multireference many-body perturbation theories. *The Journal of Chemical Physics* **2005**, *122*, 134105.
- (42) Ten-no, S. Stochastic determination of effective Hamiltonian for the full configuration interaction solution of quasi-degenerate electronic states. *The Journal of Chemical Physics* **2013**, *138*, 164126.
- (43) Wilson, K. G. The renormalization group: Critical phenomena and the Kondo problem. *Rev. Mod. Phys.* **1975**, *47*, 773–840.
- (44) Schollwöck, U. The density-matrix renormalization group. *Reviews of Modern Physics* **2005**, *77*, 259–315.

- (45) Bauman, N. P.; Bylaska, E. J.; Krishnamoorthy, S.; Low, G. H.; Wiebe, N.; Granade, C. E.; Roetteler, M.; Troyer, M.; Kowalski, K. Downfolding of many-body Hamiltonians using active-space models: Extension of the sub-system embedding sub-algebras approach to unitary coupled cluster formalisms. *The Journal of chemical physics* **2019**, *151*.
- (46) Aryasetiawan, F.; Tomczak, J. M.; Miyake, T.; Sakuma, R. Downfolded self-energy of many-electron systems. *Physical review letters* **2009**, *102*, 176402.
- (47) Bauman, N. P.; Low, G. H.; Kowalski, K. Quantum simulations of excited states with active-space downfolded Hamiltonians. *The Journal of chemical physics* **2019**, *151*.
- (48) Huang, R.; Li, C.; Evangelista, F. A. Leveraging small-scale quantum computers with unitarily downfolded hamiltonians. *PRX Quantum* **2023**, *4*, 020313.
- (49) Bauman, N. P.; Bylaska, E. J.; Krishnamoorthy, S.; Low, G. H.; Wiebe, N.; Granade, C. E.; Roetteler, M.; Troyer, M.; Kowalski, K. Downfolding of many-body Hamiltonians using active-space models: Extension of the sub-system embedding sub-algebras approach to unitary coupled cluster formalisms. *The Journal of Chemical Physics* **2019**, *151*, 014107.
- (50) Bauman, N. P.; Kowalski, K. Coupled Cluster Downfolding Theory: towards universal many-body algorithms for dimensionality reduction of composite quantum systems in chemistry and materials science. *Materials Theory* **2022**, *6*, 1–19.
- (51) Kowalski, K.; Peng, B.; Bauman, N. P. The accuracies of effective interactions in downfolding coupled-cluster approaches for small-dimensionality active spaces. *The Journal of Chemical Physics* **2024**, *160*.
- (52) Low, G. H.; Chuang, I. L. Hamiltonian Simulation by Qubitization. *Quantum* **2019**, *3*, 163.



- (53) Babbush, R.; Gidney, C.; Berry, D. W.; Wiebe, N.; McClean, J.; Paler, A.; Fowler, A.; Neven, H. Encoding Electronic Spectra in Quantum Circuits with Linear T Complexity. *Phys. Rev. X* **2018**, *8*, 041015.
- (54) Martyn, J. M.; Rossi, Z. M.; Tan, A. K.; Chuang, I. L. Grand Unification of Quantum Algorithms. *PRX Quantum* **2021**, *2*, 040203.
- (55) Motta, M.; Ye, E.; McClean, J. R.; Li, Z.; Minnich, A. J.; Babbush, R.; Chan, G. K. Low rank representations for quantum simulation of electronic structure. *arXiv:1808.02625* **2018**,
- (56) Motta, M.; Ye, E.; McClean, J. R.; Li, Z.; Minnich, A. J.; Babbush, R.; Chan, G. K.-L. Low rank representations for quantum simulation of electronic structure. *npj Quantum Information* **2021**, *7*, 83.
- (57) Lee, J.; Berry, D. W.; Gidney, C.; Huggins, W. J.; McClean, J. R.; Wiebe, N.; Babbush, R. Even more efficient quantum computations of chemistry through tensor hypercontraction. *PRX Quantum* **2021**, *2*, 030305.
- (58) von Burg, V.; Low, G. H.; Häner, T.; Steiger, D. S.; Reiher, M.; Roetteler, M.; Troyer, M. Quantum computing enhanced computational catalysis. *Physical Review Research* **2021**, *3*, 033055.
- (59) Reiher, M.; Wiebe, N.; Svore, K. M.; Wecker, D.; Troyer, M. Elucidating reaction mechanisms on quantum computers. *Proceedings of the national academy of sciences* **2017**, *114*, 7555–7560.
- (60) Kim, I. H.; Liu, Y.-H.; Pallister, S.; Pol, W.; Roberts, S.; Lee, E. Fault-tolerant resource estimate for quantum chemical simulations: Case study on Li-ion battery electrolyte molecules. *Physical Review Research* **2022**, *4*, 023019.

- (61) Goings, J. J.; White, A.; Lee, J.; Tautermann, C. S.; Degroote, M.; Gidney, C.; Shiozaki, T.; Babbush, R.; Rubin, N. C. Reliably assessing the electronic structure of cytochrome P450 on today’s classical computers and tomorrow’s quantum computers. *Proceedings of the National Academy of Sciences* **2022**, *119*, e2203533119.
- (62) Su, Y.; Berry, D. W.; Wiebe, N.; Rubin, N.; Babbush, R. Fault-tolerant quantum simulations of chemistry in first quantization. *PRX Quantum* **2021**, *2*, 040332.
- (63) Stair, N. H.; Huang, R.; Evangelista, F. A. A multireference quantum Krylov algorithm for strongly correlated electrons. *Journal of chemical theory and computation* **2020**, *16*, 2236–2245.
- (64) Ding, Z.; Lin, L. Even shorter quantum circuit for phase estimation on early fault-tolerant quantum computers with applications to ground-state energy estimation. *PRX Quantum* **2023**, *4*, 020331.
- (65) Cortes, C. L.; Gray, S. K. Quantum Krylov subspace algorithms for ground-and excited-state energy estimation. *Physical Review A* **2022**, *105*, 022417.
- (66) Beverland, M. E.; Murali, P.; Troyer, M.; Svore, K. M.; Hoeffler, T.; Kliuchnikov, V.; Low, G. H.; Soeken, M.; Sundaram, A.; Vaschillo, A. Assessing requirements to scale to practical quantum advantage. *arXiv preprint arXiv:2211.07629* **2022**,
- (67) Hoeffler, T.; Häner, T.; Troyer, M. Disentangling hype from practicality: On realistically achieving quantum advantage. *Communications of the ACM* **2023**, *66*, 82–87.
- (68) Kolda, T. G.; Bader, B. W. Tensor decompositions and applications. *SIAM review* **2009**, *51*, 455–500.
- (69) Hong, D.; Kolda, T. G.; Duersch, J. A. Generalized canonical polyadic tensor decomposition. *SIAM Review* **2020**, *62*, 133–163.

- (70) Lee, J.; Lin, L.; Head-Gordon, M. Systematically improvable tensor hypercontraction: Interpolative separable density-fitting for molecules applied to exact exchange, second- and third-order Møller–Plesset perturbation theory. *Journal of chemical theory and computation* **2019**, *16*, 243–263.
- (71) Suzuki, K. Construction of Hermitian Effective Interaction in Nuclei:-General Relation between Hermitian and Non-Hermitian Forms. *Progress of Theoretical Physics* **1982**, *68*, 246–260.
- (72) Mottonen, M.; Vartiainen, J. J.; Bergholm, V.; Salomaa, M. M. Transformation of quantum states using uniformly controlled rotations. **2004**,
- (73) Shende, V.; Bullock, S.; Markov, I. Synthesis of quantum-logic circuits. *IEEE Transactions on Computer-Aided Design of Integrated Circuits and Systems* **2006**, *25*, 1000–1010.
- (74) Dawson, C. M.; Nielsen, M. A. The Solovay-Kitaev algorithm. **2005**,
- (75) Ross, N. J.; Selinger, P. Optimal ancilla-free Clifford+T approximation of z-rotations. **2016**,
- (76) Kliuchnikov, V.; Maslov, D.; Mosca, M. Asymptotically Optimal Approximation of Single Qubit Unitaries by Clifford and T Circuits Using a Constant Number of Ancillary Qubits. *Physical Review Letters* **2013**, *110*.
- (77) Nakatani, N.; Chan, G. K. Efficient tree tensor network states (TTNS) for quantum chemistry: Generalizations of the density matrix renormalization group algorithm. *The Journal of chemical physics* **2013**, *138*.